

**Ancient Submarine Canyons and Fans of the Carson Basin, Grand Banks,  
Offshore Newfoundland, Canada**

*R. Scott Parker*

Undergraduate Honours Thesis  
Department of Earth Sciences  
Dalhousie University



## Distribution License

DalSpace requires agreement to this non-exclusive distribution license before your item can appear on DalSpace.

### NON-EXCLUSIVE DISTRIBUTION LICENSE

You (the author(s) or copyright owner) grant to Dalhousie University the non-exclusive right to reproduce and distribute your submission worldwide in any medium.

You agree that Dalhousie University may, without changing the content, reformat the submission for the purpose of preservation.

You also agree that Dalhousie University may keep more than one copy of this submission for purposes of security, back-up and preservation.

You agree that the submission is your original work, and that you have the right to grant the rights contained in this license. You also agree that your submission does not, to the best of your knowledge, infringe upon anyone's copyright.

If the submission contains material for which you do not hold copyright, you agree that you have obtained the unrestricted permission of the copyright owner to grant Dalhousie University the rights required by this license, and that such third-party owned material is clearly identified and acknowledged within the text or content of the submission.

If the submission is based upon work that has been sponsored or supported by an agency or organization other than Dalhousie University, you assert that you have fulfilled any right of review or other obligations required by such contract or agreement.

Dalhousie University will clearly identify your name(s) as the author(s) or owner(s) of the submission, and will not make any alteration to the content of the files that you have submitted.

If you have questions regarding this license please contact the repository manager at [dalspace@dal.ca](mailto:dalspace@dal.ca).

Grant the distribution license by signing and dating below.

---

Name of signatory

---

Date

Ancient Submarine Canyons and Fans of the Carson Basin, Grand Banks,  
Offshore Newfoundland, Canada

R. Scott Parker

Submitted in Partial Fulfilment of the Requirements for the Degree of  
Bachelor of Science, Honours Co-op  
Department of Earth Sciences  
Dalhousie University, Halifax, Nova Scotia

Submitted April, 1999

COPYRIGHT BY R. SCOTT PARKER 1999



Dalhousie University

Department of Earth Sciences

Halifax, Nova Scotia

Canada B3H 3J5

(902) 494-2358

FAX (902) 494-6889

DATE

April 21/99

AUTHOR

R. Scott Parker

TITLE

Ancient Submarine Canyons and Fans  
of the Carson Basin, Grand Banks,  
Offshore Newfoundland, Canada

Degree

Honours Co-op

Convocation

Year

1999

Permission is herewith granted to Dalhousie University to circulate and to have copied for non-commercial purposes, at its discretion, the above title upon the request of individuals or institutions.

THE AUTHOR RESERVES OTHER PUBLICATION RIGHTS, AND NEITHER THE THESIS NOR EXTENSIVE EXTRACTS FROM IT MAY BE PRINTED OR OTHERWISE REPRODUCED WITHOUT THE AUTHOR'S WRITTEN PERMISSION.

THE AUTHOR ATTESTS THAT PERMISSION HAS BEEN OBTAINED FOR THE USE OF ANY COPYRIGHTED MATERIAL APPEARING IN THIS THESIS (OTHER THAN BRIEF EXCERPTS REQUIRING ONLY PROPER ACKNOWLEDGEMENT IN SCHOLARLY WRITING) AND THAT ALL SUCH USE IS CLEARLY ACKNOWLEDGED.



## ABSTRACT

The Carson Basin lies beneath the Grand Banks, offshore Newfoundland, and is composed of several depocenters, the deepest of which holds over 7 km of Mesozoic and Cenozoic strata. To date only four exploration wells have been drilled. The basin lies to the southeast of the more intensely studied and developed Jeanne d'Arc Basin, which contains the Hibernia production platform and other developing oil-fields. A basement high separates the Carson Basin from the southern Jeanne d'Arc. The basins formed in response to the opening of the North Atlantic Ocean in a complex series of rifting events.

Submarine canyons and erosional scours have been recognized in the northern end of the Carson Basin at depths of 1100 m, and are buried and filled by the Banquereau Formation. The canyons were mapped using industry seismic reflection profiles. Two canyon complexes, informally named the Bonniton and St. George Canyons, incise an interpreted paleocontinental shelf-break. The upper reaches of the Bonniton Canyon carve a V-shaped erosional notch at least 6.5 km wide, with canyon walls dipping as much as 34.5 degrees. The Bonniton Canyon is over 39 km long, and trends roughly northwest-southeast. The St. George Canyon is over 30 km long and also trends northwest-southeast. Both canyons have deposited submarine fans basinward over a wide area, with a maximum thickness of approximately 900 m.

Synthetic seismograms created from well logs, along with biostratigraphic studies, indicate that the canyon incision correlates with a basinwide erosional unconformity that occurred in the Early Eocene. The Early Eocene Unconformity corresponds with a relative drop in sealevel on the shelf adjacent to the canyons, resulting in a change in marine environment from outer neritic to nearshore marine.

Early Eocene erosional channels and gullies of the Jeanne d'Arc Basin have previously been interpreted as submarine canyons. The Early Eocene erosion and deposition occur stratigraphically higher than the ridge separating the Jeanne d'Arc Basin from the Carson Basin, indicating possible interaction between the two basins. With the recognition of large submarine canyons and fans to the southeast in the Carson Basin, the Early Eocene erosional features of the Jeanne d'Arc Basin may be interpreted as subaerially exposed incised valleys. The northwest-southeast direction of transport for the East and West Cormorant Canyons is very similar to the Bonniton and St. George Canyon trend. A prograding clastic wedge at the outlet of the Cormorant Canyons was deposited on the high between the two basins. The prograding package may be the primary source of unstable material ultimately transported to the submarine fans of Carson Basin.

The Carson Basin is relatively underexplored when compared to other basins on the Grand Banks. The submarine fans of the Carson Basin are areally extensive, thick deposits which may act as both reservoir and trap for hydrocarbons present in the basin. Stratigraphic pinchouts and salt tectonism create favourable conditions for hydrocarbon plays, however the deep water environment and questionable source rock potential will continue to curtail exploration in the near future.

## TABLE OF CONTENTS

ABSTRACT .....	i
TABLE OF CONTENTS .....	ii
TABLE OF FIGURES .....	iv
TABLE OF TABLES .....	viii
ACKNOWLEDGMENTS .....	ix
CHAPTER 1: INTRODUCTION	
1.1 General Statement .....	1
1.2 Objectives and Scope of Project .....	4
1.3 Organization of Thesis .....	4
CHAPTER 2: DATA AND METHODS	
2.1 Introduction .....	7
2.2 Well Data .....	7
2.3 Cross-Section Construction .....	9
2.4 Synthetic Seismograms .....	9
2.5 Seismic Data .....	10
2.6 Mapping Procedures .....	11
CHAPTER 3: BACKGROUND GEOLOGY	
3.1 Formation and Filling of Grand Banks Rift Basins .....	14
3.2 Structure of Carson Basin .....	18
3.3 Stratigraphy of Carson Basin .....	23
3.4 Submarine Canyons and Fans .....	23
3.4.1 Submarine Canyons .....	23
3.4.2 Submarine Fans .....	30
CHAPTER 4: EXPLORATION WELLS OF CARSON BASIN	
4.1 General Lithology .....	37
4.2 Unconformities .....	39
4.3 Synthetic Seismograms .....	42
4.4 Paleoenvironment .....	44
CHAPTER 5: SUBMARINE CANYONS AND FANS OF CARSON BASIN	
5.1 Introduction .....	47
5.2 Submarine Canyons .....	47
5.2.1 Morphology .....	47
5.2.2 Timing of Excavation .....	55

5.3 Major Deposition Features .....	58
5.3.1 Fan Deposition .....	58
5.3.2 Canyon Fill and Progradation .....	63
<b>CHAPTER 6: DISCUSSION AND CONCLUSIONS</b>	
6.1 Introduction .....	68
6.2 Correlation with Previously Recognized Erosional Features .....	68
6.3 Paleoenvironment .....	71
6.4 Summary .....	73
6.5 Recommendations for Future Work .....	73
<b>REFERENCES</b> .....	75
<b>APPENDIX 1: WELLS</b>	
Osprey G-84 .....	Appendix 1.1
Bonnition H-32 .....	Appendix 1.2
Skua E-41 .....	Appendix 1.3
St. George J-55 .....	Appendix 1.4
<b>APPENDIX 2: WELL LITHOSTRATIGRAPHY AND BIOSTRATIGRAPHY PICKS</b>	
Osprey Lithostratigraphic Picks .....	Appendix 2.1
Osprey Biostratigraphic Picks .....	Appendix 2.2
Bonnition Lithostratigraphic Picks .....	Appendix 2.3
Bonnition Biostratigraphic Picks .....	Appendix 2.4
Skua Lithostratigraphic Picks .....	Appendix 2.5
Skua Biostratigraphic Picks .....	Appendix 2.6
St. George Lithostratigraphic Picks .....	Appendix 2.7
St. George Biostratigraphic Picks .....	Appendix 2.8
<b>APPENDIX 3: SYNTHETIC SEISMOGRAMS</b>	
Intersecting Seismic Lines .....	Appendix 3.1
Osprey G-84 .....	Appendix 3.2
Bonnition H-32 .....	Appendix 3.3
Skua E-41 .....	Appendix 3.4
St. George J-55 .....	Appendix 3.5
<b>APPENDIX 4: SEISMIC PROGRAMS AND SECTIONS INTERPRETED FOR PROJECT</b>	
List of Seismic Lines .....	Appendix 4.1
<b>APPENDIX 5: GREYSCALE FIGURES AND UNINTERPRETED SEISMIC SECTIONS</b>	

## TABLE OF FIGURES

<b>Figure 1.1:</b> Map showing bathymetry and general location of study area, Grand Banks, Newfoundland, Canada. The boxed area includes much of the southern Jeanne d'Arc Basin along with the Carson Basin.	2
<b>Figure 1.2:</b> Schematic map of the major rift basins of the Grand Banks. The Carson Basin and southern Jeanne d'Arc Basin are included in the noted study area. (Grant and McAlpine 1990)	3
<b>Figure 1.3:</b> Location map of the four Carson Basin wells, along with the present day bathymetry. Note that each well has been drilled in less than 105 m of water. The bulk of Carson Basin extends to the east of these wells in much deeper water.	5
<b>Figure 2.1:</b> Example of "Weight by Standard Deviation" operation to correct for 2-D seismic misties. (Landmark 1996)	12
<b>Figure 3.1:</b> Major structural elements of the Grand Banks rift basins. (Welsink et al. 1989)	15
<b>Figure 3.2:</b> Generalized geology at the level of the Avalon Peneplain. Note the three primary source areas for basin fill: the Avalon Uplift (including the South Bank High), the Bonavista Platform, and the Outer Ridge Complex. (Grant and McAlpine 1990)	17
<b>Figure 3.3:</b> Map of Sedimentary Thickness for the Grand Banks rift basins. Thickness measured from seafloor to basement in kilometers. Note the 500 m isobath for present day water depths.(Grant and McAlpine 1990)	19
<b>Figure 3.4:</b> Map of Sedimentary Thickness for Carson Basin and the southern Jeanne d'Arc Basin. Note the intervening basement high and the 500 m isobath for present day water depths. (modified from Grant and McAlpine 1990)	20
<b>Figure 3.5:</b> Lithostratigraphic chart for the Jeanne d'Arc Basin including the six major tectonic sequences of the continental margin. (DNAG timescale). (Friis 1997, modified from McAlpine 1990)	21
<b>Figure 3.6:</b> Generalized cross-section of the Carson Basin. Note the basement high which separates the Inner and Outer Carson Basin. (Grant et al. 1988)	22
<b>Figure 3.7:</b> Schematic model of how existing and buried canyons may interact. A) Former canyons transport upper-slope material from shelf-edge depocenters to the deep sea. B) Former canyons infill when sediment supply is diminished. C) The resumption of slope sedimentation and a shift in depocenter begin cutting new erosional channels, which in some cases are captured by seafloor troughs formed over buried canyons. D) Where repeated sediment flows occur, erosional channels mature into canyons that eventually reopen and deepen the underlying buried canyons. (Pratson et al. 1994)	26

<b>Figure 3.8:</b> Submarine canyon, offshore Australia. Top: uninterpreted, bottom: interpreted. The broad, V-shaped canyon shows truncation of the underlying reflectors. Note that within the canyon, the fill onlaps the truncation surface. (Posamentier and Erskine 1991)	28
<b>Figure 3.9:</b> A modern erosional remnant from the Mississippi Canyon area. (Posamentier and Erskine 1991)	29
<b>Figure 3.10:</b> Phases of a Canyon-Fan Complex as defined by Sequence Stratigraphy. (Posamentier and Erskine 1991)	31
<b>Figure 3.11A:</b> Mesozoic canyon-fan systems, Offshore Ivory Coast. i) Continental slope surface with three canyons and two fans. Slope relief is on the order of 1500 m. ii) Time-thickness (isochron) map of fans. (Mitchum 1985)	33
<b>Figure 3.11B:</b> Longitudinal seismic section showing canyon and submarine fan (section A-A' in Figure 3.11A). (Mitchum 1985)	34
<b>Figure 3.11C:</b> Transverse seismic sections in four positions of the canyon-fan system. (Mitchum 1985)	35
<b>Figure 4.1:</b> Cross-section from northeast to southwest through the four exploration wells of Carson Basin. Major formations are plotted along with unconformities picked using both lithology and biostratigraphy. Note that sonic travel time increases to the right. Lithology colours: grey = shale, orange = siltstone, yellow = sandstone, blue = limestone, purple = dolomite, and green = evaporites.	38
<b>Figure 4.2:</b> Cross-section from northeast to southwest through the four exploration wells of Carson Basin. Only unconformities are plotted for simplicity.	41
<b>Figure 4.3:</b> Synthetic seismogram calculated for the Skua well. EEU = Early Eocene Unconformity, PU = Paleocene Unconformity, CU = Cenomanian Unconformity, AU = Albian-Aptian Unconformity, TU = Tithonian Unconformity. Note the abrupt change in sonic character at the Early Eocene Unconformity.	43
<b>Figure 4.4:</b> Synthetic seismogram calculated for the Bonniton well. EEU = Early Eocene Unconformity, TU = Tithonian Unconformity. Synthetic is compared to a seismic profile in Figure 5.2.	45
<b>Figure 4.5:</b> Bonniton Depositional Environment. Note the nearshore marine environment which occurs at the Early Eocene Unconformity. (Grant et al. 1988)	46



<b>Figure 5.1:</b> Grid of seismic lines used in studying Carson Basin. The colours represent two-way travel time (“depth”) of the Early Eocene Unconformity. The horizon ranges from 800 to 6200 ms. Note the sparsity of data in the southeastern region and the irregularity of the grid as a whole. Seismic profiles used as figures are indicated, including part of Lithoprobe lines 85-4/4A which were not digitized.	48
<b>Figure 5.2:</b> Transverse seismic profile of the Bonniton Canyon (shaded green). Note the truncation of underlying seismic reflectors, onlap of canyon fill, and slight negative relief over the canyon. The Bonniton well lies to the northwest of the canyon. The green line traces the Early Eocene Unconformity. The synthetic seismogram for the Bonniton well is included, although comparison at this scale is difficult. (Line PCP81-067D)	49
<b>Figure 5.3:</b> Longitudinal seismic section down the Bonniton Canyon. Truncation of underlying reflectors and downlap of canyon fill is observed in this profile. The green line traces the Early Eocene Unconformity, which is also the canyon base. Note that the canyon erosion extends across the entire seismic profile. The reflectors between shotpoints 400-550 that appear to cross the erosional surface are multiples. (Line PCP81-065)	50
<b>Figure 5.4:</b> Early Eocene Unconformity Time-Structure contour map. Both the Bonniton and St. George canyons traverse an interpreted paleocontinental shelfbreak. Note the large knoll or outlier between the outlets of the two canyons.	52
<b>Figure 5.5:</b> Shaded relief map of Early Eocene Unconformity surface. The diagram is illuminated from 305 degrees, with 260 colours used for the 5200 ms of relief.	53
<b>Figure 5.6:</b> Longitudinal seismic profile of the St. George Canyon. The Early Eocene Unconformity is shown in green, which is also the canyon base. The canyon begins near shotpoint 5000 (middle of the figure), and cuts downward to the southeast (towards the right). Truncation of underlying reflectors is evident. The erosional Cenomanian Unconformity is in blue, and is truncated by the canyon near shotpoint 5100. Note the large channel in the CU which occurs near shotpoint 4700. There is also a younger feature above the EEU, possibly a channel/levee complex. Future work in the Tertiary would be useful in this region. The profile also intersects with the St. George well to the northwest. (Line FC83-49A)	54
<b>Figure 5.7:</b> Seismic profile intersecting Skua well. Four widespread unconformities are present (from top to bottom): green = Early Eocene Unconformity, red = Paleocene Unconformity, blue = Cenomanian Unconformity, brown = Albian-Aptian Unconformity. (Line CGB82-115)	56
<b>Figure 5.8:</b> Submarine fan seismic profile. Major features include a hummocky surface, mounded shape, lateral pinchouts, and downlapping of internal reflectors onto the basin floor. Note the region of little to no reflection at the base of the mound, suggesting chaotic sedimentation. The green line traces the Early Eocene Unconformity and basinal correlative conformity. (Line 6161-83)	59

- Figure 5.9:** Grid of seismic lines used in studying Carson Basin. The colours represent two-way travel time “thickness” of the submarine fans. The thickness ranges from 0 to 450 ms. Note the lack of seismic control in the fan region. 60
- Figure 5.10:** Contour map of fan thickness, measured in time. Contours more than 10 minutes of latitude or longitude from an interpreted seismic line are omitted. 61
- Figure 5.11:** Lithoprobe line which travels from the southern Jeanne d’Arc Basin (top left) to the deep water extent of the Carson Basin (bottom right) and captures all of the major features studied in this thesis. Separating the Jeanne d’Arc Basin from the Carson Basin is a wide basement high, where sedimentary cover is thin. To the southeast of this high is the Bonniton Canyon. The Early Eocene Unconformity surface that is traced across the basin (green line) is pierced by salt in the bottom part of the line. Further to the southeast is a complete submarine fan. (Lithoprobe Lines 85-4, 85-4A. The bottom 10 seconds of data have been truncated for the purposes of the figure.) 62
- Figure 5.12:** Fan thickness contours (in time) overlain on the Early Eocene Unconformity shaded relief map. The two areas of greatest thickness correspond to the canyon outlets, supporting the interpretation of the packages as submarine fans. 64
- Figure 5.13:** Seismic profile showing pinchout of a submarine fan against a basement or salt-influenced high. The green line traces the Early Eocene Unconformity and basal correlative conformity. (Line 6132-83) 65
- Figure 5.14:** Seismic profile showing five major packages above the Early Eocene Unconformity. The overlapping canyon fill (green) highlights an erosional remnant. The canyon fill is overlain by a progradational package (red). Rise in relative sealevel resulted in a package (blue) that overlaps the canyon fill and progradational package. Oligocene/Miocene delta progradation (yellow) steps out over much of the section, and is overlain by deep water pelagic sedimentation which continues today. (Line 6130-83) 67
- Figure 6.1:** Basemap showing Eocene and Paleocene erosional and depositional features of the Jeanne d’Arc and Carson Basins. Note the prograding complex just west of the Bonniton and St. George canyons. Dashed progradational area and Carson Basin wells added outside boundary of original figure. Boxes outline locations of 3-D surveys in Jeanne d’Arc Basin. (Modified from Deptuck 1998). 70

## TABLE OF TABLES

<b>Table 2.1:</b> Table of wells in Carson Basin and data used from GSC-Atlantic Basin Database. AU = sonic log, DEN = density log, GR = gamma-ray log. Refer to Appendix 1 for well histories, and Appendix 2 for Lithostratigraphy and Biostratigraphy picks used.	8
<b>Table 3.1:</b> Summary of Seismic Recognition Criteria for Submarine Fans. (after Mitchum 1985, and Posamentier and Erskine 1991)	36
<b>Table 4.1:</b> Unconformities and gaps in the Skua and Bonniton Wells. The Skua well shows all five of the unconformities observed in the basin, and the Bonniton well shows only two. (All data from Basin Database; see Appendix 2 for complete summary.)	40

## ACKNOWLEDGEMENTS

This honours thesis could not have been accomplished without the constant input, support, and guidance of a host of helpful souls. Thanks go to Phil Moir for inviting me to conduct a research project at the Atlantic Geoscience Center, and for allowing me free rein with both equipment and data. Arthur Jackson, resident computer guru at AGC, deserves thanks for constant assistance with equipment and extraction of data from the massively complicated (to me at least) database. I also wish to thank Nancy Morash, Saint Mary's co-op student, for helping me sort through 30 years of paper seismic profiles. Andrew MacRae's handy new computer script for extracting lithology and well logs from the Basin Database saved me at least two weeks of work, and definitely a few computer-induced headaches. The comments and suggestions of Al Grant on my final draft were of immense value. Also at AGC, I wish to thank my supervisor John Shimeld for putting up with constant interruptions of his work, and for recognizing that an honours project is a wonderful opportunity to learn many new skills. Thanks for your encouragement, time, and lively debates.

At Dalhousie University, Mark Deptuck has earned my gratitude for his eternal enthusiasm and for the initial inspiration of my work. Mark never failed to get excited about any new development, and is an endless font of ideas. I am also very grateful to Dr. Martin Gibling for the large role he played in my work; his gentle prodding helped a rookie researcher cover as many angles as possible. Additionally, his critical and detailed readings raised the level of my writing. Most importantly, I wish to recognize Martin's positive influence throughout my undergraduate studies, as he constantly challenged my abilities and encouraged my growth as an earth scientist.

And finally, I would be remiss if I did not mention those who have supported me from the beginning. Without my girlfriend and life partner Taryn, I would never have survived the past five years of university. Thank you for continuing to share in my life with all of its ups and downs. My parents, Dianne and Gordon, cannot be thanked enough for instilling in me a strong work ethic and the desire to always do better. And finally, I thank my grandmother, Helen, for showing me that learning is a life long process.

## **1.0 INTRODUCTION**

### **1.1 General Statement**

The Carson Basin is located on the Grand Banks, offshore Newfoundland, Canada (Figure 1.1). The Carson Basin straddles the present day shelf-break, with water depths ranging from 50 to more than 2000 m. The basin lies to the southeast of the more intensely studied and developed Jeanne d' Arc Basin (Figure 1.2), which contains the Hibernia oil-field and production platform along with other developing fields. Industry and scientific activity in the Carson Basin has been minimal in recent years. Consequently, the hydrocarbon potential of the Carson Basin is still unknown.

Interest has grown in submarine canyons and fans in recent years because they have been recognized as a new hydrocarbon play. Canyons and fans have been recognized in the Jeanne d' Arc Basin, where the scientific community and industry have focused heavily as a result of its large, proven reserves. The Hibernia Canyon has been imaged by an industry 3-D survey, and also has been penetrated by a well, allowing detailed study (Boyd 1997, Friis 1997, Deptuck 1998, Shimeld et al. in prep.). In addition, many other canyons in the Jeanne d' Arc Basin have been recognized and mapped (Deptuck 1998). Seismic coverage in the Carson Basin is much more limited; nevertheless, a number of canyon features have been noted and mapped in this study. These features have a wide range of implications: Was the region subaerially exposed? Is there evidence of terrestrial deposition? What tectonic or eustatic regimes are related to canyon erosion? Do major stratigraphic units and unconformities of the Jeanne d' Arc Basin correlate with those of the Carson Basin? Do the basins have similar or different evolutions? What do these differences reflect? Are canyon fills and basinward lobes potential traps or reservoirs? Although not all these issues can be explored here, this study raises new evidence and serves as a building block for future research in the region.



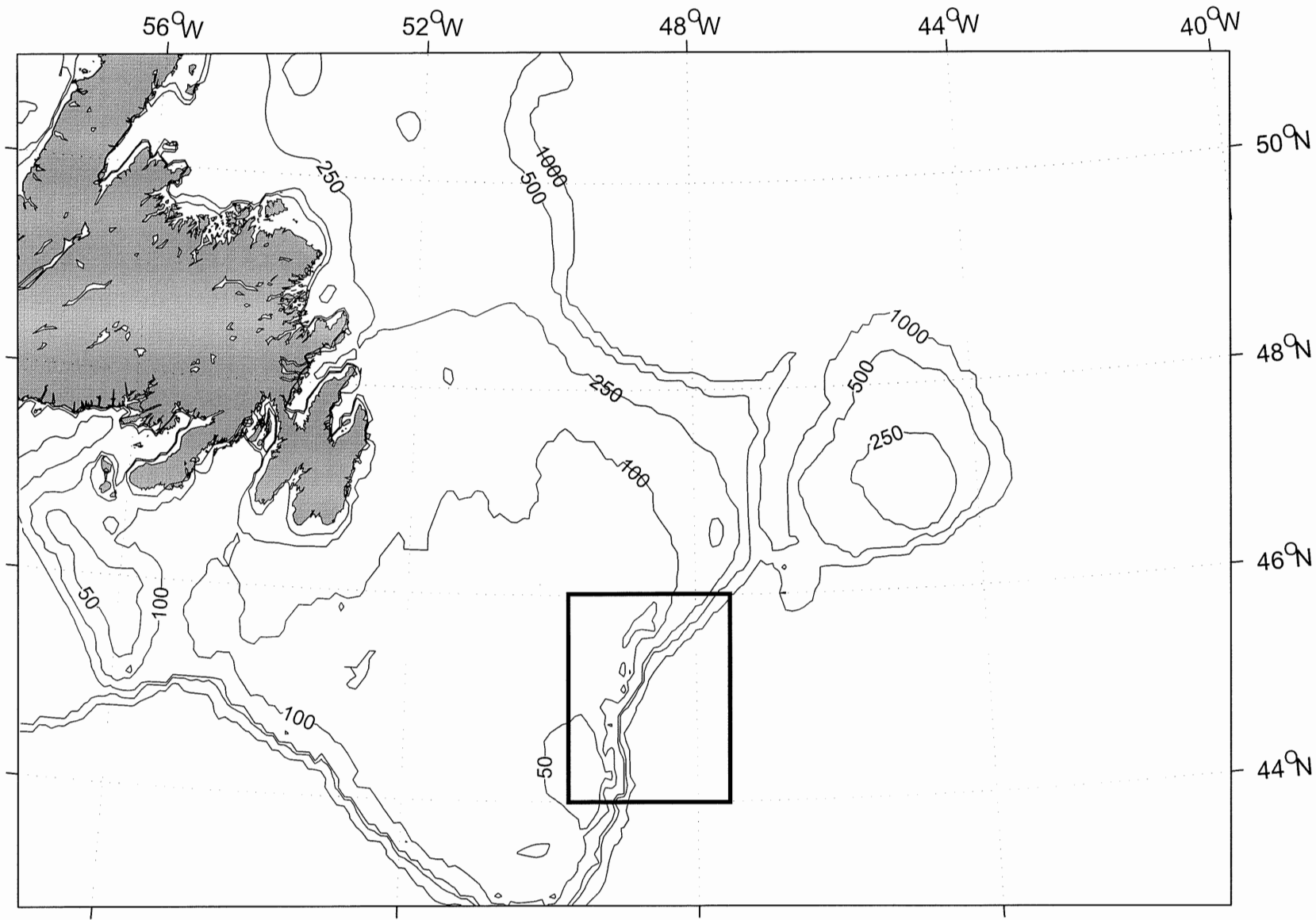


**Figure 1.1:** Map showing bathymetry and general location of study area, Grand Banks, Newfoundland, Canada. The boxed area includes much of the southern Jeanne d'Arc Basin along with the Carson Basin.

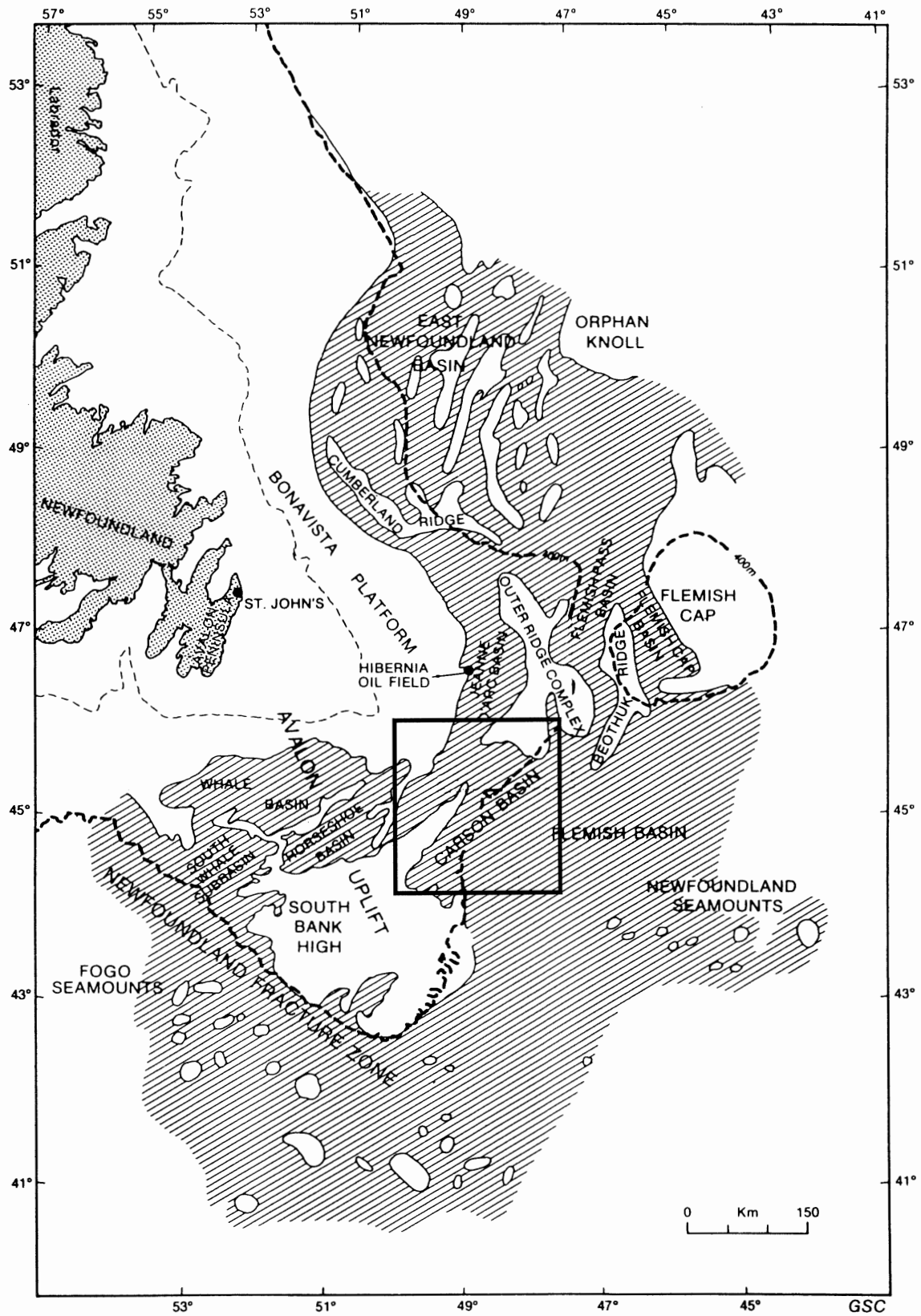


**Figure 1.2:** Schematic map of the major rift basins of the Grand Banks. The Carson Basin and southern Jeanne d'Arc Basin are included in the noted study area. (Grant and McAlpine 1990)

Recommendations for future work are included in the final section.

Study of the Carson Basin relies primarily on reflection seismic profiles collected by the petroleum industry from 1968 to 1985. In addition, four wells are present in the basin: the Bonniton, Skua, and Osprey wells were drilled in the early 1970's, whereas the fourth (St. George) was drilled in 1986 (see Appendix 1). All four wells were drilled in less than 105 m of water (Figure 1.3) because of economic and technological limitations. None of the wells encountered significant shows of hydrocarbons, and all were subsequently abandoned. The majority of the Carson Basin remains untested as a result of the drilling limitations.

### **1.2 Objectives and Scope of Project**

The primary focus of this project is the recognition, mapping, and temporal constraintment of erosional canyon features in the northern part of the Carson Basin. Basinward depositional lobes related to canyon excavation were also studied. To better understand the environment and time of deposition, the major seismic reflectors are related to the exploration wells using synthetic seismograms, yielding lithologic and biostratigraphic control of the seismic profiles. Finally, this research is related to previous canyon studies in the Jeanne d'Arc area with the aim of evaluating interaction between the basins.

### **1.3 Organization of Thesis**

Chapter Two outlines the methods applied and the data available for this study. Chapter Three offers a brief history of the formation of the Grand Banks rift basins, and also provides an introduction to submarine canyons and fans. Chapter Four examines the four wells present in the Carson Basin. Chapter Five presents the submarine canyons and fans of Carson Basin, and discusses the timing of their formation. Chapter Six relates the studied features to previous work in the Jeanne

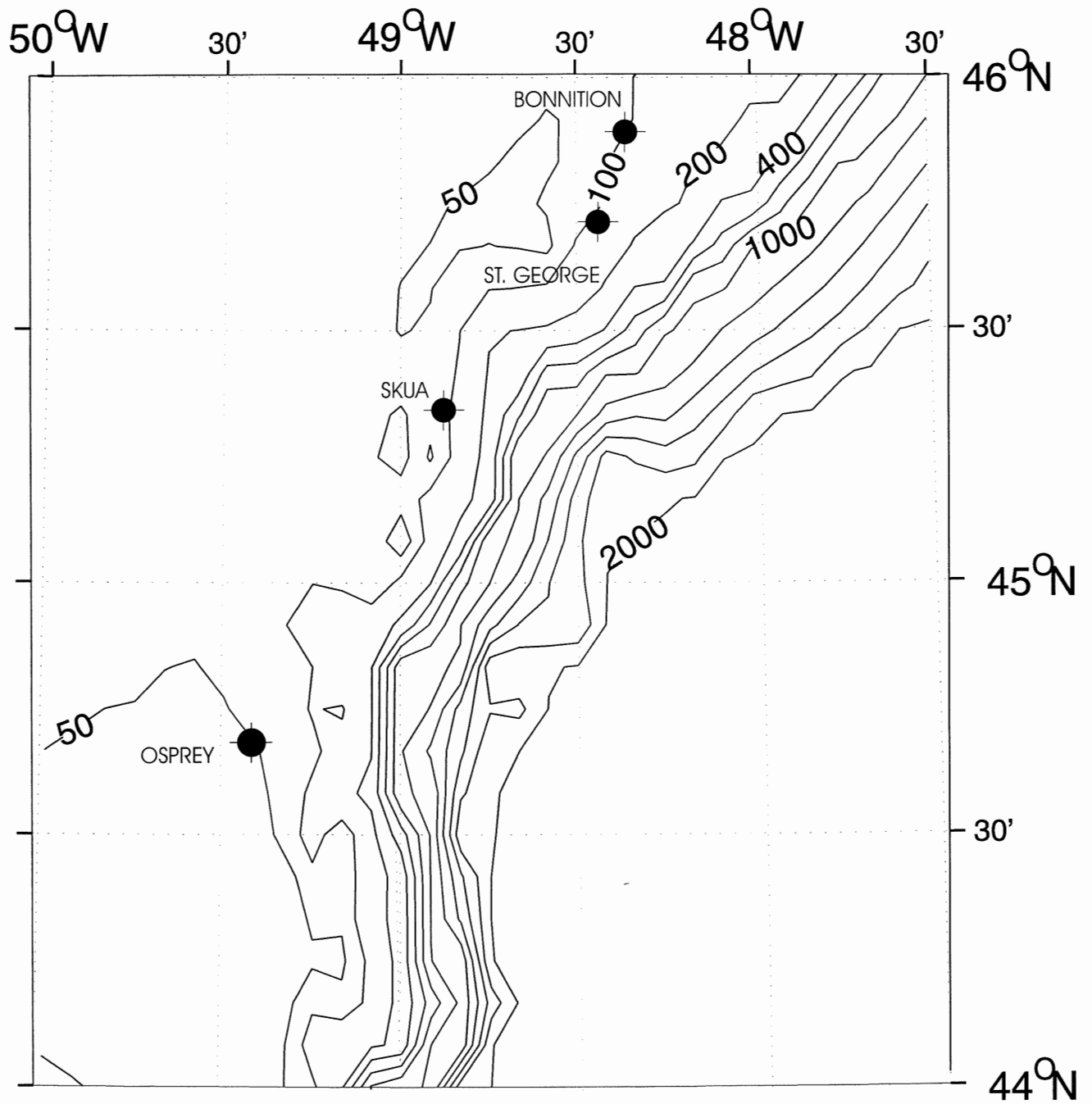


**Figure 1.3:** Location map of the four Carson Basin wells, along with the present day bathymetry. Note that each well has been drilled in less than 105 m of water. The bulk of Carson Basin extends to the east of these wells in much deeper water.

d'Arc Basin, and concludes with implications and recommendations for future work.

A large amount of summary information is contained in the appendices, and they are referred to throughout the text. Many figures in the thesis involve seismic profiles interpreted with the aid of colour. Appendix Five contains black and white versions of these profiles to facilitate photocopying of such figures, and also to provide the opportunity for the reader to view profiles unbiased by interpretation. Other colour figures that would be difficult to photocopy are also included in grayscale.



## **2.0 DATA AND METHODS**

### **2.1 Introduction**

This study relied on industry reflection seismic and four deep exploration wells. The vast majority of reflection seismic was shot over the Carson Basin prior to 1985 and is in the public domain, with seismic sections available from the Canada-Newfoundland Offshore Petroleum Board (CNOPB). Research prior to 1988 in the Carson Basin did not use data from the St. George J-55 well drilled in 1986, as well data are proprietary for two years. Research in the last ten years has focused primarily on the Jeanne d' Arc Basin, leaving the St. George well relatively under-utilized. However, the only available biostratigraphic analysis for St. George is from the company that drilled the well, and the resolution and quality of the biostratigraphic work was geared towards reconnaissance-scale exploration.

### **2.2 Well Data**

The four wells drilled in the Carson Basin are presented in Table 2.1., which summarizes the year drilled, company, and total depth reached. The table also summarizes the well logs used in conjunction with the seismic data, and the authors of the lithostratigraphic and biostratigraphic picks used in this study. The on-line GSC-Atlantic Basin Database was the primary source for all well data, including digitized well logs. Appendix 2 lists the lithostratigraphic and biostratigraphic picks used for each well. CanStrat logs are the source for lithology and grain size information contained in the database. These logs are constructed based on cuttings brought to the surface during drilling, resulting in a vertical resolution of 1 m under ideal conditions. However, drilling complications such as borehole caving and lost mud circulation can lead to depth errors of tens of meters (Shimeld, pers. comm. 1999). Cuttings are less precise than cores, however no cores were obtained from any of the

<b>Wells</b>	<b>Year</b>	<b>Company</b>	<b>Total Depth</b>	<b>Logs Used</b>	<b>Lithostratigraphy</b>	<b>Biostratigraphy</b>
<b>Osprey G-84</b>	1973	Amoco- Imperial- Skelly	3473.8 m	AU, DEN, GR	CNOPB (1990), McAlpine (1988)	Doevan (1980), Bujak and Williams (1979)
<b>Bonniton H-32</b>	1973	Mobil-Gulf	3048.0 m	AU, DEN, GR	CNOPB (1990), McAlpine (1988)	Ascoli (1988)
<b>Skua E-41</b>	1974	Amoco- Imperial- Skelly	3238.8 m	AU, DEN, GR	CNOPB (1990), McAlpine (1988)	Robertson Research (1982), Bujak 1979
<b>St. George J-55</b>	1986	Canterra-PCI	4100.2 m	AU, DEN, GR	CNOPB (1990), McAlpine (1988)	Canterra Energy (1986)

**Table 2.1:** Table of wells in Carson Basin and data used from GSC-Atlantic Basin Database.

AU = sonic log, DEN = density log, GR = gamma-ray log.

Refer to Appendix 1 for well histories, and Appendix 2 for Lithostratigraphy and Biostratigraphy picks used.

wells.

### **2.3 Cross-Section Construction**

The lithologic cross-section as shown in Figure 4.1 was created using information contained in the Basin Database. A program created by Andrew MacRae of GSC-Atlantic allowed extraction of lithology and grain-size information, along with well log curves. Using CorelDraw 8, these graphics files were then compiled at the same scale to build lithologic columns for the wells. The columns were correlated and annotated using the lithostratigraphic picks of McAlpine (1988) and the CNOBP (1990). The sonic and gamma-ray logs were plotted alongside the lithologies to allow fine-tuning of the correlations. Figure 4.1 is a structural cross-section, showing the relation of formations as they exist today.

### **2.4 Synthetic Seismograms**

Unix-based computer workstations using Landmark software were used to generate synthetic seismograms. Landmark's OpenWorks is the primary software which stores and organizes data, and through it many different modules or tools can be used. OpenWorks stores both seismic and well data, although in this study only well data were available in digital format. Syntool is one of the modules, and it converts digital sonic and density logs to synthetic seismograms. Well curve data from each well were formatted for use by Syntool and entered into OpenWorks from the GSC-Atlantic database. The resultant acoustic velocity profile for each well allows a correlation between the depth and the time in seconds it would take a seismic wave to travel through the formations. Where velocities or densities change abruptly, reflections can be predicted to occur, and Syntool creates a synthetic seismic trace plotting these reflections. The impedance contrasts allow the synthetic seismograms to be correlated with seismic profiles that intercept the location of the four

wells. The major reflections on the seismic sections were then correlated to formations, lithologies, and unconformities from the well data. Figure 4.4 shows an example of a synthetic seismogram for the Bonniton well. Appendix 3 contains all synthetics generated for the project and lists the intersecting seismic sections; many synthetics were plotted at different scales to match seismic sections from different programs.

Difficulties were encountered with all of the synthetic seismograms. The reflections of the Bonniton synthetic seismogram were consistently offset by 100 milliseconds when compared with intersecting seismic profiles. Similarly, the Skua synthetic reflections were offset by 50 milliseconds. The discrepancy is caused by the lack of sonic log readings in the top interval of the wells. The acoustic velocities for this interval must be estimated, and are often incorrect. To compensate, a bulk shift of -100 ms was applied to the Bonniton synthetic seismogram, while -50 ms was applied to the Skua well. The shifted synthetic reflections compare much better to the seismic profiles.

## **2.5 Seismic Data**

Appendix 4 summarizes the seismic programs and sections that were used in this study. The data range in age from 1979 to 1985, although older data are available for the Carson Basin. Older data were used for reconnaissance throughout the basin, however only the lines in Appendix 4 were studied in any detail.

Where seismic lines intersect, common horizons or reflectors should logically coincide. However, this is not always the case, and different times (or depths) may be obtained from horizons which occur in the same geographic location. These differences between profiles are known as “misties”. Misties between seismic data of different vintages are the result of errors in navigation data, different processing techniques, noise in the data, digitization errors, and other factors. Misties

are inevitable when using data from numerous programs; efforts were made during the digitization process (discussed in section 2.6 below) to minimize this problem.

Many seismic lines had been previously interpreted at the GSC-Atlantic for the construction of regional maps; however, only three to five major horizons were mapped. More detailed interpretation was conducted for this study, focusing primarily on erosional canyon features in the northern end of the Carson Basin. Paper sections were used exclusively, and interpretation was done by hand.

## **2.6 Mapping Procedures**

Interpreted horizons were entered into Landmark's SeisWorks 2-D by hand-digitizing each paper section. The raw data and seismic grids are shown in Figures 5.1 and 5.9. The Mistie Module of SeisWorks was then run in order to correct errors using a variable shift. Variable shifts move the horizon up or down as needed to "tie" or agree at seismic line intersections. The amount of shift to apply was determined using a standard deviation weighting function. The shift amount is divided in proportion to the standard deviation of the misties for each line. Therefore, the more variance in misties that occurs along a line, the more shift applied to the horizon pick on that line. Hence, the most reliable lines are moved the least, keeping overall adjustment to the horizon to a minimum. Figure 2.1 shows an example of the procedure. Time restrictions prevented a more detailed mistie analysis.

The resultant x,y,z data (location with depth in milliseconds) were then plotted using Generic Mapping Tools (GMT), a public domain gridding and contouring package. The erosional surface data were gridded using a Delauney Triangulation method and contoured. The triangulation gridding used to construct the map shows strongly in regions of sparse data (note the triangular shaped



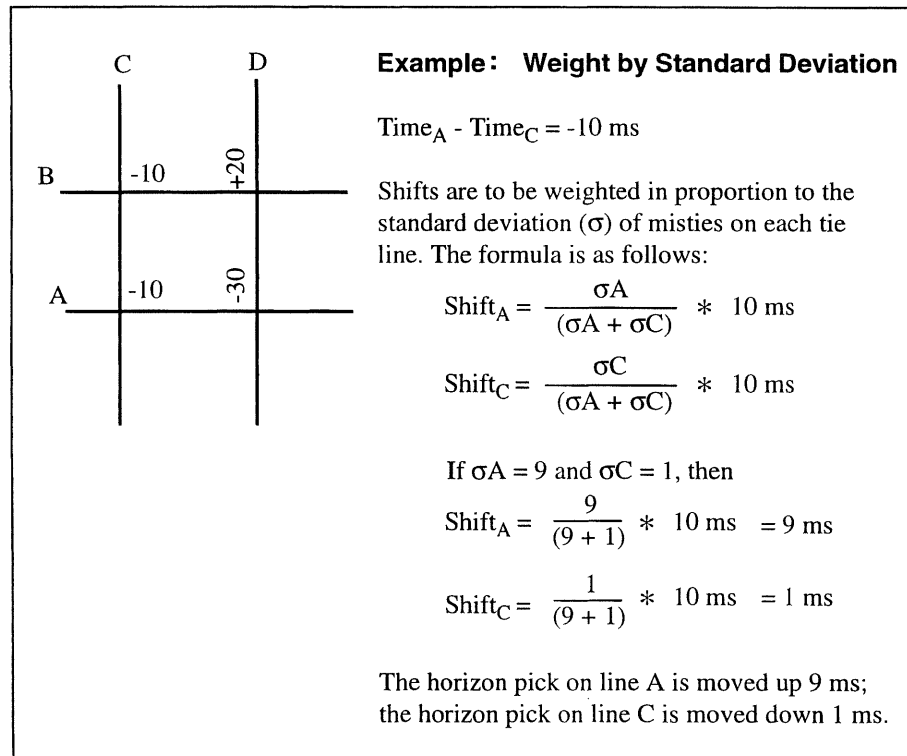


**Figure 2.1:** Example of “Weight by Standard Deviation” operation to correct for 2-D seismic misties. (Landmark 1996)

contours in the southeast of Figure 5.4), however it is a robust method which produces excellent results in densely sampled areas, and technically acceptable results in sparsely sampled areas.

A shaded relief map was also constructed for the erosional surface (Figure 5.5). The image is illuminated from an angle of 305 degrees, and the 5200 milliseconds (ms) of relief are categorized using 260 colours, resulting in one displayed shade per 20 ms of relief.

A time-thickness map was also constructed for basinward submarine fans (Figure 5.10). The submarine fan thickness data were gridded and contoured using a Surface operation with a tension factor of 0, giving a minimum curvature solution. Tension factors greater than 0 tended to create maximums higher than the control points. Such maximums were avoided in order to keep the thickness of the fans within the range bounded by the digitized data. Additionally, any grid point or contour more distant than 10 minutes of latitude or longitude from a digitized (“true”) data point was clipped. The clipping operation was added because of the sparsity of the seismic data in the fan region.

### **3.0 BACKGROUND GEOLOGY**

#### **3.1 Formation and Filling of Grand Banks Rift Basins**

The Grand Banks of Newfoundland are underlain by a series of interconnected, fault-bounded sedimentary basins which formed during the Mesozoic (Figure 3.1) (Grant and McAlpine 1990). These basins formed in response to the opening of the North Atlantic Ocean in a complex series of rifting events (Welsink et al. 1989).

Paleozoic and Precambrian rocks of the Appalachian Orogen compose the basement of the Grand Banks (Williams 1979). These basement rocks are a product of terrane accretion and deformation during the Taconian (Middle Ordovician), Acadian (Devonian), and Alleghanian (Permo-Carboniferous) orogenies (Williams 1984). The architecture of the terranes and crustal lineaments subsequently influenced the distribution and form of the Mesozoic rift basins (Tankard and Welsink 1989).

The continental margin around Newfoundland has been influenced by at least two sea floor spreading episodes. The first episode occurred from the Late Triassic to the Early Jurassic. This period of spreading relates to rifting between North America and Africa, and is characterized by deposition of red beds, evaporites, and carbonates which overlie pre-Mesozoic basement (Grant and McAlpine 1990). These sediments are initially continental, but gradually change to reflect deposition in a marine environment as a result of flooding from the Tethys Sea. The evaporites and salt deposits of the Osprey and Argo Formations suggest restricted basins in an arid climate. This first episode of rifting was aborted north of the Newfoundland Fracture Zone, a transform margin located along the southwest edge of the Grand Banks as shown in Figure 3.1 (Grant and McAlpine 1990).

As plate motion was accommodated by transform faults, shallow marine shales and

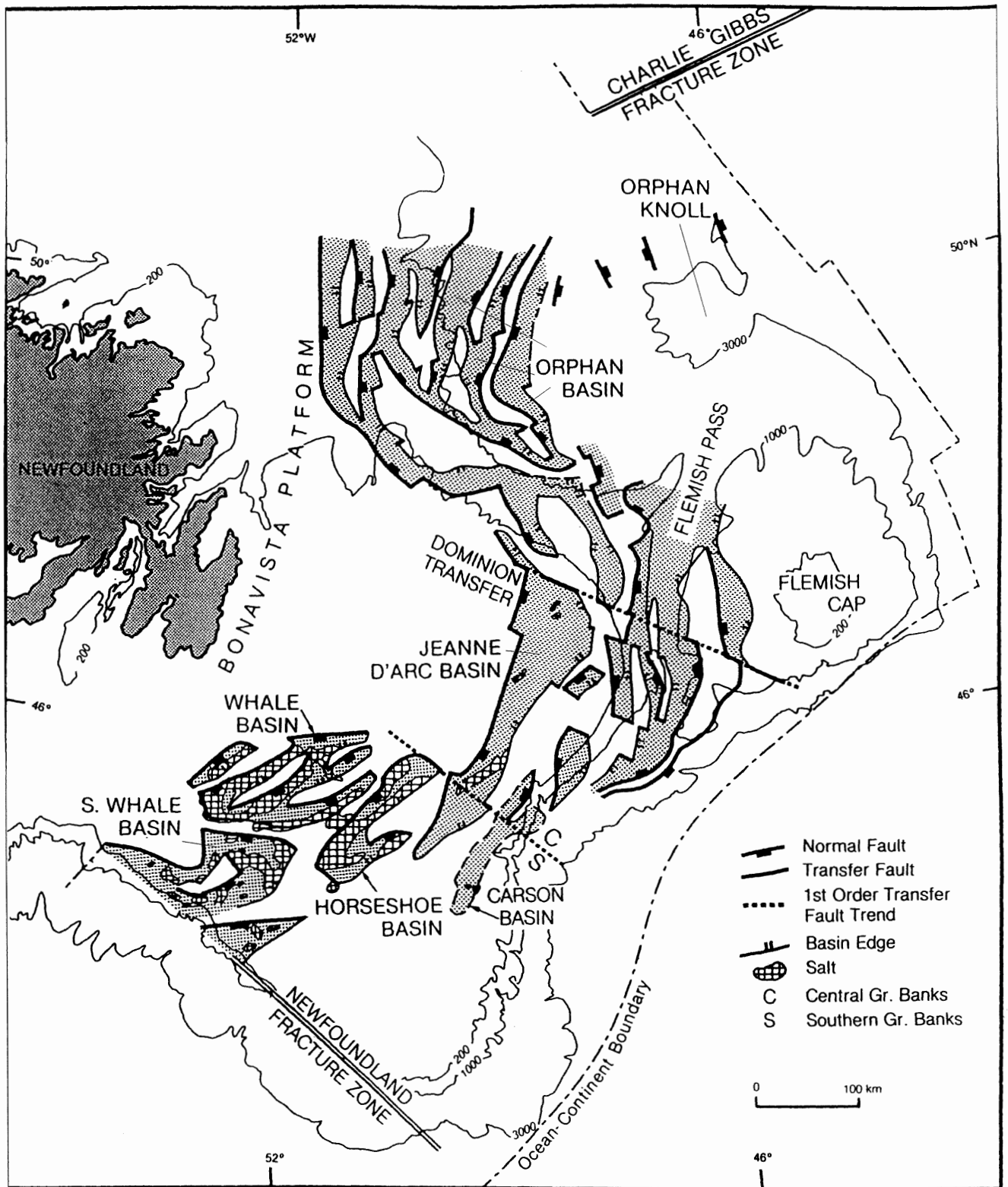


Figure 3.1: Major structural elements of the Grand Banks rift basins. (Welsink et al. 1989)

limestones were deposited during a quiescent period from Early to Late Jurassic (Grant and McAlpine 1990). An epeiric sea flooded the older, rifted topography during this quiet period (McAlpine 1990).

Renewed rifting during the Late Jurassic continued through the Neocomian (Early Cretaceous) (McAlpine and Grant 1990). The Avalon Uplift accompanied the return of rifting, and deposition of clastic sequences resulted from erosion of the uplift. Basinward subsidence rates were very high, resulting in fluvial fan and fan-delta conglomerates and coarse sandstones (McAlpine 1990). The erosion of the uplift formed a peneplain known as the Avalon Unconformity as shown in Figure 3.2 (Grant and McAlpine 1990). Source areas for basin fill material include the Avalon Uplift, the Bonavista Platform, and the Outer Ridge Complex (McAlpine 1990). This episode of rifting renewed the spread between North America and Europe, and was also influenced by opening of the Labrador Sea. The northwest-southeast trend of this opening was the second sea floor spreading regime which affected the formation of the Grand Banks Mesozoic basins (Grant and McAlpine 1990).

Basin subsidence waned by the end of the Neocomian, although slow regional subsidence continued as rifting gave way to a drifting margin during the Barremian to Cenomanian. As the Grand Banks became a passive margin setting in the Late Cretaceous to Paleocene, deposits in the Jeanne d'Arc Basin record marginal marine or continental environments (McAlpine 1990). These nearshore environments gradually changed to distal turbidites and deep water chalky limestones as sediment supply decreased and distance from the shoreline increased.

Finally, deepwater mudstones, neritic shales, and marls were deposited during the Tertiary when sediment supply was minimal (Grant and McAlpine 1990). During the Oligocene and

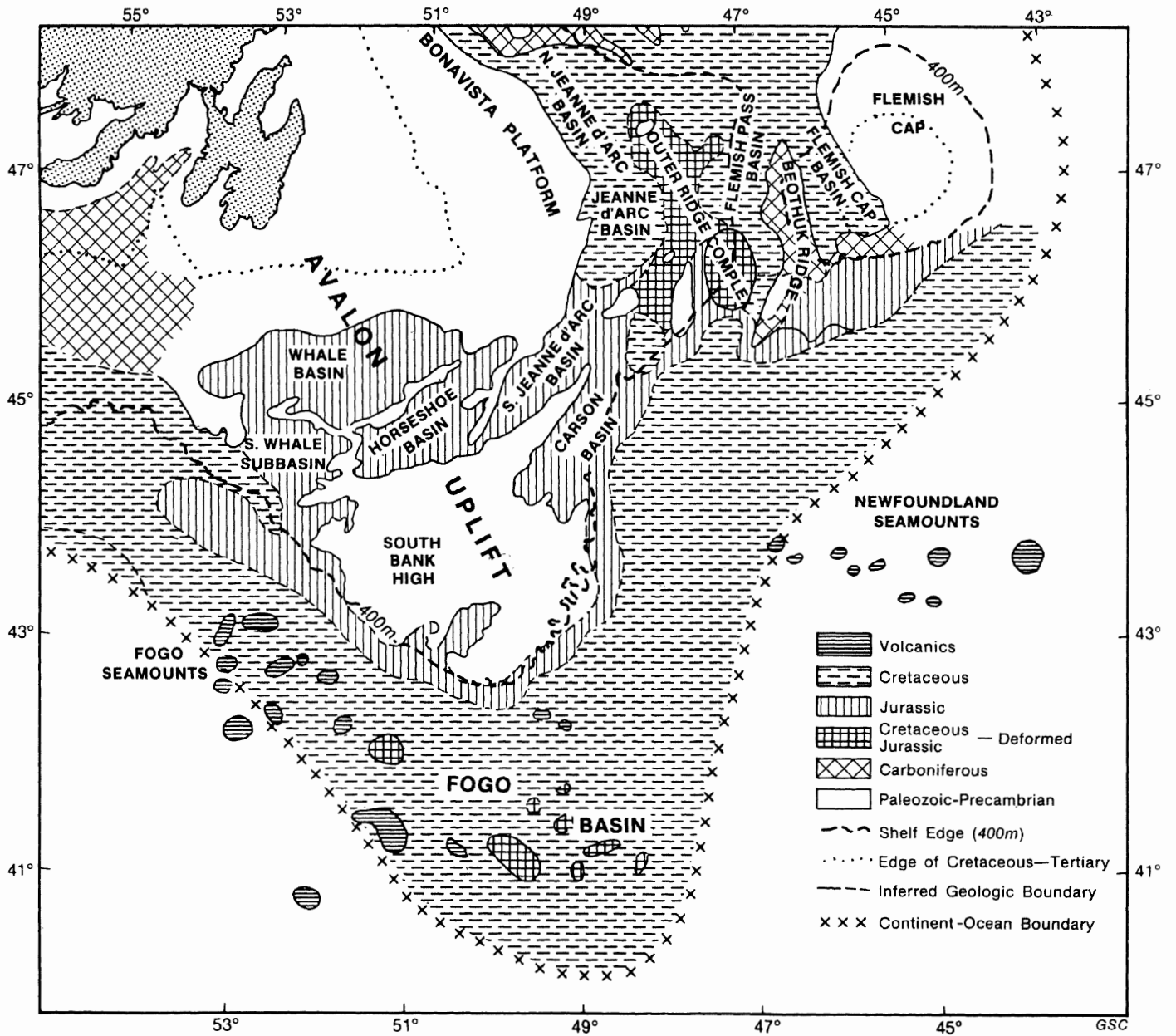


**Figure 3.2:** Generalized geology at the level of the Avalon Penneplain. Note the three primary source areas for basin fill: the Avalon Uplift (including the South Bank High), the Bonavista Platform, and the Outer Ridge Complex. (Grant and McAlpine 1990)

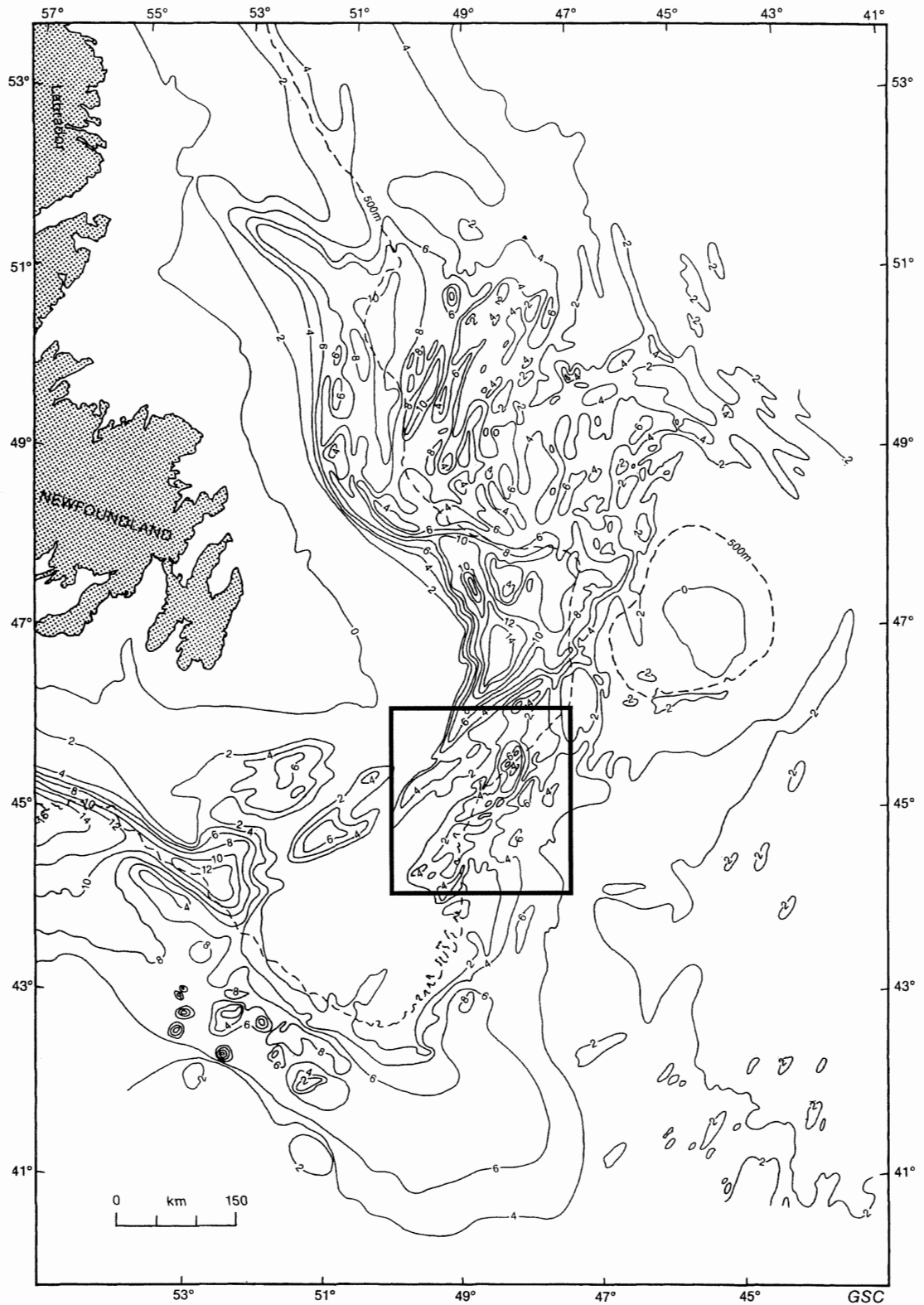
Miocene, much of the Grand Banks was subjected to much lower sealevels, which allowed sandy intervals to prograde towards the shelf edge, and may have subaerially exposed regions of the Grand Banks (Grant and McAlpine 1990). Deep neritic conditions later returned to the entire area, and this depositional period extends to the present. Figure 3.3 shows the sediment accumulations which exist offshore Newfoundland, and Figure 3.4 shows the Mesozoic and Cenozoic sediment thicknesses for the Carson Basin and the southern extent of the Jeanne d'Arc Basin. The Carson Basin is composed of several depocenters, the deepest of which may contain over 7 km of Mesozoic and Cenozoic sediments (Grant et al. 1988).

Unconformities occur in the Late Cretaceous and Tertiary. The Late Cretaceous unconformities are interpreted to correspond to the break-up between Labrador and Greenland, whereas the Tertiary unconformities have been related to the break-up between Greenland and northern Europe (McAlpine 1990). These unconformities are important in the formation of canyon features in Carson Basin, and will be discussed in the following chapter.

The history of Grand Banks basin rifting and fill has been divided into six distinct episodes as summarized in Figure 3.5. These six sequences are based on the Jeanne d'Arc as most recently defined by McAlpine (1990); however, they generally correlate to the Carson Basin (Grant et al. 1988).

### **3.2 Structure of Carson Basin**

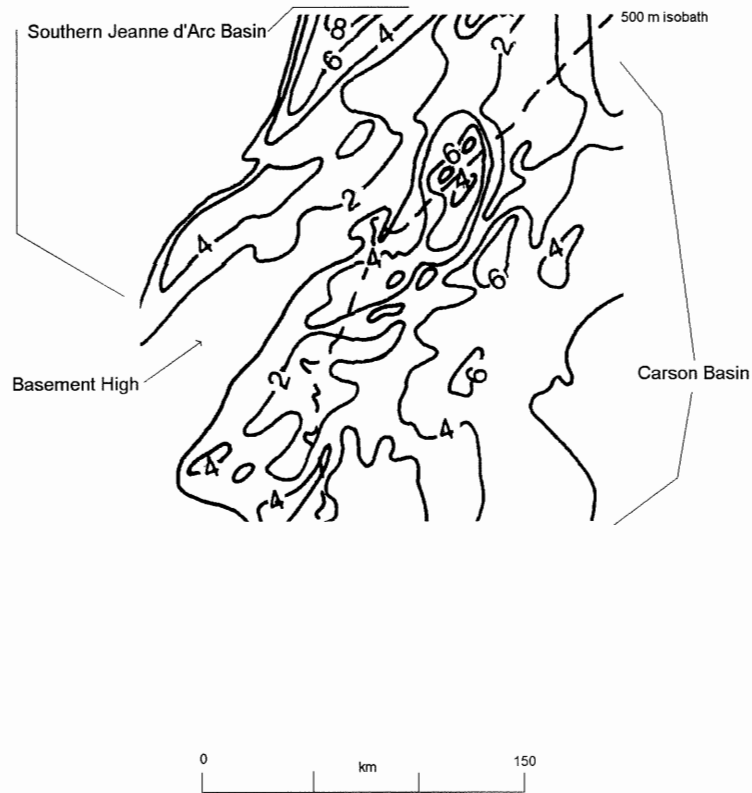
The Carson Basin is separated from the southern Jeanne d'Arc Basin to the west by a basement high. Figures 1.2 and 3.2 show that the basin terminates to the southwest against the South Bank High, and in the north the basin extends into the Outer Ridge Complex (Grant et al. 1988). A basement block ridge separates the inner and outer Carson Basins as shown in Figure 3.6. Deep



**Figure 3.3:** Map of sedimentary thickness for the Grand Banks rift basins. Thickness measured from seafloor to basement in kilometers. Note the 500 m isobath for present day water depths. (Grant and McAlpine 1990)



Figure 3.4: Map of sedimentary thickness for the Carson Basin and the southern Jeanne d'Arc Basin. Note the intervening basement high and the 500 m isobath for present day water depths. (modified from Grant and McAlpine 1990)



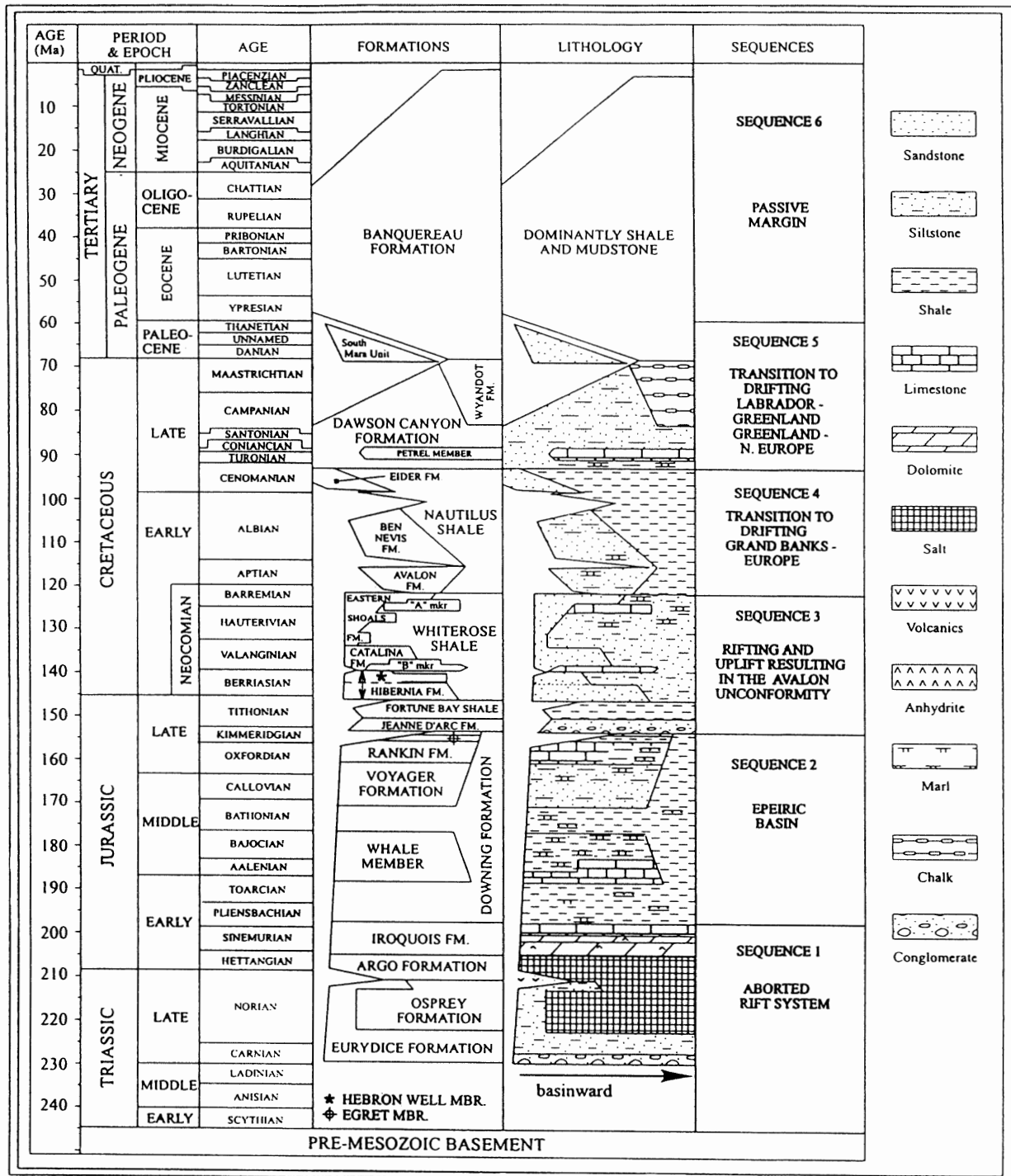
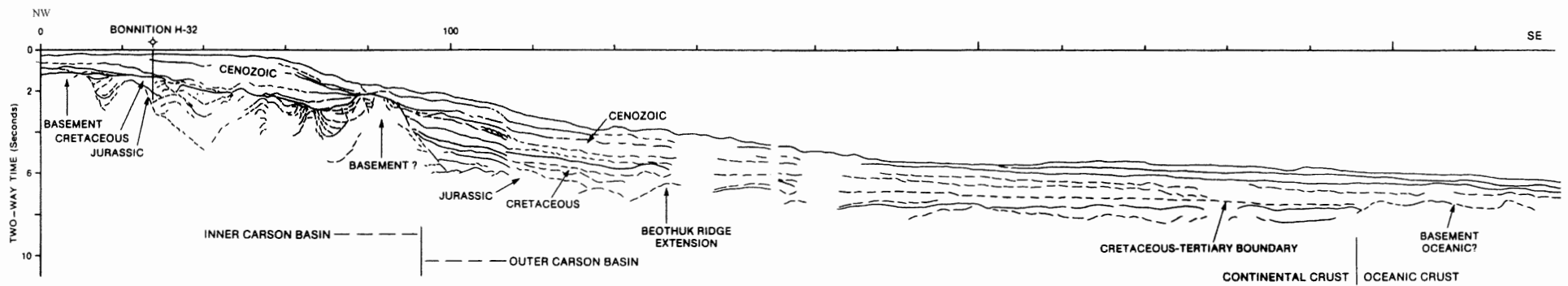


Figure 3.5: Lithostratigraphic chart for the Jeanne d'Arc Basin including the six major tectonic sequences of the continental margin. (DNAG Timescale). (Friis 1997, modified from McAlpine 1990)



**Figure 3.6:** Generalized cross-section of the Carson Basin. Note the basement high which separates the Inner and Outer Carson Basin. (Grant et al. 1988)

seismic events suggest that salt flowage may be associated with this structure (Grant et al. 1988). The outer Carson Basin extends off the shelf into deeper water.

### **3.3 Stratigraphy of Carson Basin**

Mesozoic sediments tend to occupy the structural basins of the Grand Banks, whereas Cenozoic sediments form a regional blanket over the continental margin (Grant et al. 1988). The Mesozoic and Cenozoic stratigraphy of the Jeanne d'Arc Basin has been well documented (Figure 3.5). The formation names used in the Carson Basin rely on those defined for the Jeanne d'Arc Basin, but should be considered general equivalents only. The lithologies present in the four exploration wells of Carson Basin are discussed in the following chapter.

### **3.4 Submarine Canyons and Fans**

Understanding of modern submarine canyons and fans has progressed with technology. Early studies by marine surveyors used sounding charts to detect canyon heads which created lows on the shelf break (Pratson et al. 1994). As more advanced bathymetric surveys using acoustic profiling were created, canyons were traced out to deeper water, and fans became available for study as well. Modern technologies such as side-scan sonar have allowed imaging of features to precise resolutions. The study of modern canyons and fans can yield many insights into ancient submarine systems, although many smaller scale features apparent in modern systems cannot be resolved in ancient settings using seismic data.

#### *3.4.1 Submarine Canyons*

In the broadest sense, a canyon is the available avenue of transport for coarse sediment across the outer shelf and upper slope (Mitchum 1985). Topographic lows already present, such as synclines, grabens, or reef breaks, may serve as this avenue. However, canyon systems are commonly

erosional, and truncate the strata at the canyon walls (Mitchum 1985). The formation of modern submarine canyons is a widely debated topic. A detailed, comprehensive study undertaken by Shepard and Dill (1966) of 96 canyons led them to define submarine canyons as "...valleys that have a V-shaped profile, high steep walls with rock outcrop, a winding course, and possibly numerous tributaries from both sides." The V- or U-shaped incisions eventually diminish in relief as the canyons approach the basin and the flow competence decreases (Ryan et al. 1978). The decrease in transport velocity often results in deposition of submarine fans (discussed below), although they are not always found with submarine canyons (Mitchum 1985). Presently, submarine canyons are recognized as both sinuous and linear features. For example, on the continental margin of the United States, two populations of canyons occur: a relatively few, large sinuous canyons, and a much greater number of smaller, more linear canyons (Pratson and Coakley 1996). The difference may reflect the maturity of the canyons, although there is continued debate about canyon formation mechanisms, as discussed below.

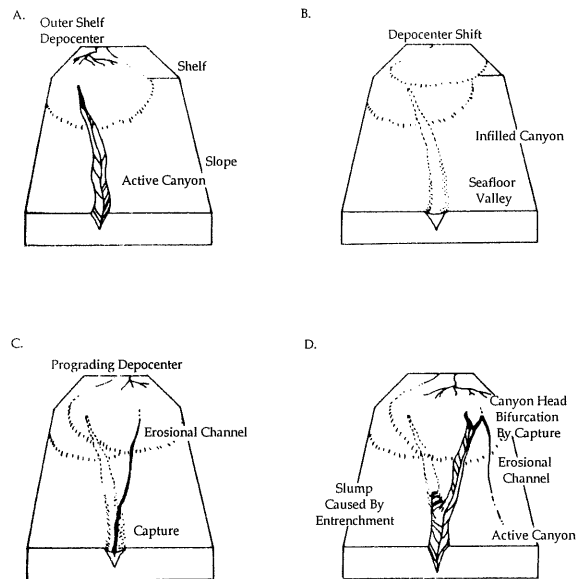
Canyons act as conduits to move sediment from river or inner-shelf environments to the shelf rise and basin floor. The size and character of the canyon are related to the margin type and underlying strata (Nelson 1984). Initially, researchers attempted to relate canyon formation to one unifying mechanism. Shepard (1981) concluded that submarine canyons are not created by a single formation mechanism, but rather are of composite origin. Contributing mechanisms of formation may include:

- 1) erosion by turbidity currents and debris flows,
- 2) submarine fault valleys later modified by marine erosion,
- 3) initial subaerial erosion, submerged and enlarged by marine processes,

- 4) slumping of oversteepened canyon walls weakened by biologic burrowing, and
- 5) flushing by tidal currents.

Evidence suggests that many large submarine canyons are the result of several stages of erosion and deposition, although reactivation of canyons may obscure previous episodes (Shepard 1981). Explanations which conclude that submarine canyons are produced during relatively short glacial lowstands are dismissed by Shepard (1981). He points out that canyons are often excavated thousands of feet into crystalline rock, which is not likely to be accomplished by a short series of turbidites, despite their erosive magnitude. Hence, submarine canyon formation is an intermittent but nevertheless ongoing process. Pratson et al. (1994) document buried submarine canyons on the New Jersey continental slope which have had their downslope portions “pirated” and exhumed by modern canyons. They contend that since lower canyon sections are not always completely buried, the older canyons create a preferential “funnel” for renewed sedimentation from the shelf-edge, as shown in Figure 3.7. This “downslope erosion model” assumes that sediment flow and erosion begins on the upper continental slope or shelf break and advances the canyon system basinward (Pratson et al. 1994). Other workers (for example, Twichell and Roberts 1982) have suggested a headward or “upslope erosion model” where canyons are eroded by retrogressive mass-wasting at the canyon head. Although this helps explain canyons that do not breach the shelf break, such canyons may be improperly categorized, as buried upslope extensions have been found for many canyons previously thought not to extend to the shelf-break (Pratson et al. 1994). However, in the case where headward eroding canyons reach the shelf-break and encounter a new sediment source, it may be difficult to distinguish whether upslope or downslope erosion was the primary formation mechanism (Pratson and Coakley 1996). Presently the downslope erosion model is in favour.

Figure 3.7: Schematic model of how existing and buried submarine canyons may interact. A) Former canyons transport upper-slope material from shelf-edge depocenters to the deep sea. B) Former canyons infill when sediment supply is diminished. C) The resumption of slope sedimentation and a shift in depocenter begin cutting new erosional channels, which in some cases are captured by seafloor troughs formed over buried canyons. D) Where repeated sediment flows occur, erosional channels mature into canyons that eventually reopen and deepen the underlying buried canyons. (Pratson et al. 1994)



C) The resumption of slope sedimentation and a shift in depocenter begin cutting new erosional channels, which in some cases are captured by seafloor troughs formed over buried canyons. D) Where repeated sediment flows occur, erosional channels mature into canyons that eventually reopen and deepen the underlying buried canyons. (Pratson et al. 1994)

When submarine canyons are being actively excavated, they are repeatedly flushed by sediment gravity flows and are therefore a zone of sediment bypass (Posamentier and Erskine 1991). Coarse-grained sediments are transported through the canyon system and are deposited basinward (see section 3.4.2 below). Canyon cutting ceases when the system achieves equilibrium through retrogressive slumps, and when the energy level of flows decreases (Posamentier and Erskine 1991). The energy level may decrease because of decreased sediment supply, renewed sea-level rise, or tectonic influence. As the energy level decreases, the amount of material passing through the system decreases, along with the grain size of the sediments. Sediments carried from the shelf source or from the over-steepened canyon wall no longer pass through the entire system, and sediment deposition gradually begins to backstep into the canyon (Posamentier and Erskine 1991). The canyon eventually fills with slump deposits, fine-grained flows, and even finer grained hemipelagic sediments that are able to collect in the new lower energy environment (Posamentier and Erskine 1991). The site of deposition moves landward as sea-level stabilizes at low-stand and begins to rise. Final filling of the canyon may occur when prograding complexes of deltaic sandstones reach the top of the canyon fill (Posamentier and Erskine 1991). Canyon fill is generally thought to have little or no hydrocarbon exploration potential as a reservoir unit; however, work by Boyd (1997) suggested the upper reaches of the Hibernia Canyon in the Jeanne d'Arc Basin contain as much as 60 % sandstone. Potential also exists where reservoir rocks have been truncated by the canyon incision and are overlain by fine-grained canyon fill (Posamentier and Erksine 1991).

Recognition of canyons on seismic profiles relies primarily on the V- or U-shaped erosional notch, and truncation of underlying seismic reflectors as shown in Figure 3.8. As noted above, the V-shape diminishes in relief basinward of the canyon head, and the canyon often widens. Erosional



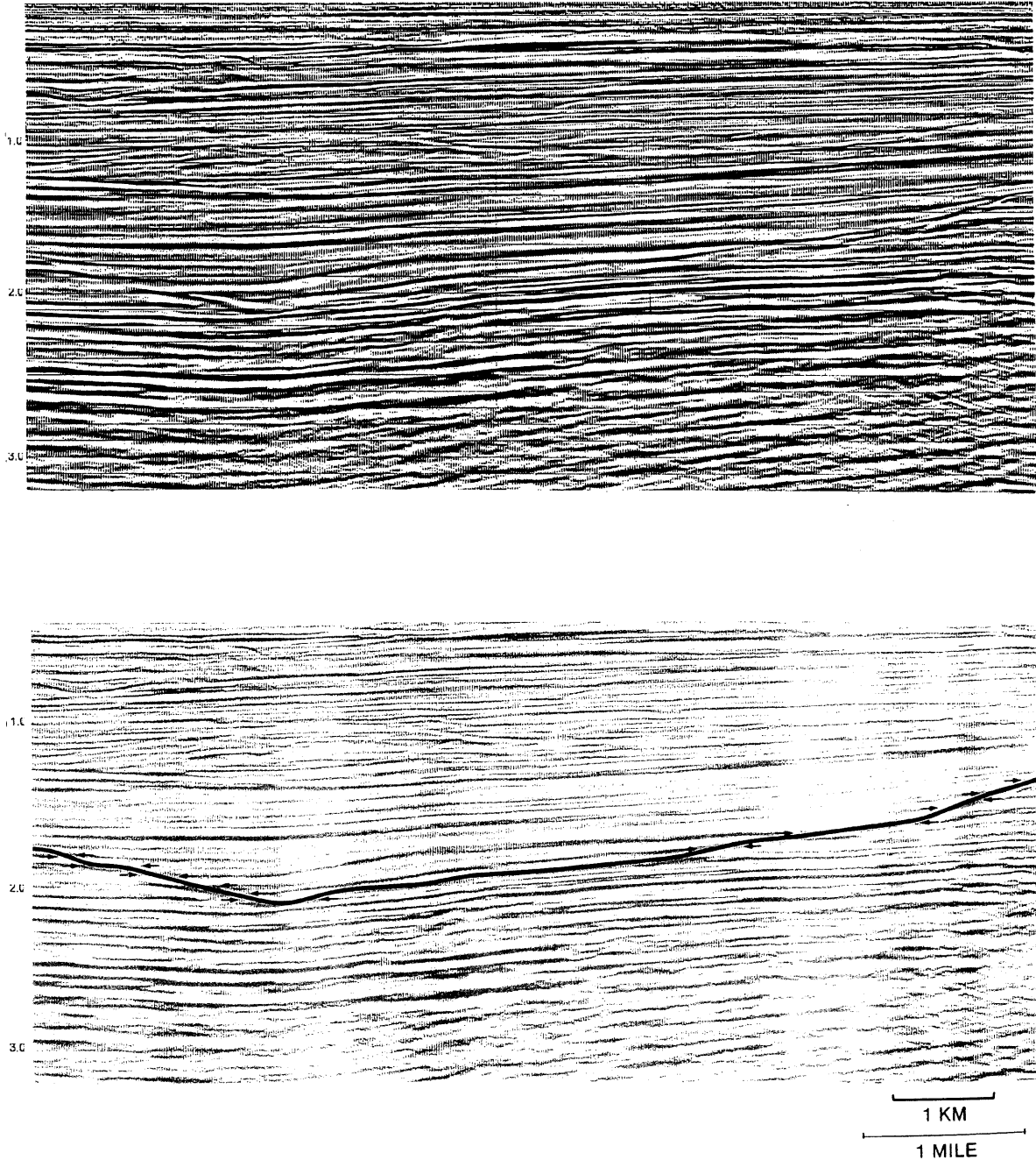


**Figure 3.8:** Submarine canyon, offshore Australia. Top: uninterpreted, bottom: interpreted. The broad, V-shaped canyon shows truncation of the underlying reflectors. Note that within the canyon, the fill overlies the truncation surface. (Posamentier and Erskine 1991)

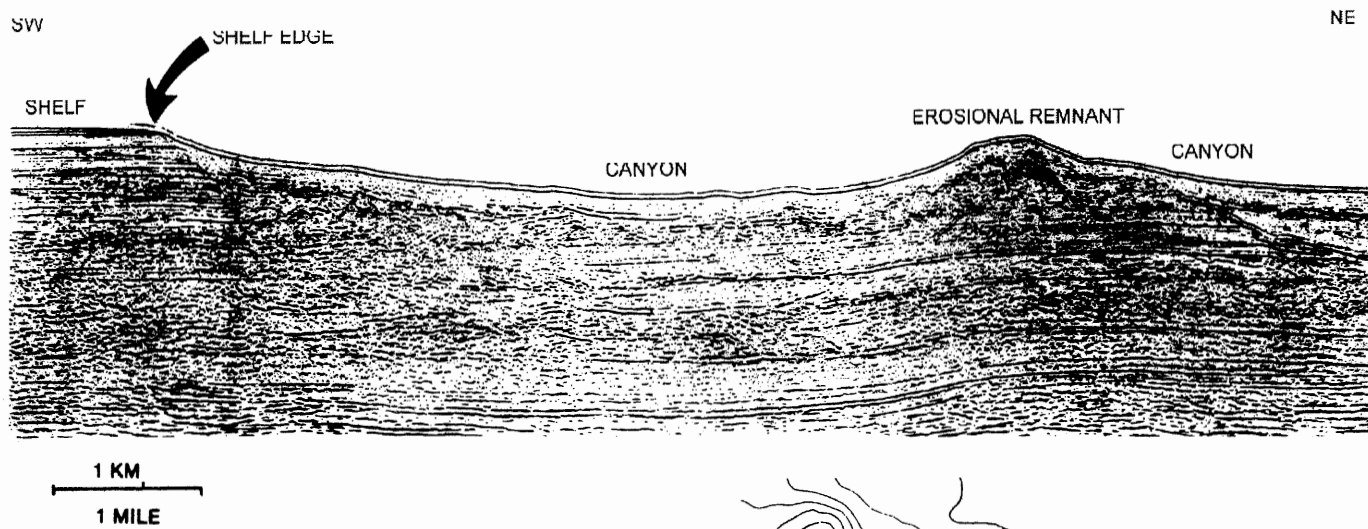
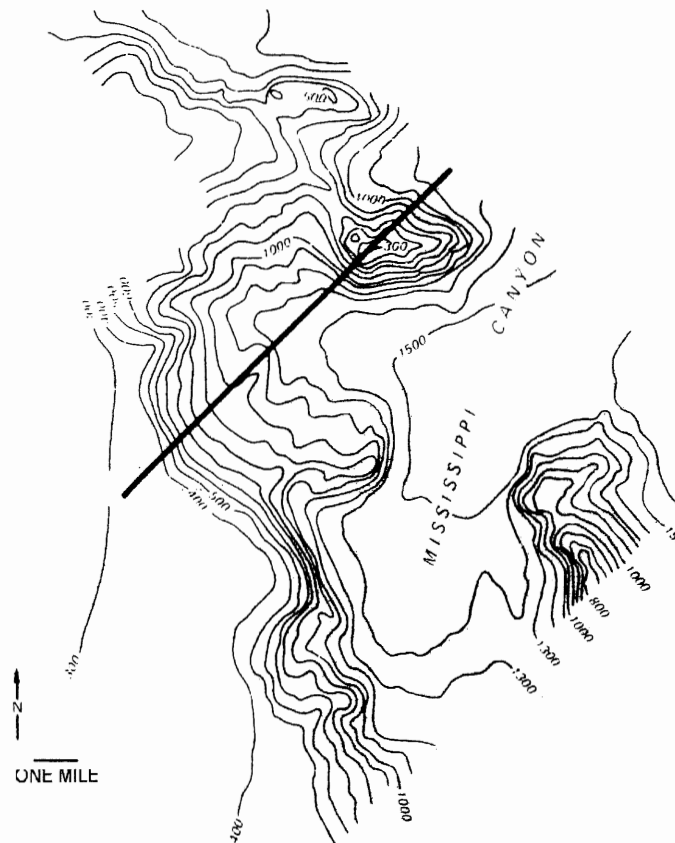


**Figure 3.9:** A modern erosional remnant from the Mississippi Canyon area. (Posamentier and Erskine 1991)



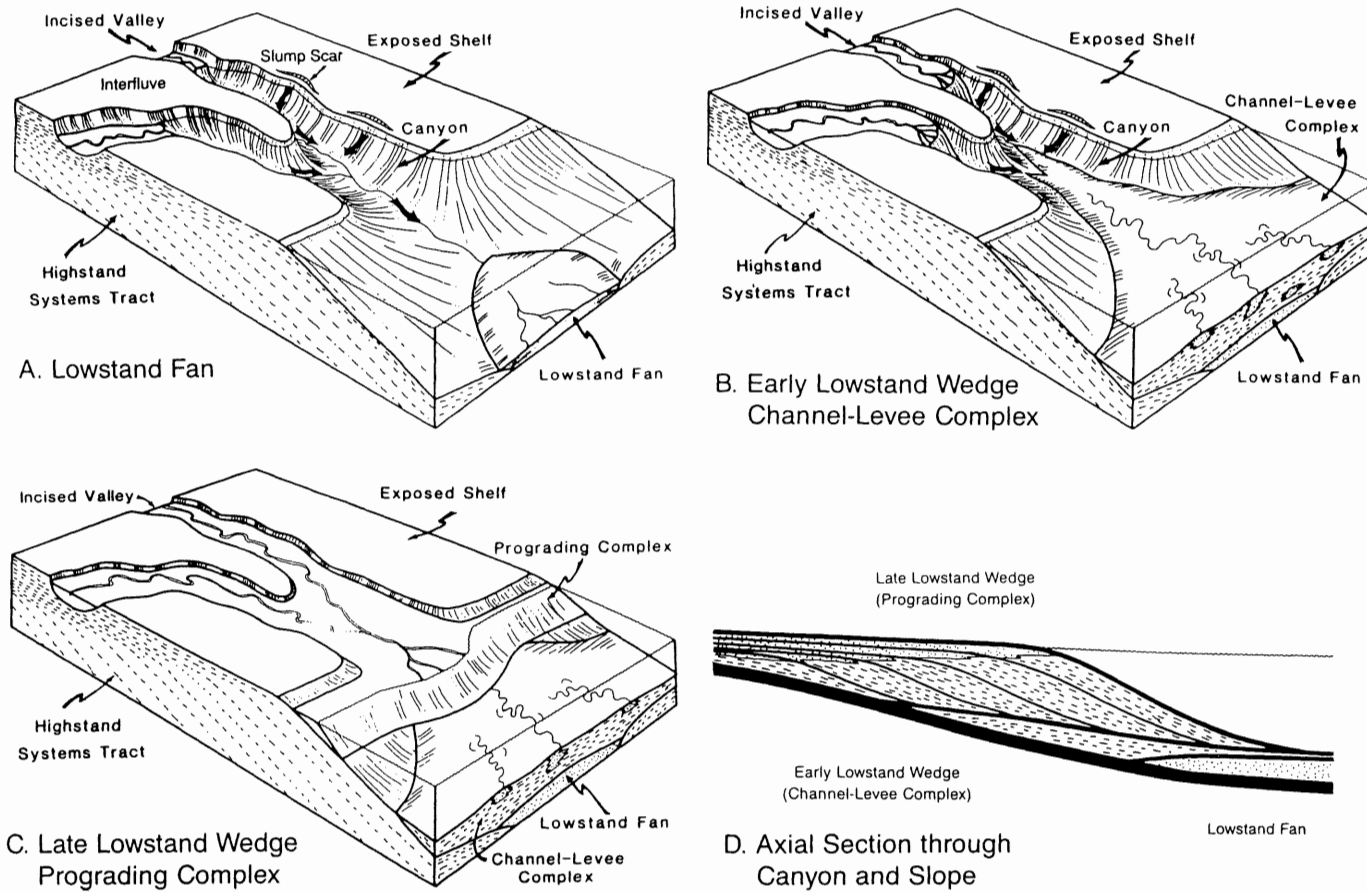
remnants occur within canyons (Figure 3.9) and are often mistaken for fan mounds (Posamentier and Erskine 1991). Canyon fill in transverse section is often characterized by reflections onlapping the erosional truncation surface, also apparent on Figure 3.8. In longitudinal seismic sections, canyon fill reflectors show down-canyon, prograding units (Mitchum 1985).

#### *3.4.2 Submarine Fans*

Submarine fans are fan or cone-shaped physiographic features composed of terrigenous sediment carried seaward by submarine canyons (Posamentier and Erskine 1991). The deposition of fans is often thought to be related to lowstand periods as shown in Figure 3.10 (Posamentier and Vail 1988). Included in this figure are sequence stratigraphic relationships which attribute fan deposition to the “lowstand systems tract”. Although this paper utilizes some seismic stratigraphic terms, they are used primarily to differentiate sedimentary packages and to characterize the nature of the seismic reflections. However, the studied features will not be placed in specific systems tracts as defined by the nomenclature of sequence stratigraphy.

Incision of continental shelves and deposition of fans beyond the shelf-break does indeed require lowered relative sealevel. However, it is important to note that many fans can be deposited during much higher relative sealevel conditions. Many modern fans such as the Amazon, Mississippi, and Bengal remain active despite the relative highstand conditions present today. This present activity can be attributed in part to the high volumes of sediment which are supplied to the continental shelf (Burgess and Hovius 1998). The Mississippi Canyon as shown in Figure 3.9 is also still active, despite the higher sea-level since its initial excavation. Similarly, the Baltimore Canyon on the east coast of the United States is presently active (Shepard 1981). Canyons and fans may remain active during highstands because of high fluvial discharge, headward erosion of submarine

Figure 3.10: Phases of a Canyon-Fan Complex as Defined by Sequence Stratigraphy



(Posamentier and Erskine 1991)

canyons, and shelf currents which transport sediments (Burgess and Hovius 1998). These examples show that erosion of submarine canyons and deposition of fans cannot be confined to a single stage in the base-level cycle.

Figure 3.11A shows a Mesozoic canyon-fan system offshore Ivory Coast in map view. On seismic reflection profiles, such canyon-fan systems can be divided into the canyon, lower fan, upper fan, and canyon fill (Figure 3.11B) (Mitchum 1985). The seismic character of the sand-prone lower fan is a mound shape with a convex-upward upper surface (Figure 3.11C). The internal reflections will downlap onto the basin floor (Mitchum 1985). The upper fan is characterized by sand-prone channels flanked by large silt-shale levees which decrease in relief downdip (Mitchum 1985). The surface separating the upper and lower fan usually shows the upper fan downlapping or onlapping the lower fan. The lower fan is active during coarse clastic deposition in high-energy periods, whereas the upper fan is active when the canyon system stabilizes and deposits silt and shale at its mouth (Mitchum 1985). The lower fan is considered the best hydrocarbon reservoir target because of the coarse clastics contained within it and because of the overlying mud-rich sequences (Mitchum 1985). Table 3.1 summarizes the seismic criteria used to recognize submarine fans.

Figure 3.11A: Mesozoic Canyon-Fan Systems, Offshore Ivory Coast  
 i) Continental Slope Surface with Three Canyons and Two Fans. Slope relief is on the order of 1500 m.  
 ii) Time-thickness (isochron) map of fans.

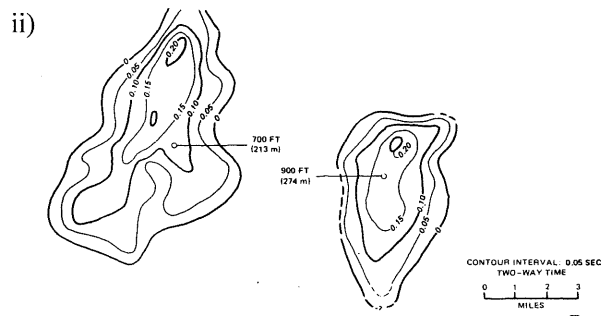
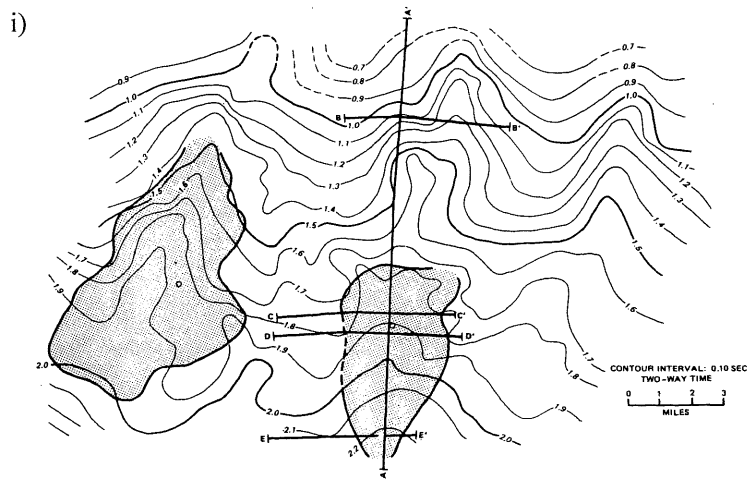
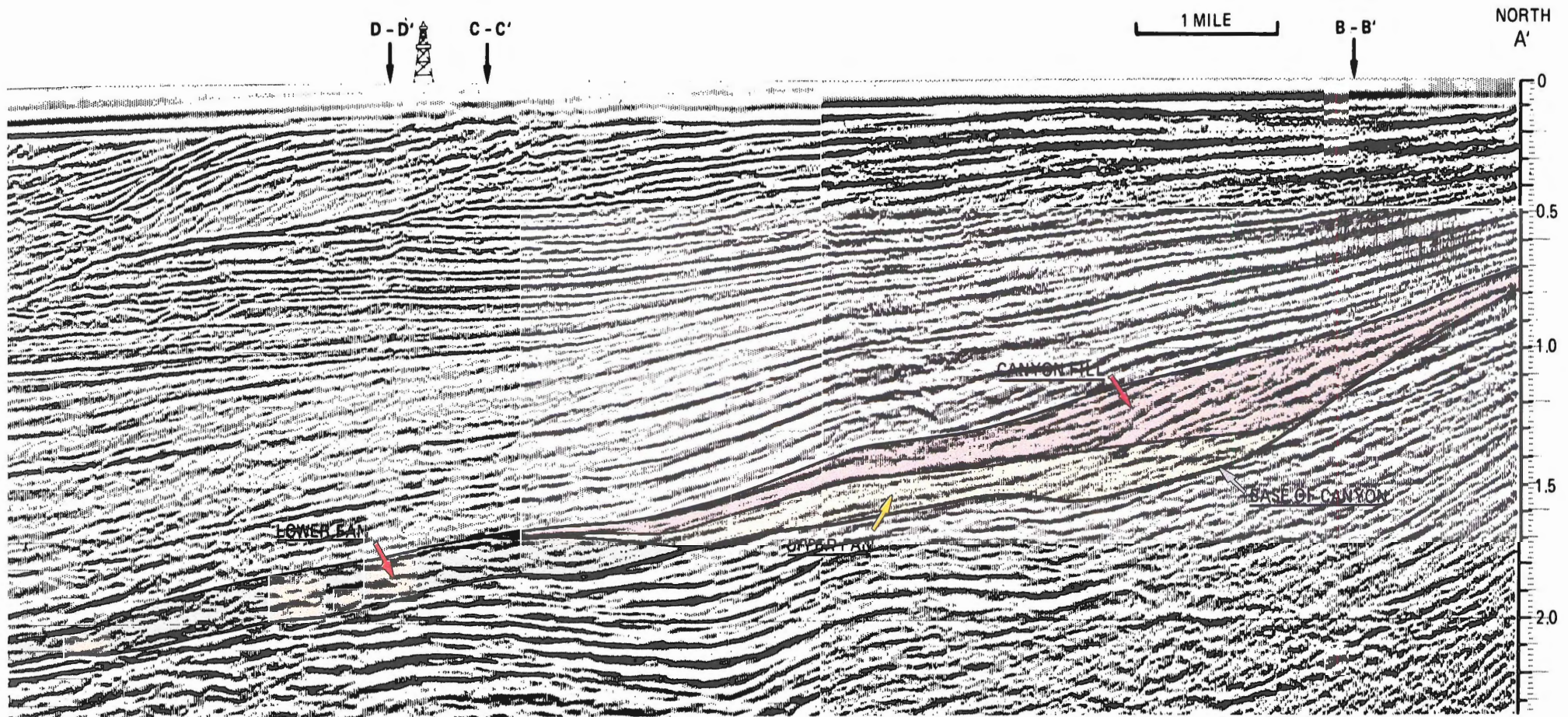




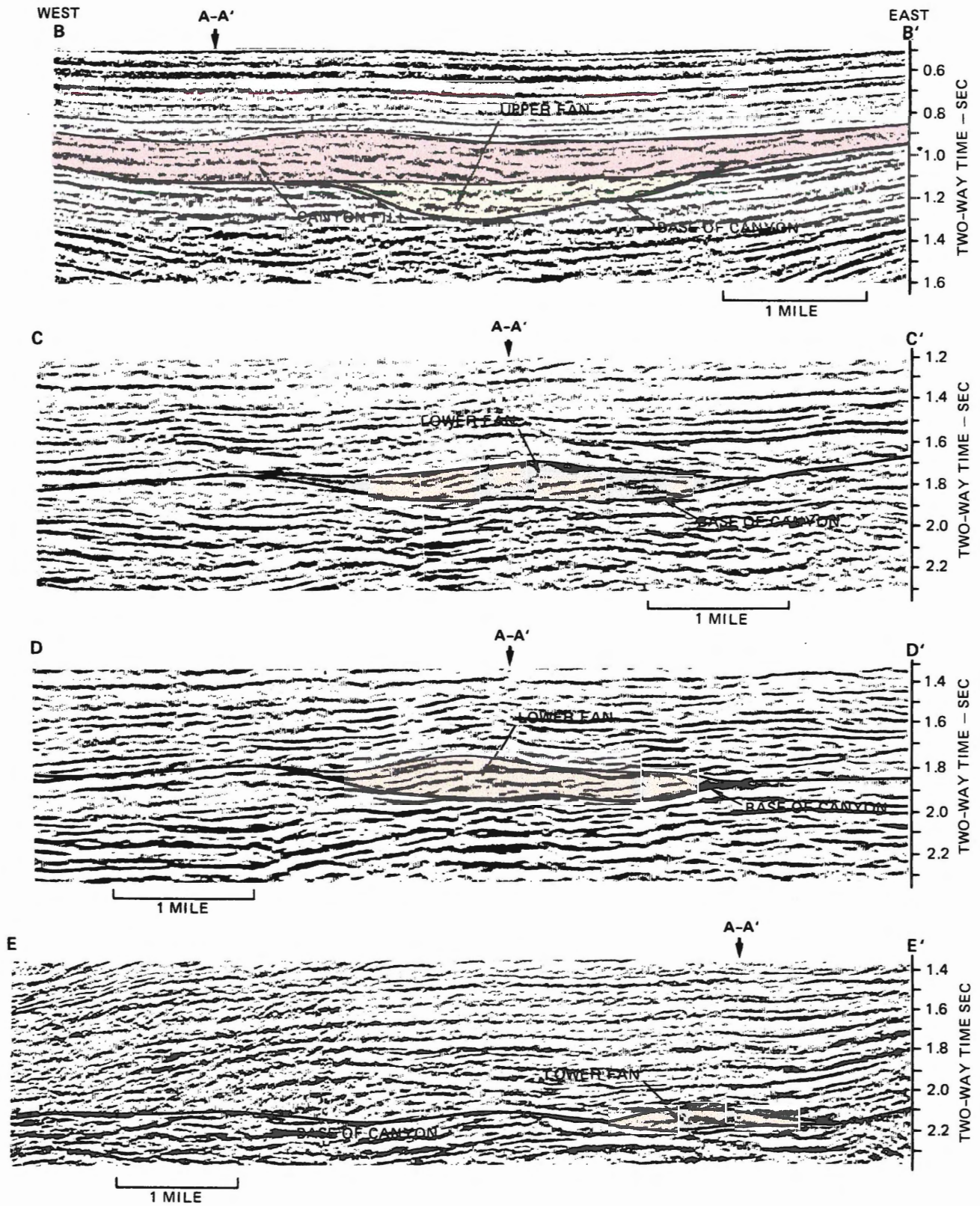
Figure 3.11B: Longitudinal Seismic Section showing canyon and submarine fan (section A-A' in Figure 3.11A).



(Mitchum 1985)



Figure 3.11C: Transverse seismic sections in four positions of the canyon/fan system.



(Mitchum 1985)



**Table 3.1:** Summary of Seismic Recognition Criteria for Submarine Fans.

<b>Upper Surface</b>	<ul style="list-style-type: none"> <li>-high amplitude, continuous reflection which onlaps or downlaps on basin margin</li> <li>-overall mound shape</li> <li>-fan pinchout geometry against bathymetric highs</li> <li>-overlying units onlap or downlap</li> <li>-often a high central channel with concave upward levees; levees become smaller downdip</li> <li>-subtle external mounding or hummocky surface</li> </ul>
<b>Lower Surface</b>	<ul style="list-style-type: none"> <li>-fills depositional lows (paleotopography)</li> <li>-depressed in center, rising to flanks</li> </ul>
<b>Internal Reflection Character</b>	<ul style="list-style-type: none"> <li>-internal bidirectional downlap (convex upward)</li> <li>-may be internally chaotic or irregularly mounded</li> <li>-stacked or slumped leveed channel complexes may exist</li> <li>-amplitude of internal reflections highly variable</li> <li>-reflections commonly discontinuous, although levees may be continuous</li> <li>-"bow-tie" diffractions possible from central channel</li> </ul>

(after Mitchum 1985, and Posamentier and Erskine 1991)

## 4.0 EXPLORATION WELLS OF CARSON BASIN

### 4.1 General Lithology

Figure 4.1 shows a cross-section through the Carson Basin wells. None of the four wells reach pre-Mesozoic basement; the oldest encountered rocks are the coarse-grained Carnian-Norian continental clastics of the Eurydice Formation penetrated in the Osprey well. Overlying these clastics is a 2 km thick evaporite deposit dominated by halite with minor red mudstones (Osprey Formation). The later Jurassic and Lower Cretaceous deposits are primarily shales, carbonates, and fine-grained clastics which have been partially eroded as a result of numerous unconformities (Grant et al. 1988). The amount of truncation increases towards the southwest part of the basin (Osprey well area), where Mesozoic cover over the Triassic evaporites is thin. Hence, while deeply buried in the north, these evaporites are much nearer the surface at the Osprey location. The exception is the occurrence of diapirs, which are found throughout the basin (see Chapter 5 for an example). The Jurassic and Cretaceous sedimentary units (the Downing Formation up through to the Dawson Canyon Formation) are better preserved in the central and northern parts of the basin.

The most complete Jurassic and Cretaceous section is present in the St. George well. Although the Bonniton well is even further north, it was drilled on the edge of the Carson Basin, and consequently has a thin accumulation of Cretaceous and Late Jurassic sedimentary units. Additionally, the unconformities present within the basin merge together at the Bonniton location. The most recent unconformity likely has eroded the previous unconformities, obscuring their occurrence. These unconformities are discussed in more detail in section 4.2 below.

The Jeanne d'Arc Basin contains rich, thick hydrocarbon source rocks of Upper Jurassic age, primarily the Kimmeridgian Egret Member of the Rankin Formation (McAlpine 1990). Organic

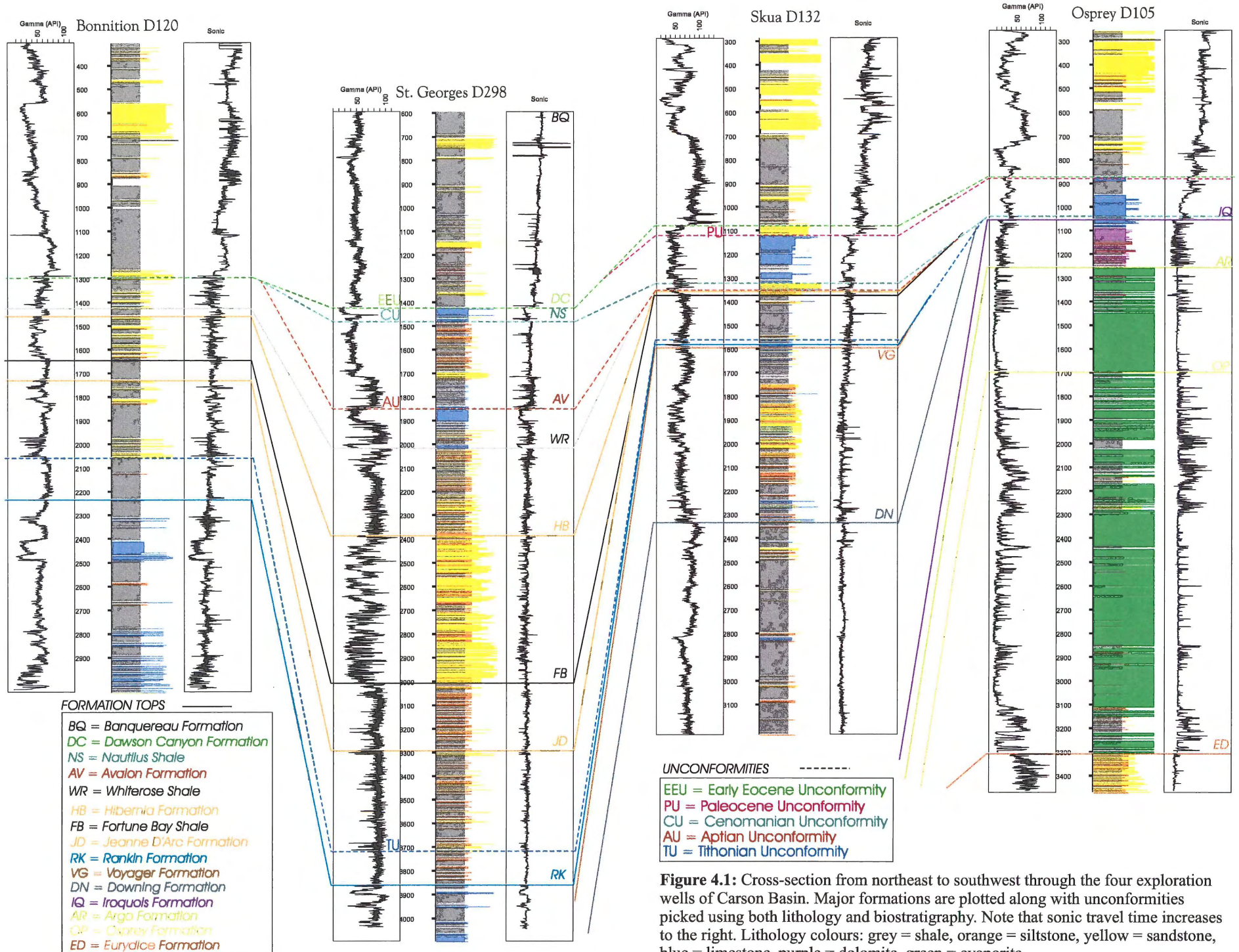


**Figure 4.1:** Cross-section from northeast to southwest through the four exploration wells of Carson Basin. Major formations are plotted along with unconformities picked using both lithology and biostratigraphy. Note that sonic travel time increases to the right. Lithology colours: grey = shale, orange = siltstone, yellow = sandstone, blue = limestone, purple = dolomite, green = evaporite.

carbon is as high as 9 %, and the Egret Member is considered an oil-prone source rock (McAlpine 1990). However, Kimmeridgian-age sediments in the Carson Basin have low organic carbon contents; the Bonniton and Skua wells register less than 1.5 % organic carbon in the Jurassic section (Powell 1985). Hardy and Jackson (1980) showed that the Upper Jurassic sediments in the Bonniton and Skua wells are in the marginally mature to mature zone for hydrocarbon generation. The low organic carbon content of the Kimmeridgian must therefore be a result of a different depositional environment than that which existed in the Jeanne d'Arc Basin (Powell 1985). This conclusion suggests that the two basins were separated by a sill, allowing the Jeanne d'Arc Basin to deposit organic matter in a restricted basin under anoxic conditions, whereas the Carson Basin was exposed to the open sea (Powell 1985). Organic matter deposited in the Carson Basin at this time would therefore have been oxidized and preserved only in modest amounts.

#### **4.2 Unconformities**

A number of unconformities exist in the Carson Basin. The five major unconformities are the Tithonian Unconformity (TU), Albian-Aptian Unconformity (AU), Cenomanian Unconformity (CU), Paleocene Unconformity (PU), and the Early Eocene Unconformity (EEU). In the past, the upper unconformities have been lumped together into the "Base Tertiary Unconformity". However, it is important in this study to distinguish between them. The unconformities of Carson Basin have been picked using both biostratigraphic and lithostratigraphic information, and are summarized in Table 4.1 for the Skua and Bonniton wells. Appendix 2 details all the picks used in this study.

Figure 4.2 again shows a cross-section through Carson Basin, with only the unconformities for simplicity. The unconformities vary across the basin, with only the Skua well containing all five unconformities. The Paleocene Unconformity (PU) does not appear in any well other than Skua,

**Table 4.1:** Unconformities and gaps in the Skua and Bonniton Wells. The Skua well shows all five of the unconformities observed in the basin, and the Bonniton well shows only two. (All data from Basin Database; see Appendix 2 for complete summary.)

**Skua Well**

<b>Unconformity:</b>	<b>Gap (hiatus or erosion):</b>	<b>Constrained By:</b>
Early Eocene	Middle-Late Paleocene	Biostrat.and Lithostrat.
Early Paleocene	Maastrichtian	Biostrat.and Lithostrat.
Cenomanian	Albian?	Lithostrat. only
Albian-Aptian	Velanginian, Hauterivian, Barremian, Aptian	Biostrat.and Lithostrat.
Tithonian	?	Lithostrat. only

**Bonnitton Well**

<b>Unconformity:</b>	<b>Gaps (hiatus or erosion):</b>	<b>Constrained By:</b>
Early Eocene	Aptian, Albian, Late Cretaceous, Paleocene	Biostrat. and Lithostrat.
Tithonian	?	Lithostrat. only



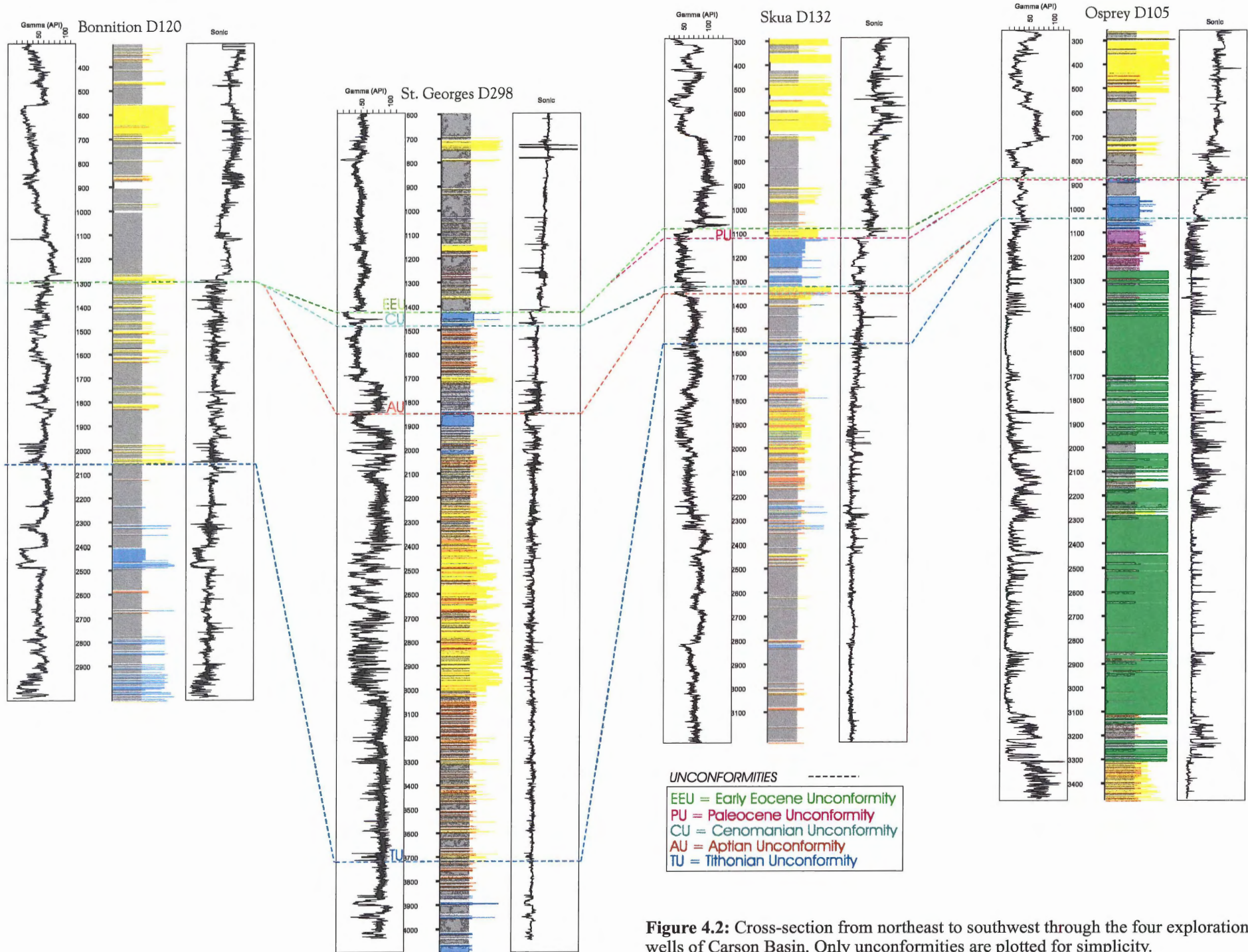


**Figure 4.2:** Cross-section from northeast to southwest through the four exploration wells of Carson Basin. Only unconformities are plotted for simplicity.

although Late Paleocene sediments may occur in the Osprey well based on two index species. The gamma-ray well log does record a sharp spike between the Early Eocene Unconformity (EEU) and the Cenomanian Unconformity (CU) in the St. George well, which could indicate the presence of the PU. However, biostratigraphic control for the St. George well is poor, and does not distinguish between a Paleocene and Eocene unconformity.

In the Bonniton well, only the Early Eocene Unconformity (EEU) is observed of the four younger unconformities. Although all the unconformities present in the basin probably occurred in the Bonniton area, they have been destroyed by subsequent erosional unconformities. Hence, the EEU, as the most recent erosional unconformity, is the only one which remains.

Alternatively, it is possible that the PU is present in the Bonniton well. The erosional unconformity that separates the Early Eocene from the Barremian is constrained by two sidewall cores 50 meters apart. Cuttings have been examined for the intervening interval, however at best the cuttings would have a resolution of plus or minus 20 meters (Ascoli, pers. comm. 1999). Hence, there is a 40 meter window within which the Paleocene Unconformity could exist, yet remain undetected. Such a 40 meter interval is also not resolvable with seismic profiles, especially since those used in this study were processed more than 15 years ago. Therefore, the PU should not be dismissed despite a lack of evidence at the present time for its existence in the Bonniton region.

### **4.3 Synthetic Seismograms**

Figure 4.3 shows a synthetic seismogram created for the Skua well, with the five unconformities plotted. The synthetic seismograms allow well depths to be correlated with the time data collected from seismic profiles. Most importantly, unconformities and formations from the wells can be directly related to the reflections mapped in this study. Note that on the synthetic

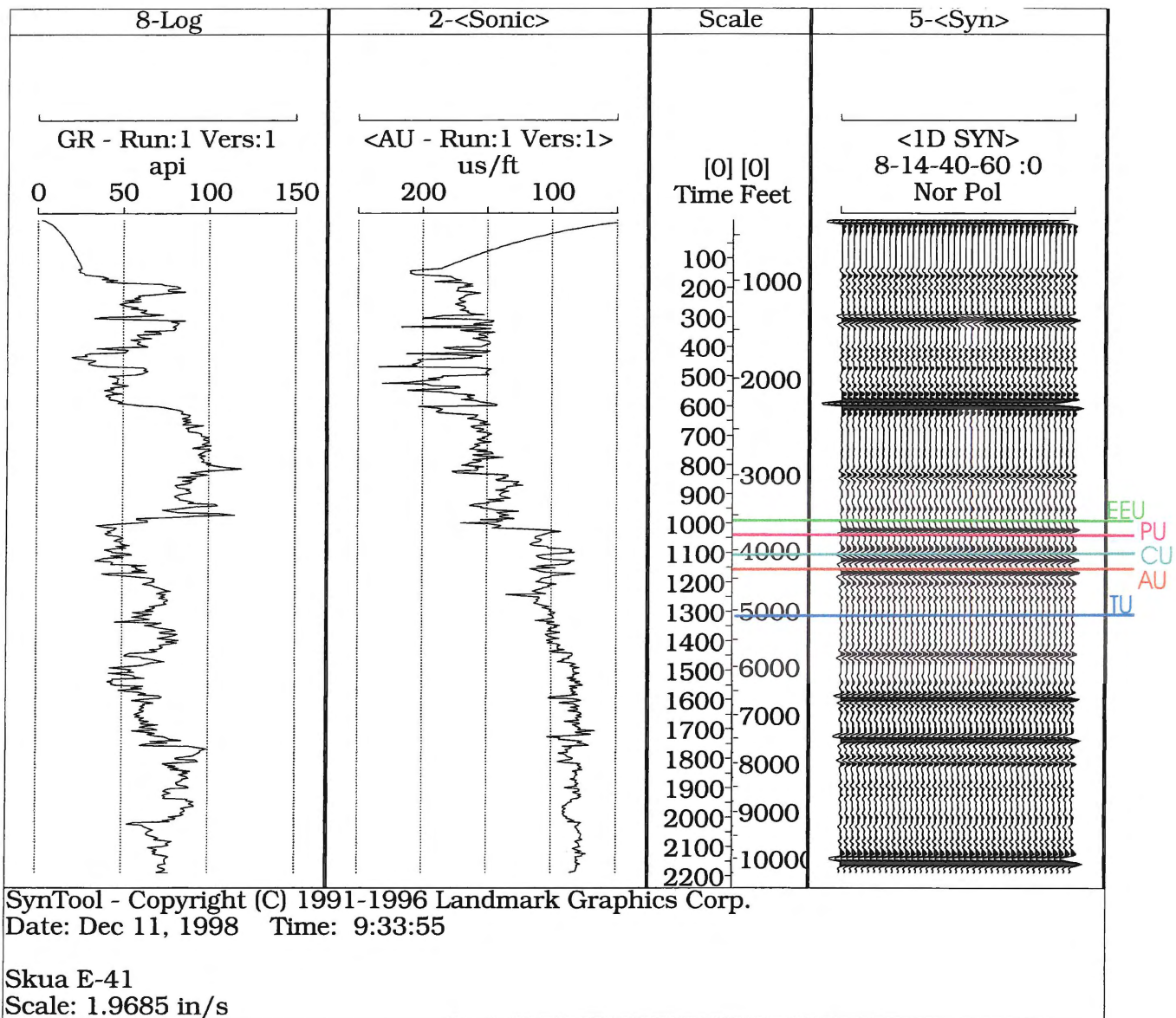


**Figure 4.3:** Synthetic seismogram calculated for the Skua well. EEU = Early Eocene Unconformity, PU = Paleocene Unconformity, CU = Cenomanian Unconformity, AU = Albian-Aptian Unconformity, TU = Tithonian Unconformity. Note the abrupt change in sonic character at the Early Eocene Unconformity.



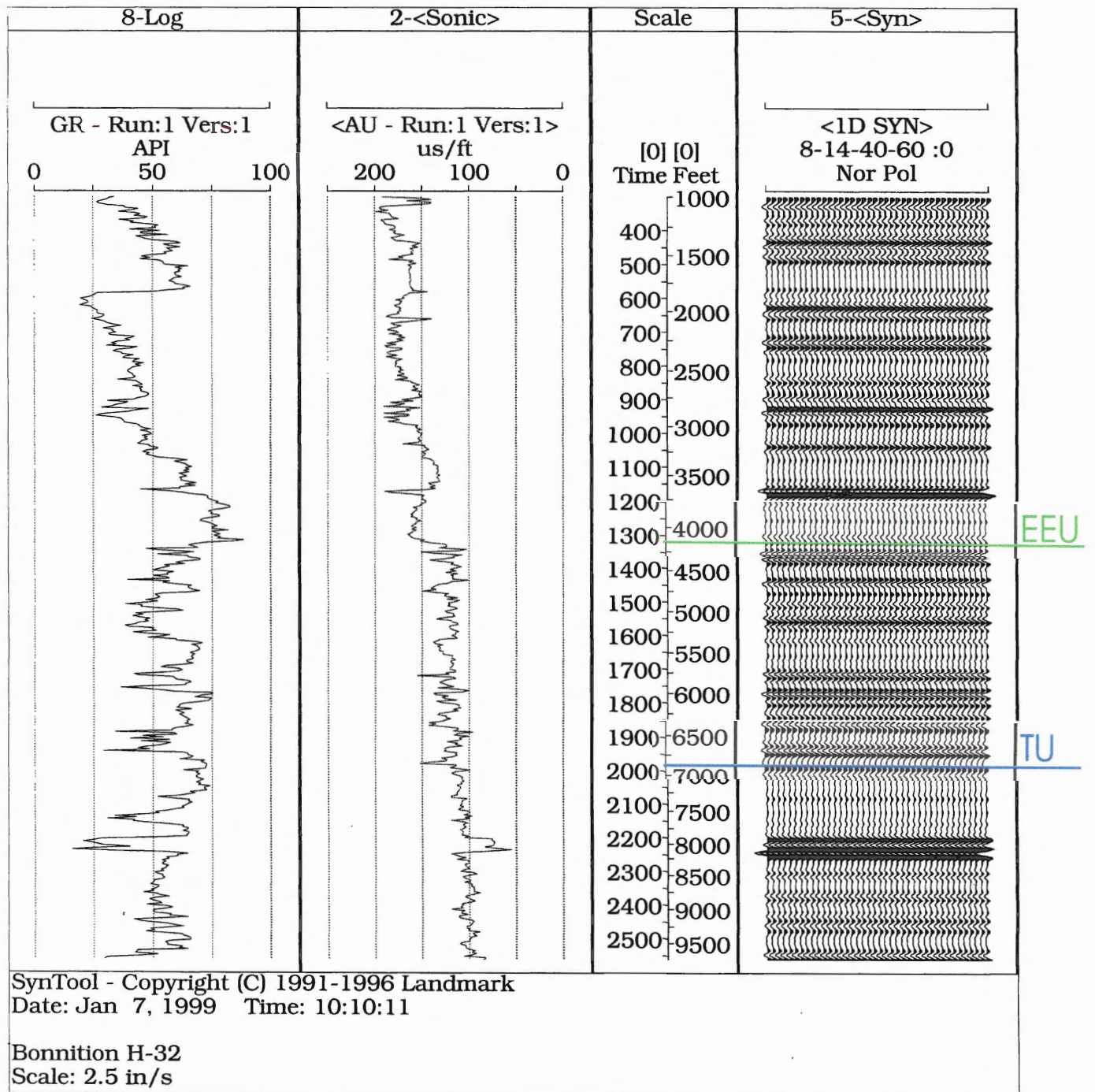
seismogram, time is the linear scale, while the depth scale is variable as a result of its dependency on velocity for depth conversion.

Figure 4.4 shows a synthetic seismogram for the Bonniton well with the EEU plotted on it. Note the strong change in character of the sonic log: from the top of the well to the EEU, there is a trend of slowly increasing velocity as compaction increases. The EEU marks an abrupt change to higher velocity, and velocity continues to increase gradually below the EEU. The sonic log supports the biostratigraphic evidence for the existence of the unconformity, as there is missing section which would normally connect these two segments to form a single overall trend. Although a sudden change in sedimentation rate could also create such an effect, the combination of the sonic log character with the biostratigraphy supports the interpretation of an erosional unconformity.

#### **4.4 Paleoenvironment**

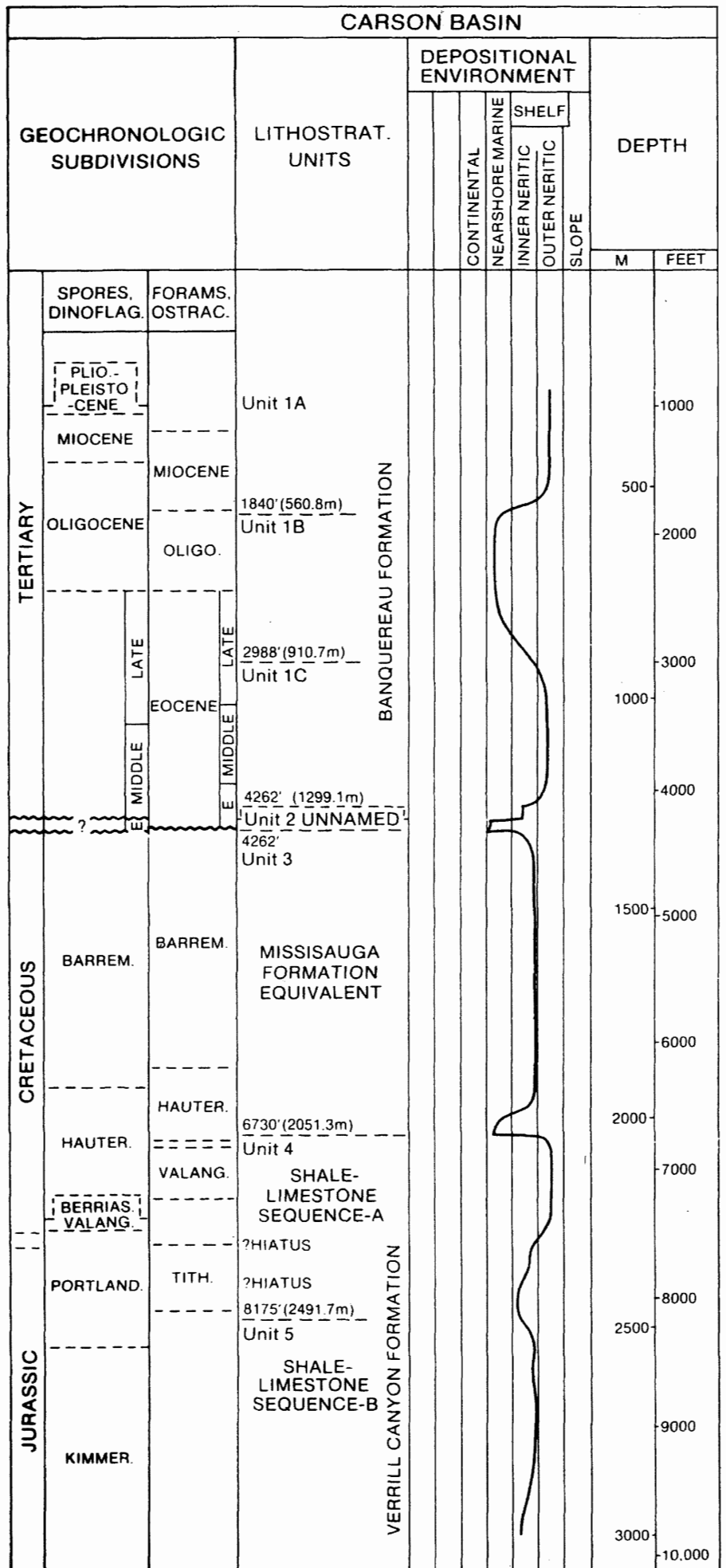
Figure 4.5 summarizes the depositional environment present in the Bonniton well over time, based on study of spores, dinoflagellates, foraminifera, and ostracods (Grant et al. 1988). A rapid shift in environment occurred at the Early Eocene Unconformity, changing from an inner/outer neritic shelf to a nearshore marine setting. By the Middle Eocene, the environment of deposition had returned to an outer neritic shelf setting. The abrupt nature of the environmental change should not be misinterpreted as an indication of the rate with which the change occurred, since the previous periods of transition have been lost to the erosional unconformities. Nevertheless, this unconformity has important implications which are discussed in Chapter 6.

Nearshore marine conditions returned during the Oligocene and Miocene, when sandy deltaic units prograded out to the shelf edge (Grant and McAlpine 1990); this change in environment is also reflected in Figure 4.5. A final stage of outer neritic environment, which occurred after the Miocene deltas, continues to the present day.



**Figure 4.4:** Synthetic seismogram calculated for the Bonniton well. EEU = Early Eocene Unconformity, TU = Tithonian Unconformity. Synthetic is compared with a seismic profile in Figure 5.2.

**Figure 4.5:** Bonnition depositional environment. Note the nearshore marine environment which occurs at the Early Eocene Unconformity. (Grant et al. 1988)



## **5.0 SUBMARINE CANYONS AND FANS OF CARSON BASIN**

### **5.1 Introduction**

The detailed mapping undertaken in the northern part of the basin relied on the irregular grid of lines shown in Figure 5.1; the specific programs and lines examined are summarized in Appendix 4. The seismic coverage virtually disappears basinward, and as a consequence the submarine fans are not imaged in their entirety. Two distinct, informally named canyon systems are identified in the mapped area: Bonniton Canyon in the north and St. George Canyon to the south. Seismic coverage over the southern canyon is less dense than for the northern one; these differences should be taken into account when comparisons are made.

### **5.2 Submarine Canyons**

#### *5.2.1 Morphology*

The criteria for seismic recognition of submarine canyons as discussed previously are clearly met by profiles available in Carson Basin. Figure 5.2 is a cross-section through the upper reaches of the Bonniton Canyon, showing a V-shaped erosional notch approximately 6.5 km wide. Truncation of the horizontal and dipping reflectors is distinctly visible at the erosional surface of the canyon. Additionally, the canyon fill onlaps the erosional surface and shows slight negative relief as a result of differential compaction. The canyon appears asymmetrical in this profile, with the right side of the canyon lower than the left side. This may be a result of later subsidence of the Carson Basin.

Truncation is also visible in Figure 5.3, a longitudinal seismic section through the Bonniton Canyon. The canyon slope gradually decreases from left to right on the section. The canyon fill can also be observed onlapping the truncation surface.



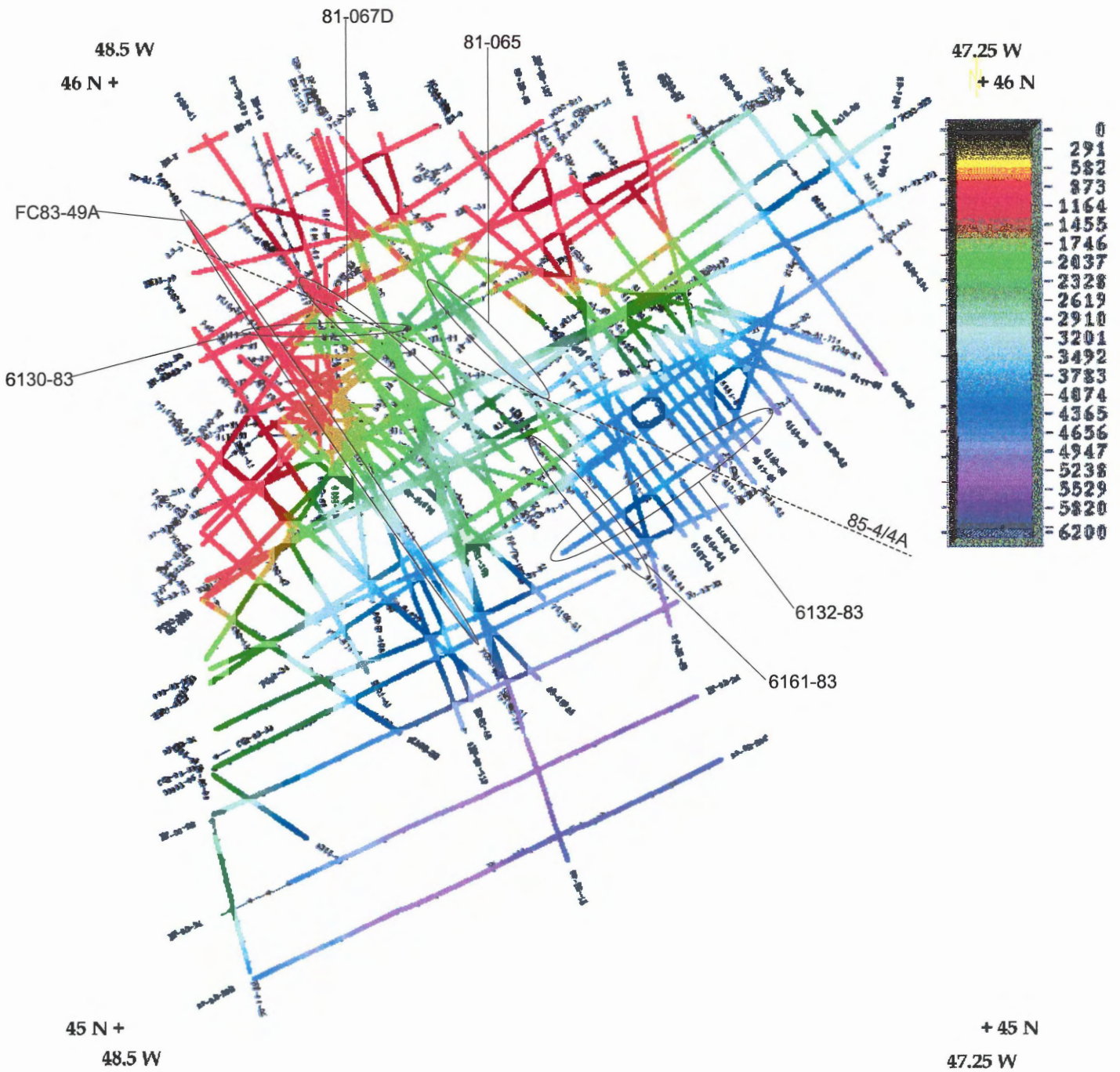


**Figure 5.1:** Grid of seismic lines used in studying Carson Basin. The colours are two-way travel time ("depth") of the Early Eocene Unconformity. The horizon ranges in depth from 800 to 6200 ms. Note the sparsity of the data in the southeastern region and the irregularity of the grid as a whole. Seismic profiles used as figures are indicated, including part of Lithoprobe lines 85-4/4A which were not digitized.



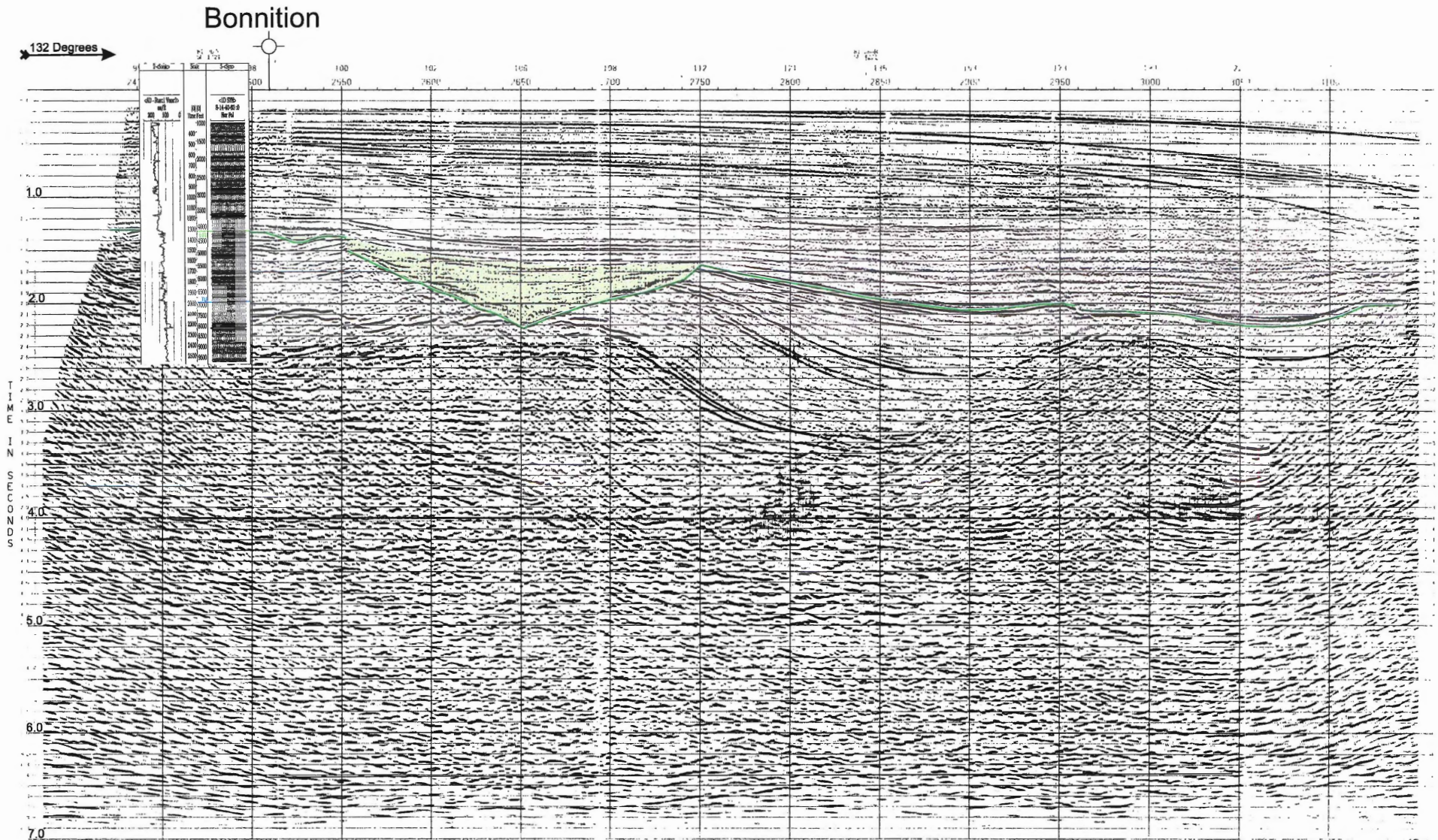


**Figure 5.2:** Transverse seismic profile of the Bonntion Canyon (shaded green). Note the truncation of underlying seismic reflectors, onlap of canyon fill, and slight negative relief over the canyon. The Bonntion well lies to the northwest of the canyon. The green line traces the Early Eocene Unconformity. The synthetic seismogram for the Bonntion well is included, although comparison at this scale is difficult.. (Line PCP81-067D)



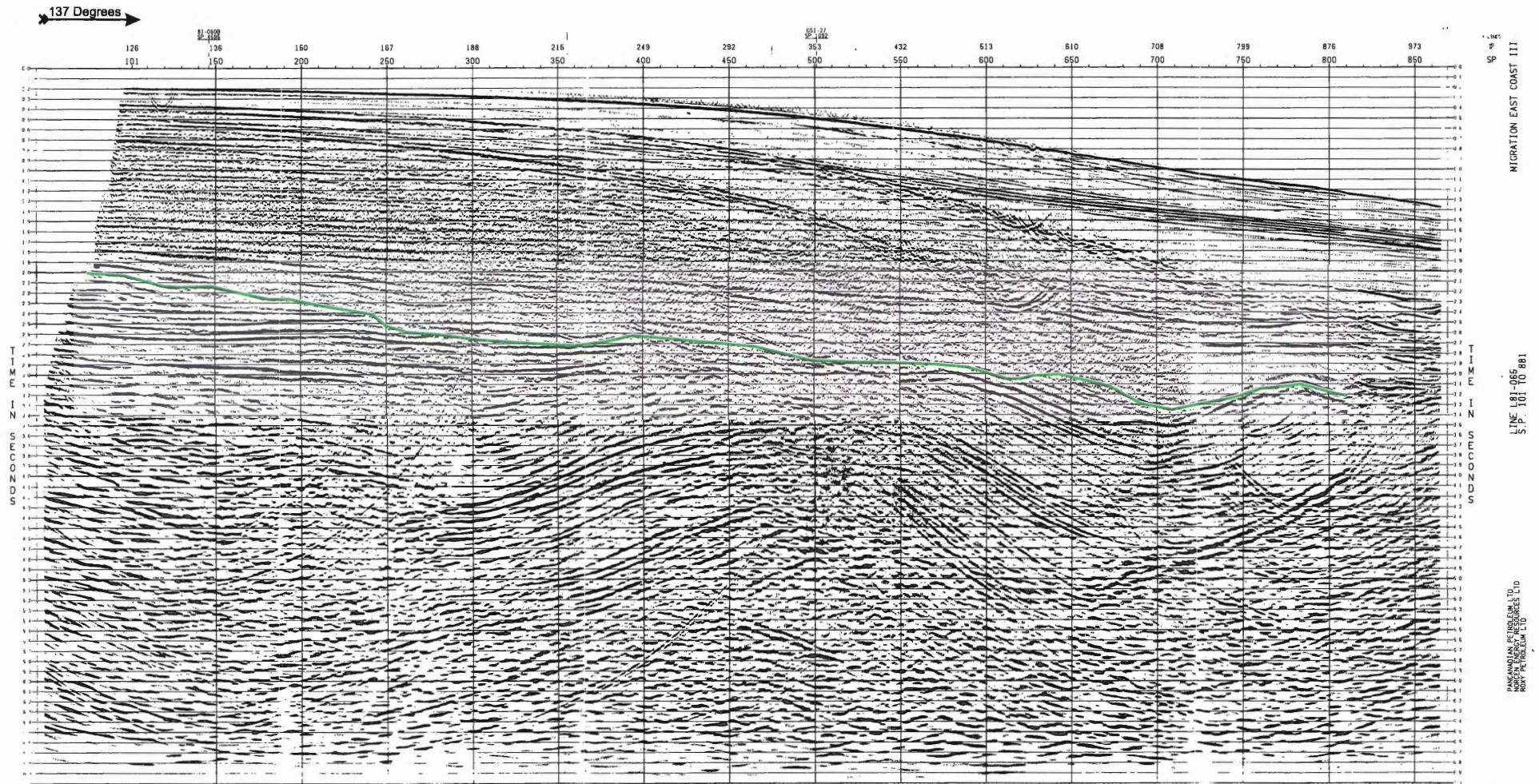


**Figure 5.3:** Longitudinal seismic section down the Bonniton Canyon. Truncation of underlying reflectors and downlap of canyon fill is observed on this profile. The green line traces the Early Eocene Unconformity, which is also the canyon base. Note that the canyon erosion extends across the entire seismic profile. The reflectors between shotpoints 400-550 that appear to cross the erosional surface are multiples.  
(Line PCP81-065)

Figure 5.4 is a time-structure contour map of the erosional unconformity to which the canyons correspond (discussed below in section 5.2.2). The canyons traverse a sharp drop in the mapped surface, where there is a zone of closely spaced contours. These closely spaced contours occur between much wider spaced contours above and below. This sudden change in slope is interpreted as the paleocontinental shelf break. The lower reaches of the two canyons flank a large ridge which can be described as a knoll or isolated outlier of the paleoshelf. The ridge may be related to large-scale salt movement, or may be an upraised basement feature. Smaller elevated features are caused by localized salt diapirs. Note that the contours are in milliseconds, as a velocity model for the Carson Basin is not available for widespread depth conversions.

Figure 5.5 is a shaded relief map which clearly displays the erosional features. The Bonniton Canyon in the north can be divided into three major segments: Segment one is a west-east trending, sinuous tributary which converges with segment two. Segment two is much deeper, also trends west to east, and shows two distinct erosional scours at its head. These two segments converge together into the remainder of the canyon (segment three), which trends northwest-southeast. The canyon extends at least 39 km from the beginning of the second segment to its lower extent past the basement ridge.

The St. George Canyon is much more direct, with no apparent tributary segments. The canyon extends over 30 km from its head to the lower reaches, trending northwest-southeast. Seismic profiles show localized channeling and erosional scours near the canyon head. Figure 5.6 is a longitudinal section through the St. George canyon, showing truncation of underlying reflectors. The canyon begins near shotpoint 5000 (middle of the figure), and cuts downward to the southeast (towards the right). The profile also intersects with the St. George well in the northwest.



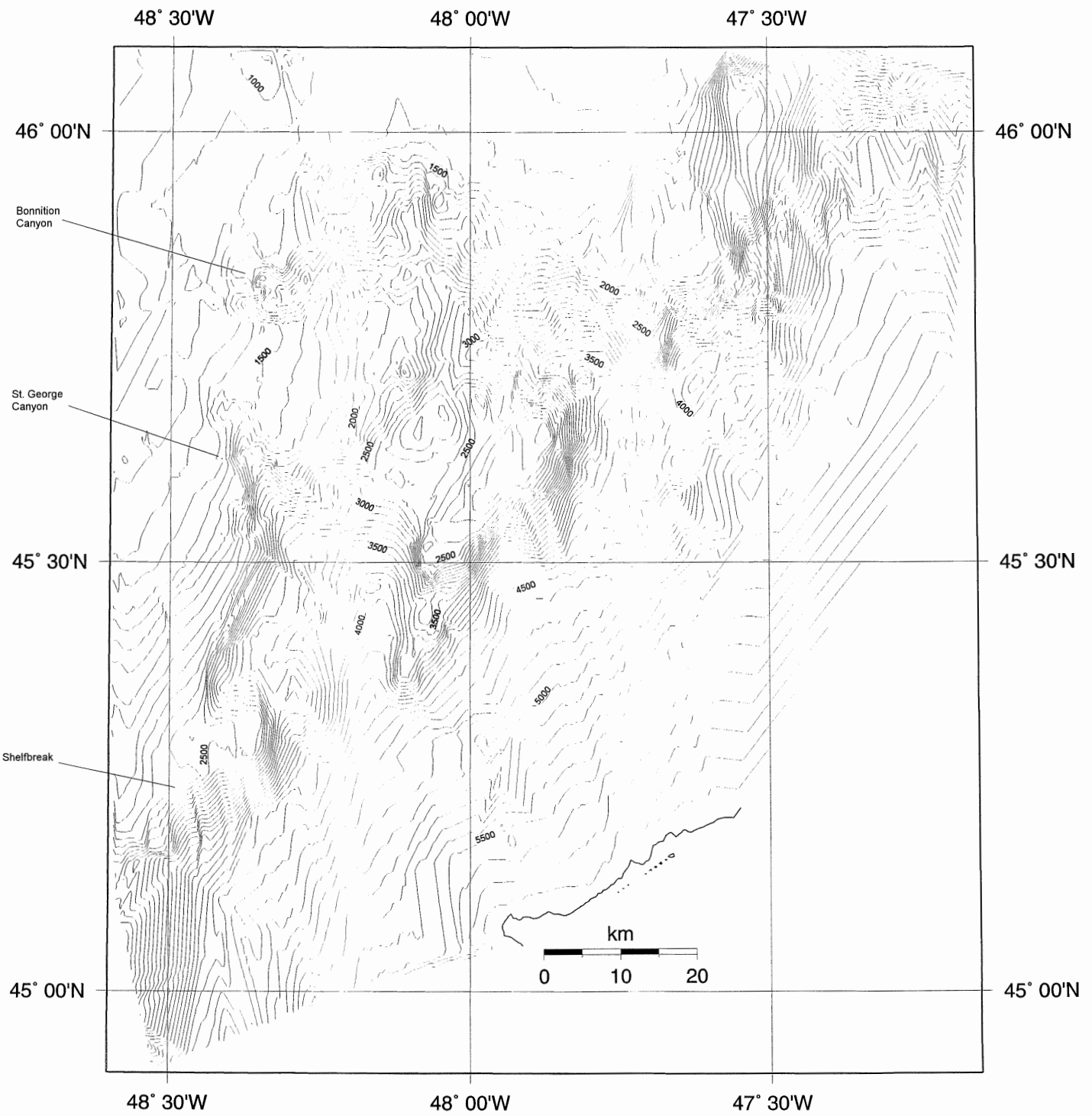


Figure 5.4: Early Eocene Unconformity Time-Structure contour map. Both the Bonnition and St. George Canyons traverse an interpreted paleocontinental shelfbreak. Note the large knoll or outlier between the outlets of the two canyons.

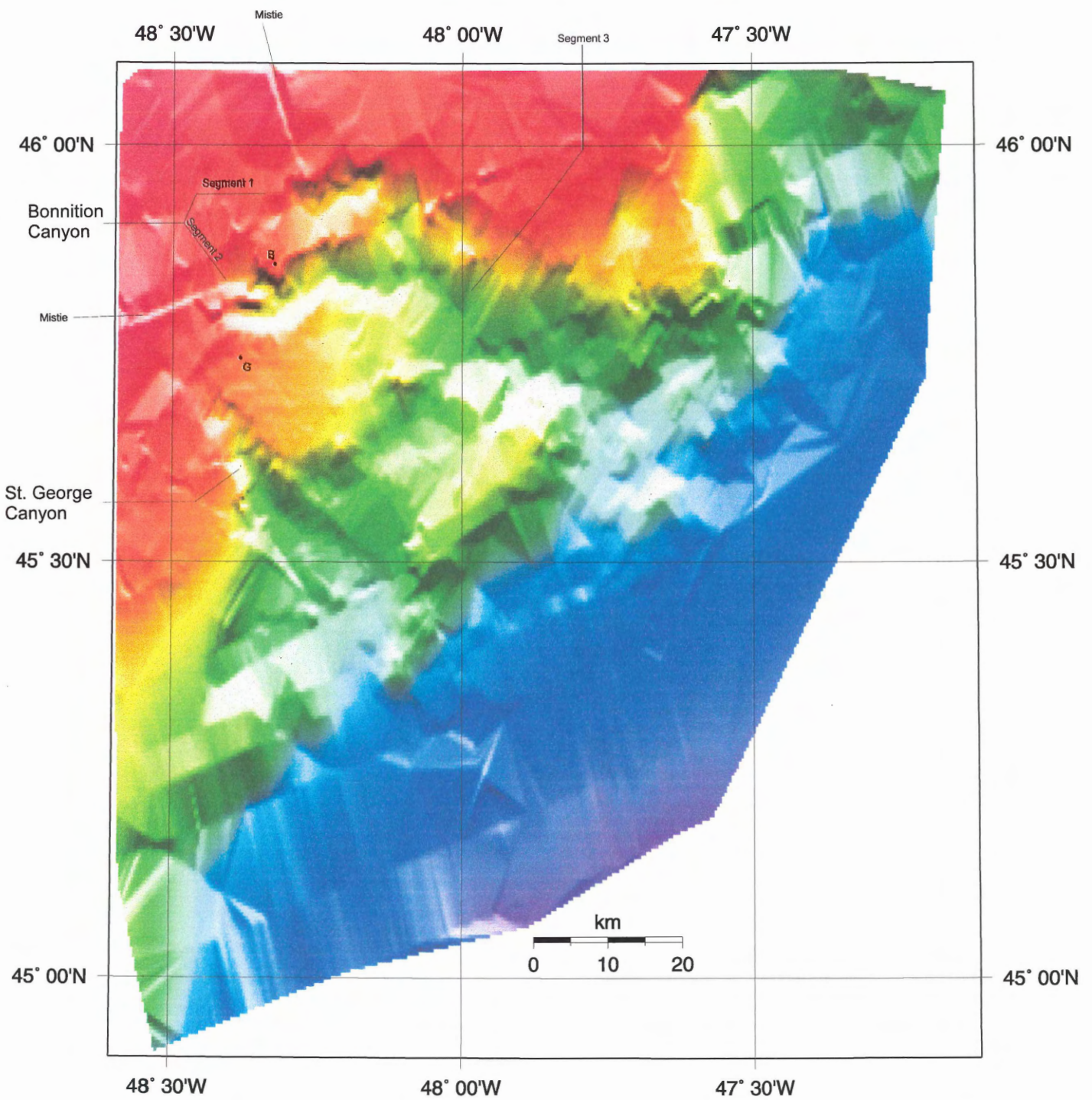
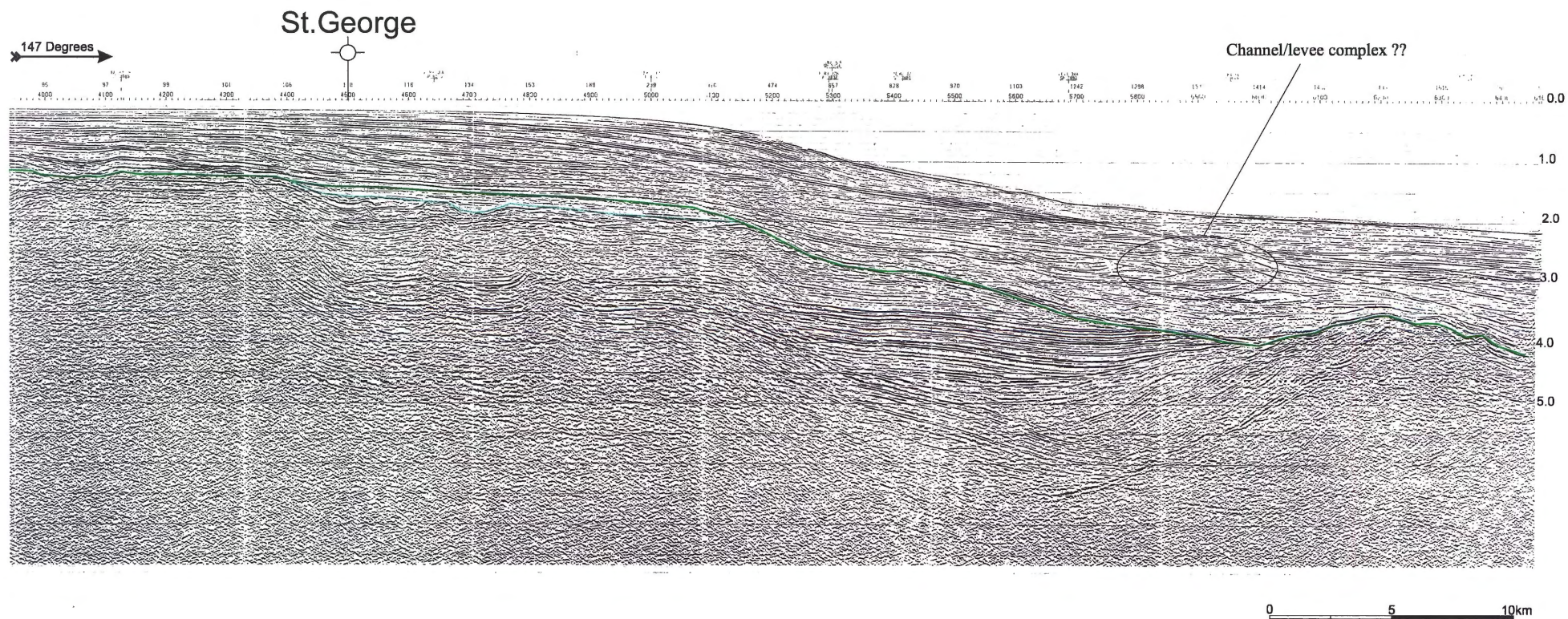


Figure 5.5: Shaded relief map of Early Eocene Unconformity surface. The diagram is illuminated from 305 degrees, with 260 colours used for the 5200 ms of relief.  
 B = location of Bonniton well, G = location of St. George well.





**Figure 5.6:** Longitudinal seismic profile of the St. George Canyon. The Early Eocene Unconformity is shown in green, which is also the canyon base. The canyon begins near shotpoint 5000 (middle of the figure), and cuts downward to the southeast (towards the right). Truncation of underlying reflectors is evident. The erosional Cenomanian Unconformity is in blue, and is truncated by the canyon near shotpoint 5100. Note the large channel in the CU which occurs near shotpoint 4700. There is also a younger feature above the EEU, possibly a channel/levee complex. Future work in the Tertiary would be useful in this region. The profile also intersects with the St. George well to the northwest. (Line FC83-49A)

Both canyons gradually widen from a steep V-shaped erosional notch to a wider, U-shaped erosional pattern. This may reflect a decrease in erosional force as sediment velocity decreases basinward. This decrease in velocity would correspond to greater distance from source areas and also to the shallower slope which is present away from the shelf break. In the upper reaches of the Bonniton Canyon, the canyon walls dip as much as 34.5 degrees. This estimate is based on an assumed constant seismic velocity of 125 microseconds/foot or 2450 meters/second measured at the erosional surface using the sonic logs of Bonniton and Skua.

Over a measured distance of 35 km, the Bonniton Canyon changes in depth by 2000 milliseconds, giving an average gradient of 57 ms/km. The Banquereau Formation overlies and fills the unconformity surface, and has a velocity ranging from 1600-2500 m/s based on sonic logs and seismic processing data. Using an average velocity of 2000 m/s, the gradient of the canyon can be estimated as:

$$(57\text{ms/km}) \times (1\text{s}/1000\text{ms}) \times (2000\text{m/s}) \times (1\text{km}/1000\text{m}) \times 100\% = 11.4 \%$$

This gradient appears sensible, since in order to incise a continental slope, the gradient of a canyon must be steeper than the slope. Continental shelf gradients are usually on the order of 3-5 degrees (Prothero and Schwab 1996).

### *5.2.2 Timing of Excavation*

As discussed in Chapter 4, only the Skua well contains all the unconformities recognized for this study. The upper four unconformities are easily distinguished in Figure 5.7 which shows a seismic section that intersects with the Skua well. No apparent reflector corresponds with the older Tithonian Unconformity (TU), which is also not apparent from the biostratigraphic information. The TU has been picked based on lithological criteria, but it is not important in this study. The upper four



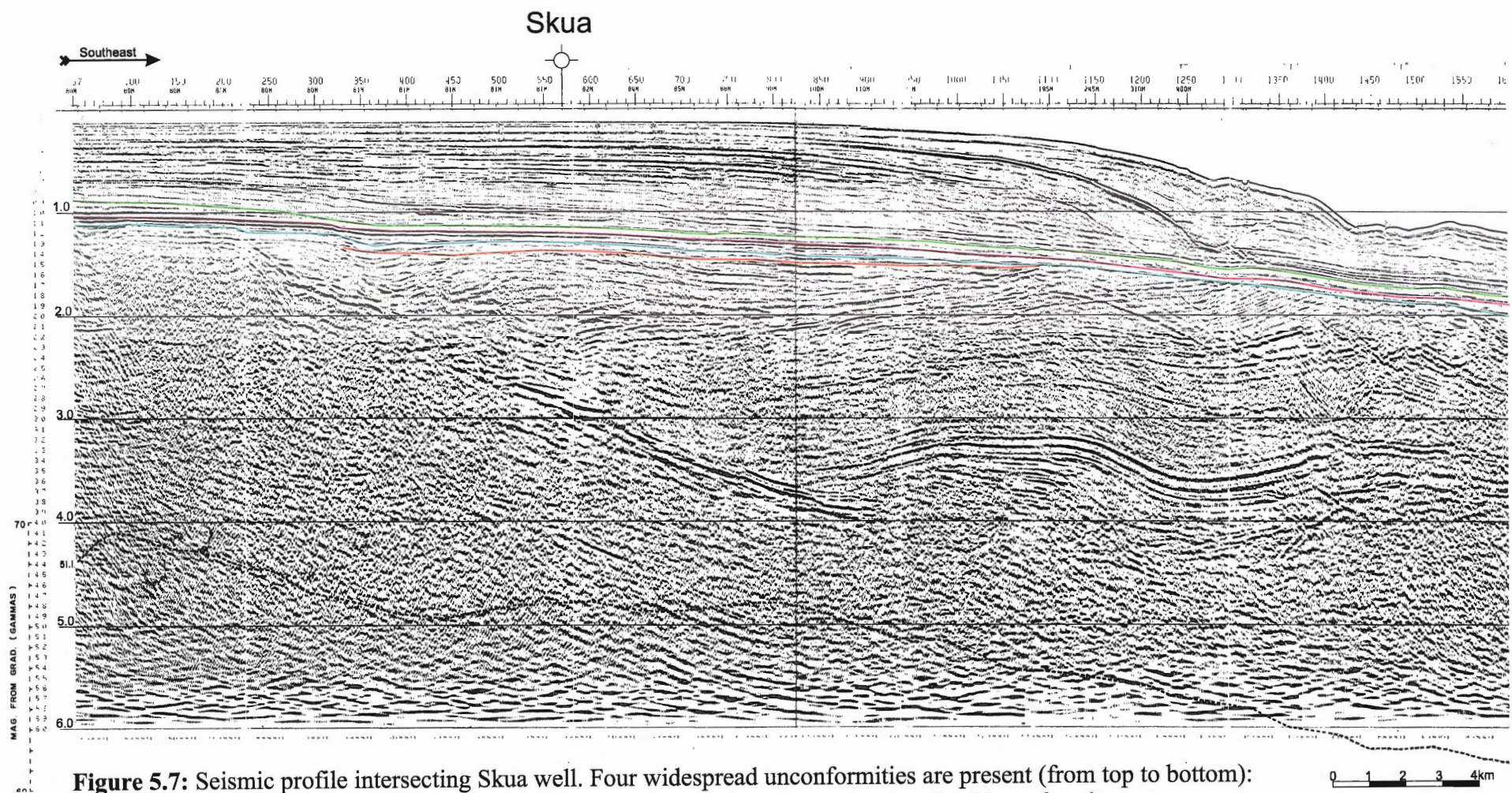


**Figure 5.7:** Seismic profile intersecting Skua well. Four widespread unconformities are present (from top to bottom): green = Early Eocene Unconformity, red = Paleocene Unconformity, blue = Cenomanian Unconformity, brown = Albian-Aptian Unconformity. (Line CGB82-115)

unconformities are widespread, continuous reflectors which are traceable across the basin except where they have been obliterated by younger unconformities.

In the Bonniton well locality, the Early Eocene Unconformity (EEU) has erased the Paleocene, Cenomanian, and Albian Unconformities. Figure 5.2 displays a seismic section which intersects both the Bonniton well and the Bonniton Canyon. This seismic profile clearly shows a single erosional surface, and not four individual ones as in the Skua profile. The synthetic seismogram for the Bonniton well (Figure 4.4) plots the EEU at a similar time-depth of approximately 1320 ms, and therefore it can be concluded that the Bonniton Canyon was cut during this erosional unconformity.

The St. George well locality contains two erosional unconformities at the canyon level, the EEU and CU (see synthetic seismograms in Appendix 3). However, examination of Figure 5.6 shows the CU being truncated by the EEU as it reaches the St. George Canyon. Hence, both of the canyons were cut during the EEU.

The noted erosion of previous unconformities by the EEU suggests that the canyons may have been eroded by older unconformities and then reactivated during the EEU. This notion is supported conceptually by the discussion in Chapter 3, where it was noted that canyon incision is an intermittent but long-term process. Indeed, channeling of the CU (Figure 5.6) points to previous episodes of incision. However, within the Bonniton and St. George Canyons, only the EEU occurs at the base. That is, the EEU is never observed at mid-level within a canyon. Cut and fill relationships are also not evident. Since there is no direct evidence to show that reactivation has occurred, it must be concluded that the canyons were formed primarily during the EEU. Although this conclusion must be tempered by the possible existence of the PU in the canyon region, the lack

of evidence from both the St. George and Bonniton wells tends to support the Early Eocene hypothesis.

Salt movement influences much of the Carson Basin, and appears to have moved throughout its development. In some cases these diapirs pierce the EEU erosional surface (shown later in Figure 5.11). Salt has therefore moved upwards as recently as the Eocene.

### **5.3 Major Deposition Features**

#### *5.3.1 Fan Deposition*

The seismic profile shown in Figure 5.8 shows the mounded shape of a submarine fan, with a hummocky, high-amplitude surface reflector. The fan surface pinches out on either side of the mound. The mound also shows bidirectional downlapping of internal reflectors onto the basin floor. Internally, the fan contains almost no reflections at the base of the mound, suggesting chaotic deposition with no horizontal stratification available to yield reflectors. This change in reflection character from the chaotic bottom sediments to the more stratified upper reflectors suggests a change in depositional energy and possibly source sediment.

Figure 5.9 shows the digitized line data for the submarine fans, located basinward of the canyons. These fans are not imaged completely by the surveys, and hence the contour map of Figure 5.10 is poorly constrained. The fans reach up to 450 milliseconds in thickness; estimating a conservative velocity of 2000 m/s, these fans could therefore be as much as 900 m thick. Large modern submarine fans range in thickness from 1.2 km (Rhone Fan) to 4.2 km (Amazon Fan) (Walker 1992). Assuming compaction has occurred since the Early Eocene, the submarine fans of the Carson Basin are comparable in thickness to the smaller end of the scale (i.e. the Rhone Fan). Comparisons for areal extent are rendered impossible because of the incomplete seismic coverage.



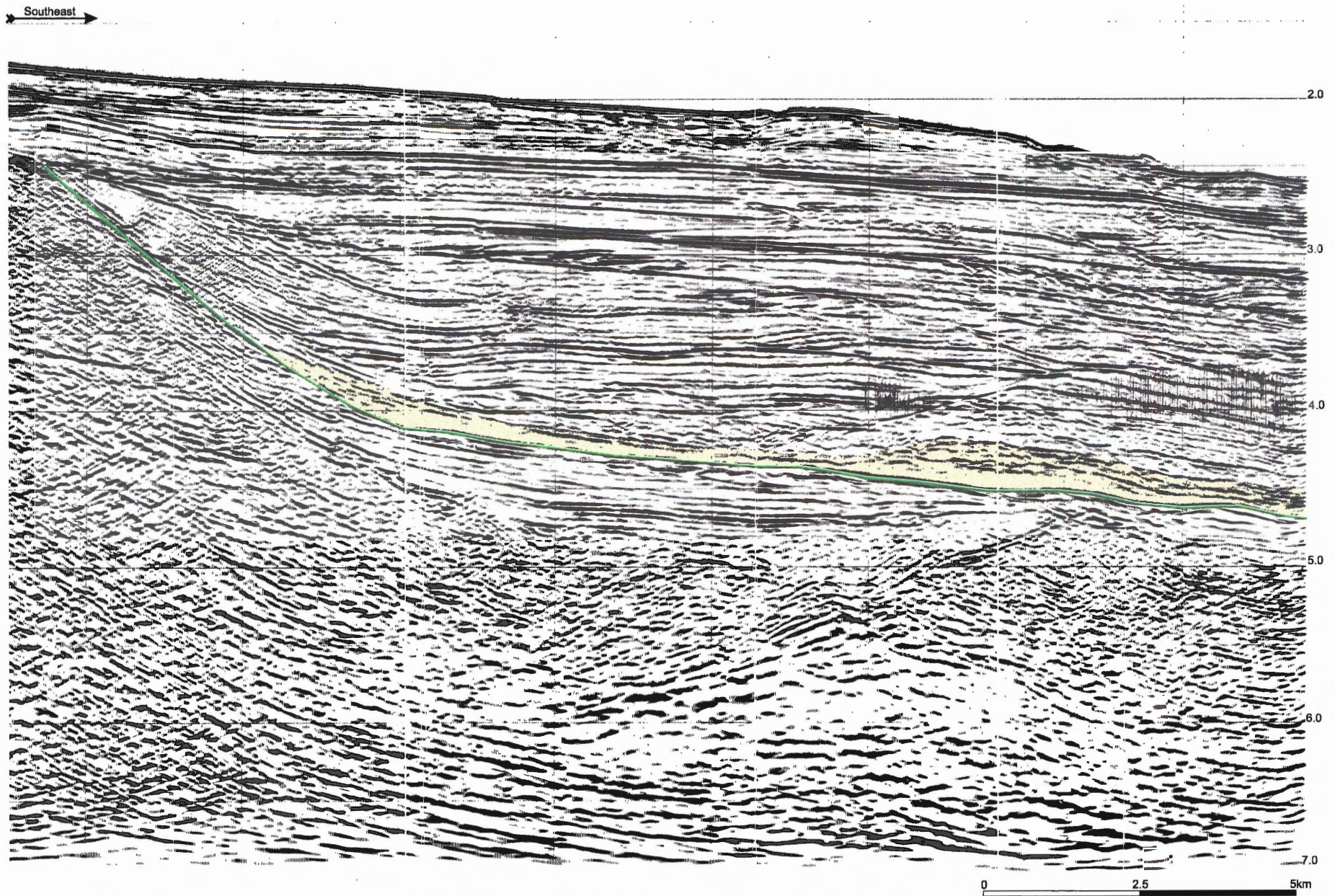


**Figure 5.8:** Submarine fan seismic profile. Major features include a hummocky surface, mounded shape, lateral pinchouts, and downlapping of internal reflectors onto the basin floor. Note the region of little to no reflection at the base of the mound, suggesting chaotic sedimentation. The green line traces the Early Eocene Unconformity and basinal correlative conformity. (Line 6161-83)



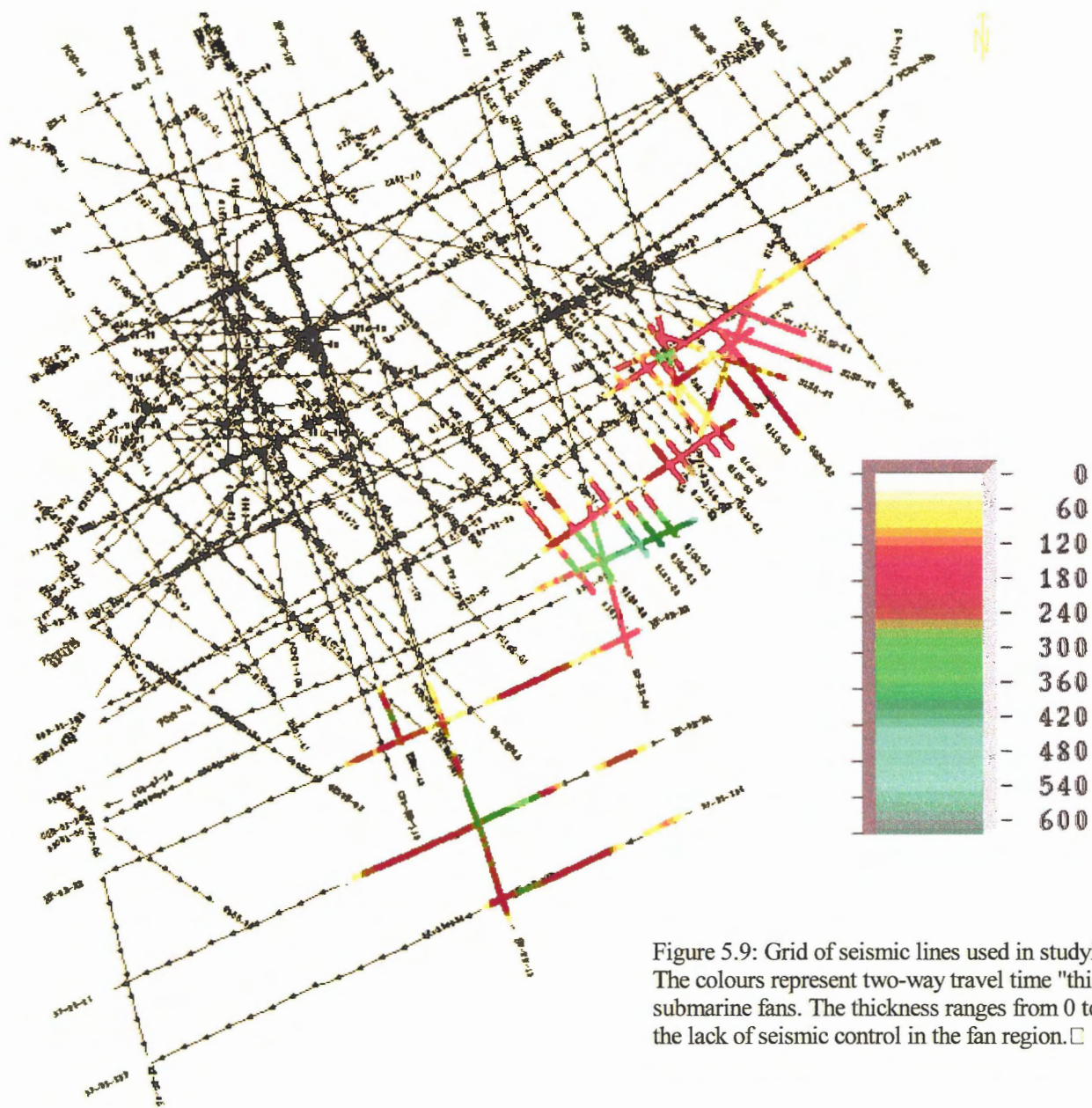


Figure 5.9: Grid of seismic lines used in studying Carson Basin. The colours represent two-way travel time "thickness" of the submarine fans. The thickness ranges from 0 to 450 ms. Note the lack of seismic control in the fan region. □

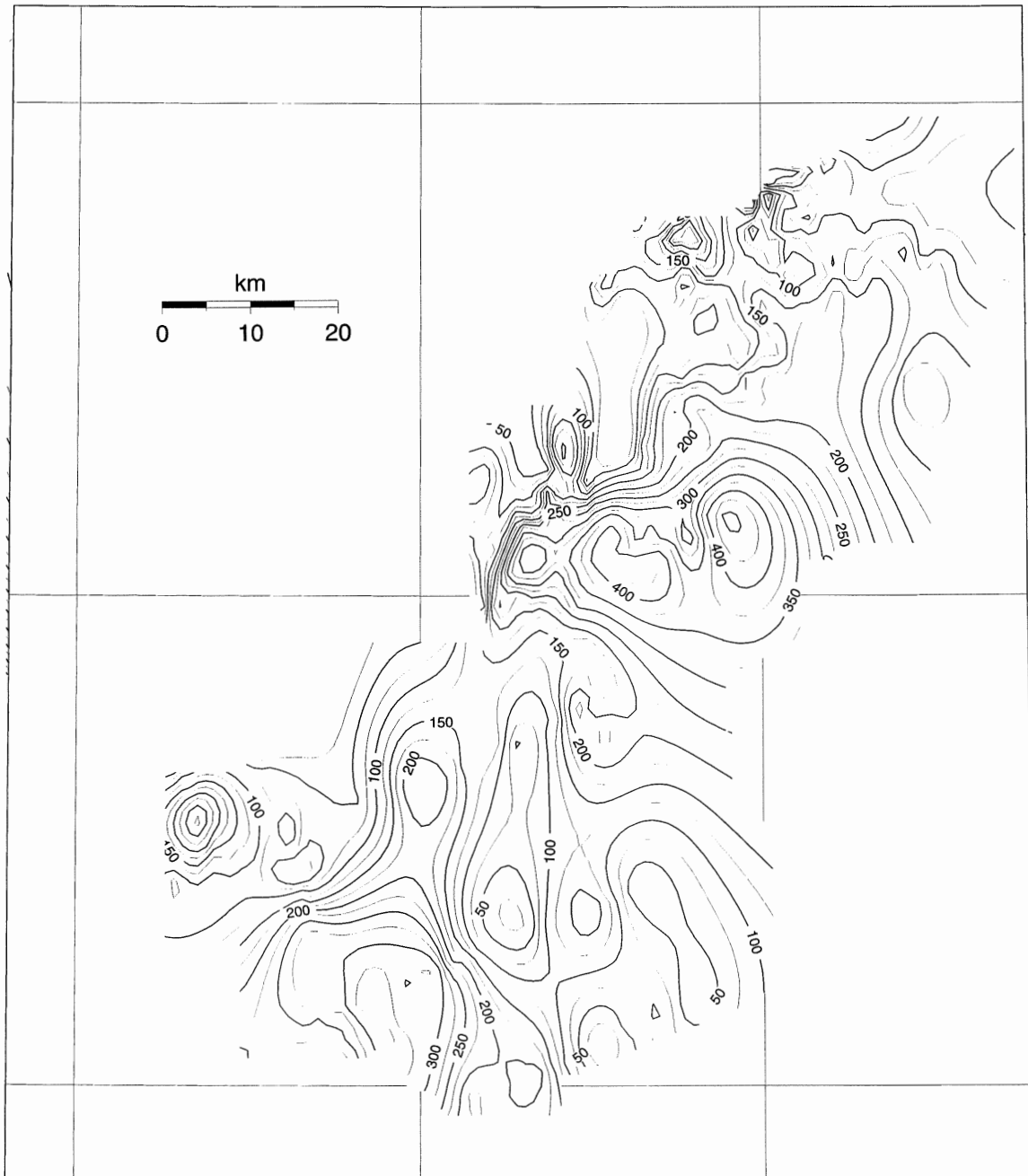
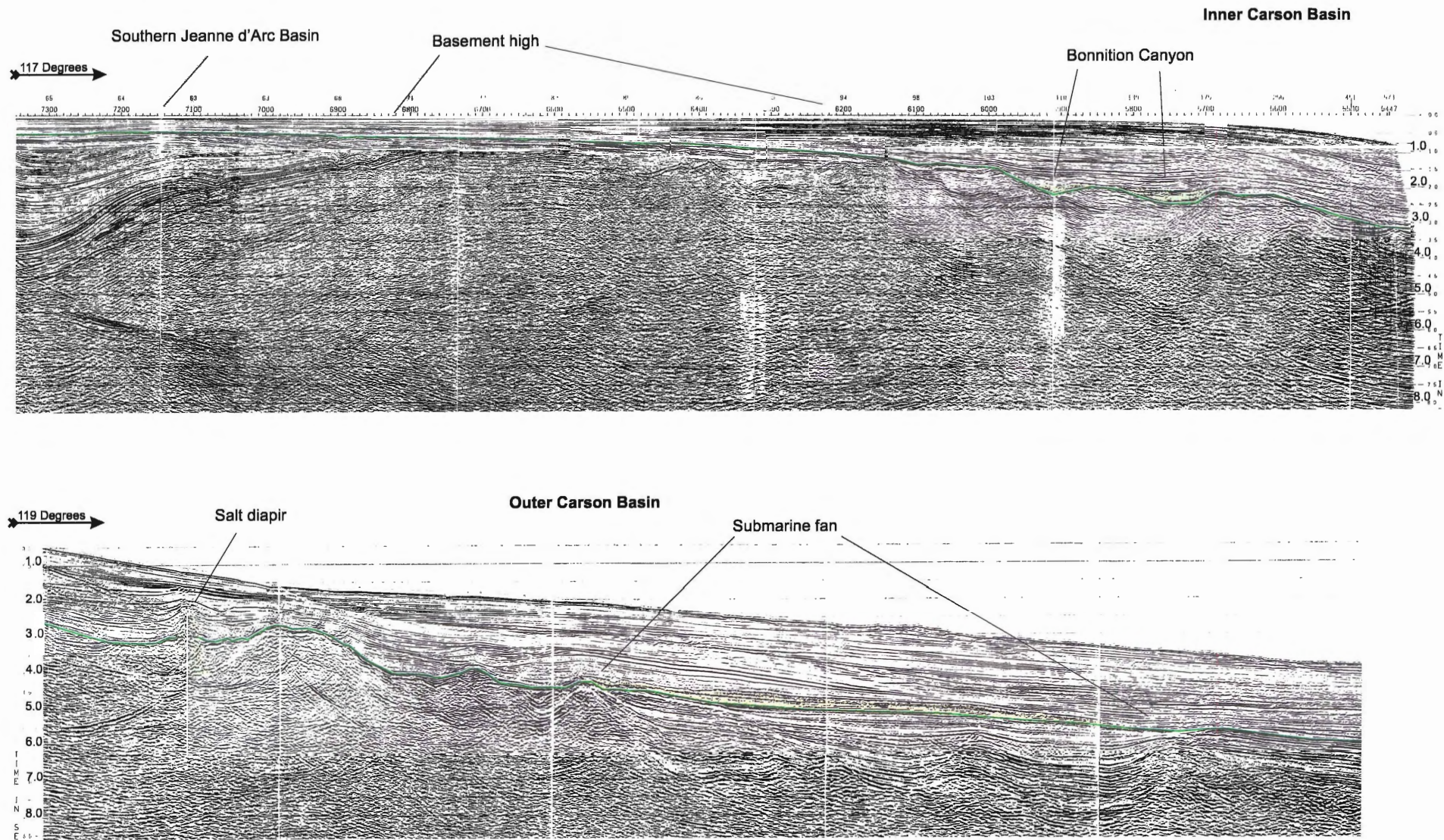


Figure 5.10: Contour map of fan thickness, measured in time. Contours more than 10 minutes of latitude or longitude from an interpreted are omitted.





**Figure 5.11:** Lithoprobe line which travels from the southern Jeanne d'Arc Basin (top left) to the deep water extent of the Carson Basin (bottom right) and captures all of the major features studied in this thesis. Separating the Jeanne d'Arc Basin from the Carson Basin is a wide basement high, where sedimentary cover is thin. To the southeast of this high is the Bonniton Canyon. The Early Eocene Unconformity surface that is traced across the basin (green line) is pierced by salt in the bottom part of the line. Further to the southeast is a complete submarine fan. (Lithoprobe 85-4, 85-4A. The bottom 10 seconds of data have been truncated for the purposes of the figure).

However, Figure 5.11 does show a complete submarine fan which is traceable over 44 km. Although the orientation of the line with respect to the fan's true length and width dimensions is unknown, the conclusion can be drawn that the fan is at least 44 km across.

Figure 5.12 shows the fan thickness map overlain on the Early Eocene erosional surface, which contains the submarine canyons of Carson Basin. The fan distribution correlates well with the trend and position of the canyons, supporting the interpretation of the packages as submarine fans. The largest deposit of fan material occurs to the southeast of the Bonniton Canyon. A second lobe corresponds to the St. George Canyon. The fan material is widespread, covering all of the intervening distance between the two thickest deposits. The seismic profiles show the fans on top of the EEU surface, traced with a green line. At basinal depths, this surface is more accurately described as the correlative conformity of the EEU.

Fans are potential hydrocarbon traps by virtue of their lateral stratigraphic pinchouts. Initial deposits of fans are often sandy, hence submarine fans can serve as both reservoirs and traps for hydrocarbons. The Carson Basin has additional factors increasing the attractiveness of these plays. Figure 5.13 shows a fan in the Carson Basin overlapping and pinching out against a local paleotopographic high. This structural influence may give rise to an upward migration path into the fan material, and also might act as an updip seal if it is salt cored. A number of variations on this play occur in the Carson Basin. However, the fans are primarily in deep water which will continue to discourage exploration in the near future.

### *5.3.2 Canyon Fill and Progradation*

No wells have penetrated the Carson Basin canyons. On seismic profiles, the canyon fill shows negative relief in the upper reaches of the canyon, while lower segments show little relief at



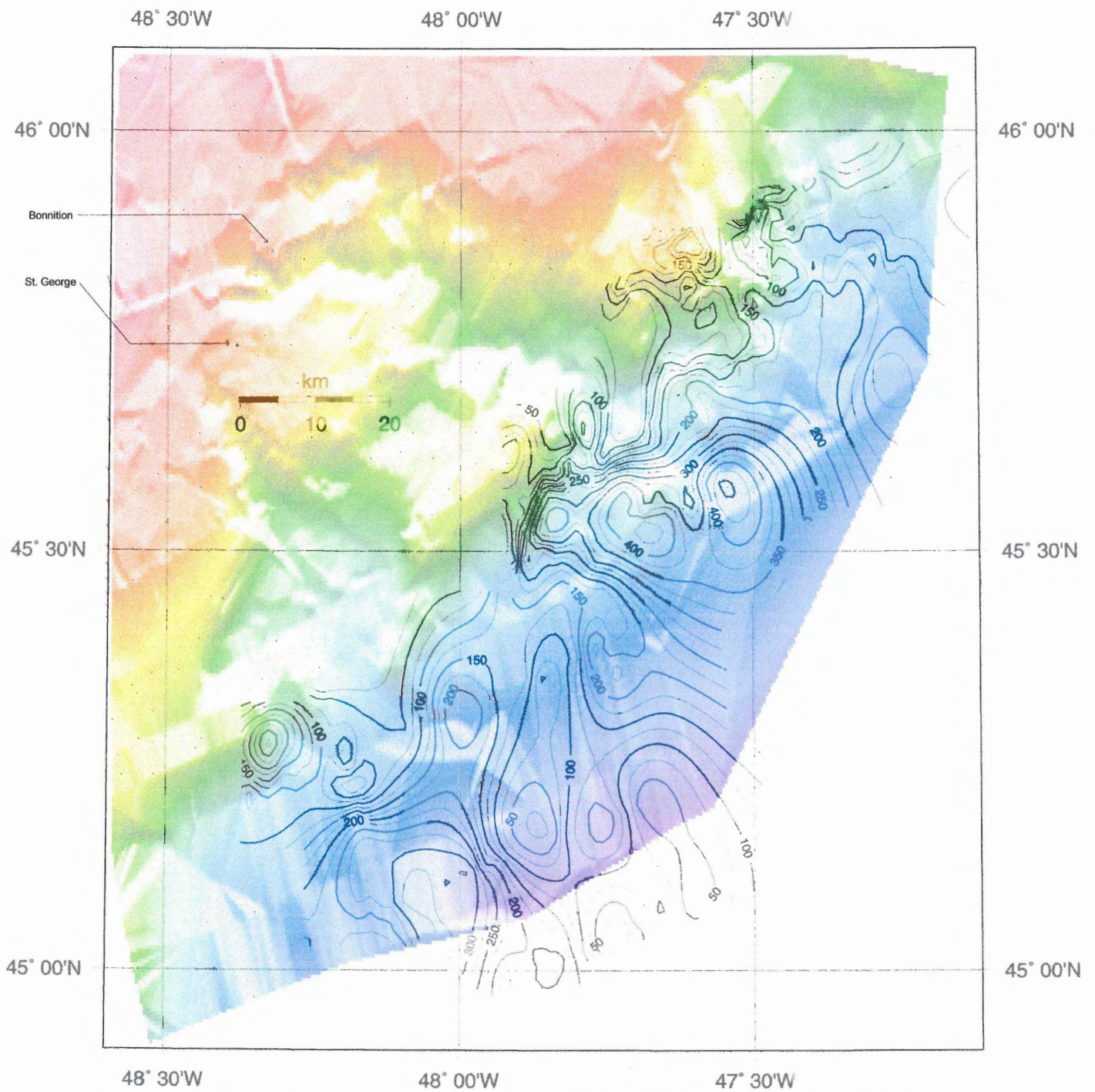
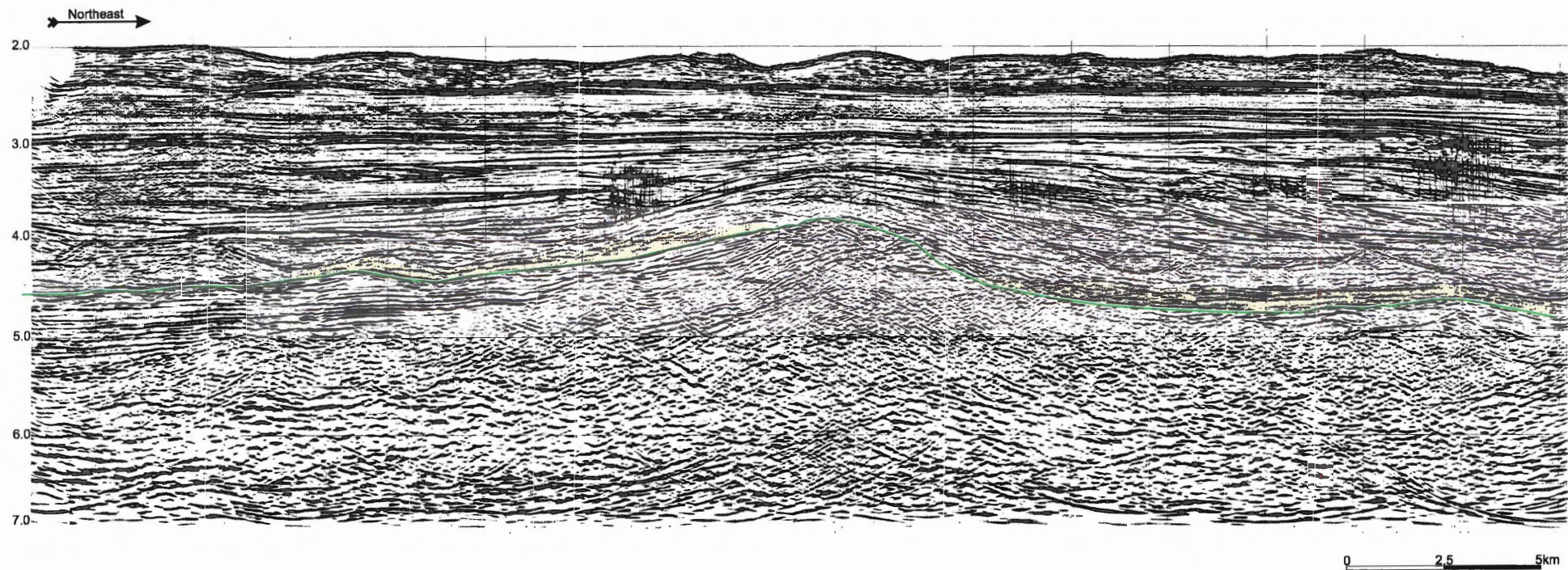


Figure 5.12: Fan thickness contours (in time) overlaid on the Early Eocene Unconformity shaded relief map. The two areas of greatest thickness correspond to the canyon outlets, supporting the interpretation of the packages as submarine fans.





**Figure 5.13:** Seismic profile showing pinchout of a submarine fan against a basement or salt-influenced high. The green line traces the Early Eocene Unconformity and basinal correlative conformity. (Line 6132-83)

all. The relief is attributed to differential compaction, although there is no evidence to account for the lack of relief (positive or negative) in the lower reaches.

The Tertiary Banquereau Formation infills the canyons and overlies the Early Eocene Unconformity basinwide. The formation is composed predominantly of shales and mudstones in the Carson Basin wells, although there are occurrences of thick sandy intervals corresponding to Oligocene/Miocene delta development (Grant and McAlpine 1990). Correlation of the canyon fill directly with other seismic packages and lithologies is difficult because of the lateral variation in thickness. The upper reaches of the Bonnetion Canyon are adjacent to the high separating Carson Basin from the southern Jeanne d'Arc Basin. Hence, units which may be hundreds of meters thick infilling the canyon are considerably thinner at the headward margins of the canyon. The red shaded area of Figure 5.14 shows a progradational package overlying the EEU and canyon fill, suggesting that a major system of sedimentary deposition was stepping out to the shelf edge. The progradational package shows no appreciable thickening where it reaches the canyon, suggesting that the canyon was already filled when this package reached the basinal area. Distal elements of this package that reached the basin earlier can be inferred, filling in the canyons and delivering sediment directly to the paleoslope and Carson Basin. Hence, the canyons were not filled passively by pelagic sedimentation; rather, they were filled by an active sedimentary system.



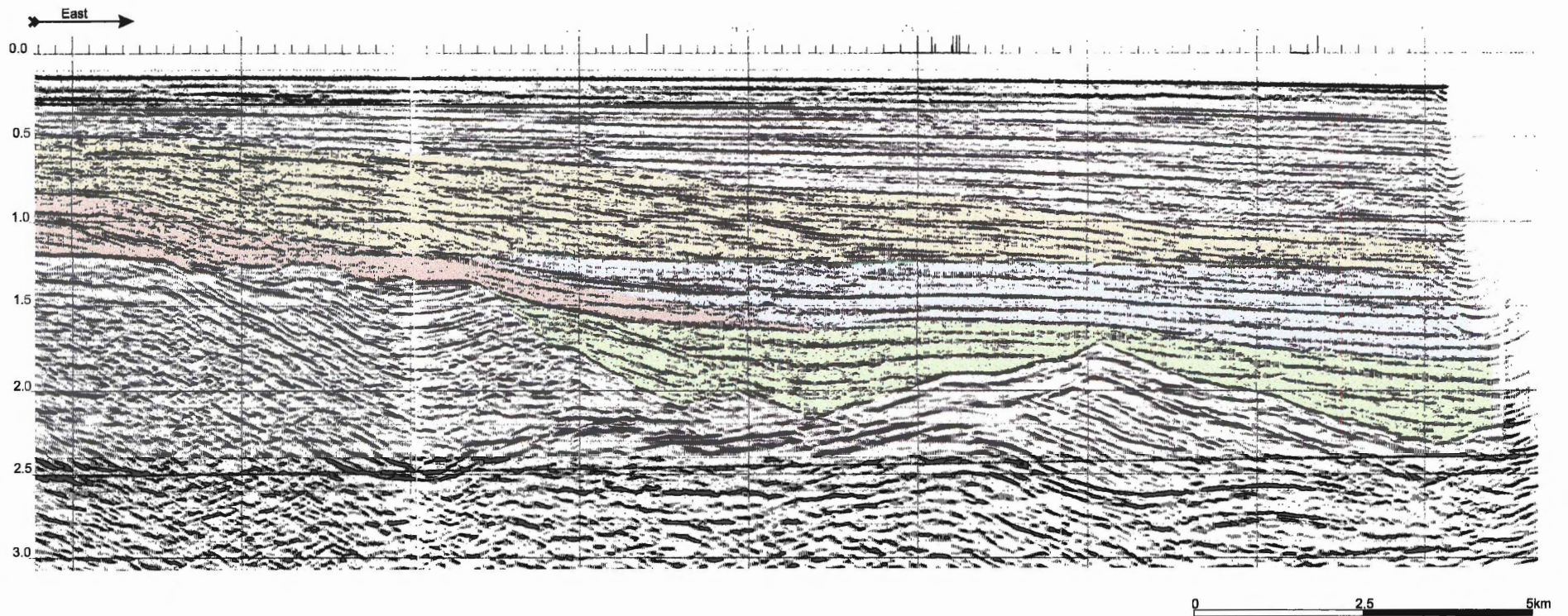


**Figure 5.14:** Seismic profile showing five major packages above the Early Eocene Unconformity. The onlapping canyon fill (green) highlights an erosional remnant. The canyon fill is overlain by a progradational package (red). Rise in relative sealevel resulted in a package (blue) that onlaps the canyon fill and progradational package. Oligocene/Miocene delta progradation (yellow) steps out over much of the section, and is overlain by deep water pelagic sedimentation which continues today. (Line 6130-83)

## **CHAPTER 6: DISCUSSION AND CONCLUSIONS**

### **6.1 Introduction**

From the Barremian through to the beginning of the Tertiary, the Grand Banks region was undergoing a transition from rifting to drifting as discussed in Chapter 3. Tectonic settings were changing rapidly as oceanic crust formed in the north, from the Newfoundland Fracture Zone to the Labrador Sea (Grant and McAlpine 1990). These tectonic changes had widespread effects, resulting in numerous unconformities which are present throughout the basins of the Grand Banks (Grant and McAlpine 1990). However, tectonic influences and sea level changes will not affect each basin contemporaneously; hence, interpretations for the Jeanne d'Arc cannot be applied without modifications to the Carson Basin. Nonetheless, the two basins may indeed be linked.

### **6.2 Correlation with Previously Recognized Erosional Features**

A number of canyon and fan systems have been recognized in the Jeanne d'Arc Basin. These systems have been examined by Boyd (1997), Friis (1997), Shimeld et al. (in prep.), and Deptuck (1998). Three main episodes of canyon development have been constrained; these episodes are closely related to the Coniacian/Santonian, Early Paleocene, and Early Eocene unconformities (Deptuck 1998).

From the Jurassic through to the early stages of the Tertiary, the Carson Basin and Jeanne d'Arc Basin were separated by a wide ridge (Figure 5.11), and therefore the two basins were not in full sedimentary communication. The Carson Basin was also consistently in deeper water than the Jeanne d'Arc Basin, as implied by the more easterly location, the interpreted paleocontinental shelfbreak, and the marked difference in source rock preservation. Hence, canyon and fan activity in the Jeanne d'Arc Basin from the Coniacian/Santonian up to the Paleocene occurred in

confinement, while the Carson Basin was open to the wider sea.

The existence of the Paleocene Unconformity across the Jeanne d'Arc Basin and in the southern regions of the Carson Basin (in the Osprey and Skua wells) demonstrates that it was a widespread event, even though the two basins may not have been in full sedimentary communication. The Hibernia and Rankin Canyons shown in Figure 6.1 were incised during this event, and trend in a similar direction to the canyons mapped in the Carson Basin. The smaller size of the Jeanne d'Arc canyons may reflect their occurrence in a confined basin. If the Paleocene and Eocene Unconformities are so close together as to be unresolvable on both seismic profiles and in the biostratigraphy, the Bonniton and St. George Canyons may have been cut during the Paleocene Unconformity and merely reactivated during the Early Eocene event.

Alternatively, the canyons may have been cut predominantly during the Early Eocene Unconformity. Figure 6.1 also shows the location of Early Eocene erosional and depositional features of the Jeanne d'Arc Basin. The Early Eocene erosion and deposition occur stratigraphically higher than the separating ridge, leading to the possibility of interaction between the two basins. The northwest-southeast direction of transport for the East and West Cormorant Canyons is very similar to the Bonniton and St. George Canyon trend. The Cormorant Canyons appear to have fed a prograding clastic wedge, which was deposited on the high which separates the Jeanne d'Arc Basin and the Carson Basin. The sediments at the outlet of the Cormorant Canyons may be the primary source of unstable material ultimately transported to the submarine fans of Carson Basin.

Early Eocene erosional features in the Jeanne d'Arc Basin have been mapped and interpreted as canyons and gullies (Deptuck 1998). With the recognition of large submarine canyons and fans to the southeast in the Carson Basin, it can be suggested that the Early Eocene erosional features of



the Jeanne d'Arc Basin are subaerially exposed incised valleys, which supplied sediment to the shelf edge in the Carson Basin. The magnitude of the Carson Basin canyons and fans certainly requires a large source of sediments, perhaps more than could be locally derived. A prime candidate is therefore a subaerially exposed Jeanne d'Arc Basin during the Early Eocene. Not shown on Figure 6.1 are a number of smaller channels identified by Deptuck (1998) that support the existence of a channelized, terrestrial environment. These channels occur south of the Cormorant Canyons (Deptuck 1998).

Three major phases of canyon incision have occurred in the southeastern Grand Banks since the Late Cretaceous, with one or more of the events affecting the Carson Basin. Coniacian/Santonian and Paleocene events were confined to the Jeanne d'Arc Basin, but Paleocene incision may have occurred simultaneously in the Carson Basin. Although the Paleocene Unconformity is recorded in the southern Carson Basin, direct evidence in the region of the Bonniton and St. George Canyons is lacking. Seismic profiles and biostratigraphic studies of the Bonniton and St. George wells cannot rule out a Paleocene origin for the canyons. Nevertheless, the Early Eocene Unconformity is recorded in both the Bonniton and St. George wells, and is closely related to the mapped erosional surface. The availability of a large amount of source sediment from the Cormorant Canyons also points to an Early Eocene age of excavation, and this age is therefore the favoured hypothesis.

### **6.3 Paleoenvironment**

The transition to a nearshore marine environment at the Early Eocene Unconformity (Figure 4.5) corresponds to the submarine canyon excavation as shown by well-to-seismic correlations using synthetic seismograms. Both the widespread erosion and change in environment point to a marked decrease in water depth in the Bonniton/St. George area during the Early Eocene. Unfortunately,



the biostratigraphic control does not provide clues as to what influenced the regional drop in water depth, be it eustatic sealevel change or regional tectonic uplift. Either change would generate increased erosion from newly exposed or uplifted sedimentary sources, and both causes would create conditions necessary for incision of the paleoshelf. Nevertheless, it can be concluded that the shoreline must have moved much closer to the shelf edge during the Early Eocene, and hence the canyons were not simply the result of a change in bottom currents or one-time turbidites. Indeed, both the magnitude of the canyons and the existence of submarine fans is consistent with a large change in sediment supply to the region. Subaerial exposure of previously submerged regions close to the Bonniton area can therefore be inferred from the fossil indicators.

The progression of the Bonniton and St. George Canyons fits the pattern of many classic submarine canyon-fan systems. A drop in relative sealevel brought the shoreline closer to the shelfbreak, increasing sediment supply to the edge of the shelf. The increased flux of sediment was transported off the shelf by channels and canyons which incised the shelfbreak. Deltas stepped out towards the shelf edge as sealevel remained low. Canyon excavation and deposition of submarine fans eventually stabilized as the system reached equilibrium. A relative rise in sealevel (indicated by the change in marine environment of the Bonniton fossils) resulted in backfilling of the canyon as the paleoshoreline moved away from the shelf edge. Delta progradation continued during the initial sealevel rise and canyon filling, and in fact the arrival of the prograding package in the canyon region occurs at the end of canyon filling (Figure 5.14). Delta progradation then faltered during the continued rise in relative sealevel, and was followed by onlap as the rise swamped progradation (Figure 5.14). The Bonniton fossils then record a transition to an outer neritic marine environment, until the return of nearshore marine conditions (delta progradation) in the Oligocene and Miocene.

These relative changes in sealevel therefore controlled canyon development and eventually buried the canyon-fan systems.

#### **6.4 Summary**

Erosion during the period of the Early Eocene Unconformity correlates with a change in environment from outer neritic to nearshore marine. The paleoshoreline regressed to the southeast, subaerially exposing the Jeanne d'Arc Basin. The exposure carved channels and incised valleys, carrying sediment southeast to the edge of the continental shelf. This shelf edge occurred in the Carson Basin, and the high sediment load coupled with lower water depths resulted in the formation of two large submarine canyons- Bonniton and St. George. These two submarine canyons cut the shelfbreak and carried sediments basinward to form thick submarine fans. A return to higher relative sealevel backfilled the canyon and progradation of the supplying clastic wedge ceased. The canyons were buried by an onlapping package, and later covered by sediments brought to the shelf edge during Oligocene and Miocene delta-building events. The end of tectonic activity coupled with thermal subsidence in the area returned deepwater conditions to the region, which have continued to the present day.

The submarine fans of the Carson Basin are areally extensive, thick deposits which may act as both reservoir and trap for hydrocarbons present in the basin. Stratigraphic pinchouts and salt tectonism create favourable conditions for hydrocarbon plays, however the present deep water environment and questionable source rock potential will continue to curtail exploration.

#### **6.5 Recommendations for Future Work**

Four recommendations could have a major impact on further studies in the Carson Basin. New biostratigraphic studies of the St. George well would be of immense value in further



constraining the Paleocene and Eocene Unconformities, creating a clearer picture of the paleoenvironment and erosional history of the northern part of Carson Basin.

Burial history and subsidence modeling of the basin and canyon fill would increase understanding of the unconformities and sedimentation rates. These studies would help create maturation curves for hydrocarbon potential, and the compaction of canyon fill could be examined as well to determine its composition.

The development of a velocity model for the formations in Carson Basin would allow depth conversions. These depth conversions may have large effects on studied features, as time-structure maps can both exaggerate and mute buried structures.

Finally, examination of non-industry seismic data from sources such as the Geologic Survey of Canada (GSC), Institute of Ocean Sciences (IOS), and Woods Hole Oceanographic Institution (WHOI) may further constrain the areal extent of the submarine fans.

## REFERENCES

- Boyd, H.K. 1997. Modelling of a Paleocene Submarine Canyon, Jeanne d'Arc Basin, Offshore Newfoundland, To Determine Canyon Fill Lithology. Honours Thesis, Department of Earth Sciences, Dalhousie University, Halifax, Nova Scotia, Canada. 46 pp.
- Burgess, P.M., and Hovius, N. 1998. Rates of Delta Progradation During Highstands: Consequences for Timing of Deposition in Deep-Marine Systems. *Journal of the Geological Society* **155**: 217-222.
- Deptuck, M.E. 1998. Characterization and Interpretation of Late Cretaceous to Eocene Erosional Features and Submarine Fans of the Jeanne d'Arc Basin, Offshore Newfoundland. Honours Thesis, Department of Geology, Saint Mary's University, Halifax, Nova Scotia, Canada. 99 pp.
- Friis, N. 1997. A Well Log and 3-D Seismic Study of the Late Cretaceous to Eocene Deposits in the Hibernia Area of the Jeanne d'Arc Basin, Offshore Newfoundland, Canada. Masters Thesis, Department of Earth Sciences, University of Aarhus, Denmark. 88 pp.
- Grant, A.C., Jansa, L.F., McAlpine, K.D., and Edwards, A. 1988. Mesozoic-Cenozoic Geology of the Eastern Margin of the Grand Banks and its Relation to Galicia Bank. *In: Proceedings of the Ocean Drilling Program, Scientific Results, 103. Edited by: Boillot, G., Winterer, E.L., et al. Ocean Drilling Program, College Station, Texas, pp. 787-808.*
- Grant, A.C. and McAlpine, K.D. 1990. The Continental Margin Around Newfoundland. *In: Geology of the Continental Margin of Eastern Canada. Edited by: Keen, M.J. and Williams, G.L. Geological Survey of Canada, Geology of Canada, no. 2, pp. 239-292.*
- Hardy, I.A., and Jackson, A.E. 1980. A Compilation of Geochemical Data: East Coast Exploratory Wells. Geological Survey of Canada, Open File Report 694.
- McAlpine, K.D. 1990. Mesozoic Stratigraphy, Sedimentary Evolution, and Petroleum Potential of the Jeanne d'Arc Basin, Grand Banks of Newfoundland. Geological Survey of Canada, Paper 89-17, 50 pp.
- Mitchum Jr., R.M. 1985. Seismic Stratigraphic Expression of Submarine Fans. *In: Seismic Stratigraphy II: An Integrated Approach to Hydrocarbon Exploration, AAPG Memoir 39. Edited By: Berg, O.R. and Woolverton, D.G. Tulsa, Oklahoma, pp. 117-138.*
- Nelson, H. C. 1984. Modern Fan Morphology. *In: Modern and Ancient Deep-Sea Fan Sedimentation: Lecture Notes for SEPM Short Course No. 14. Edited By: Nelson, H.C. and Nilsen, T.H. Tulsa, Oklahoma, pp. 38-71.*

- Posamentier, H.W. and Erskine, R.D. 1991. Seismic Expression and Recognition Criteria of Ancient Submarine Fans. *In: Seismic Facies and Sedimentary Processes of Submarine Fans and Turbidite Systems. Edited by: Weimer, P. and Link, M.H.* New York, pp. 197-222.
- Posamentier, H.W. and Vail, P.R. 1988. Eustatic Controls on Clastic Deposition II: Sequence and Systems Tract Models. *In: Sea Level Change: An Integrated Approach, SEPM Publication 42. Edited by: Wilgus, C.K., Hastings, B.S., Kendall, C.G.St.C., Posamentier, H.W., Ross, C.A., and Van Wagoner, J.C.,* pp. 125-154.
- Powell, T.G. 1985. Paleogeographic Implications for the Distribution of Upper Jurassic Source Beds: Offshore Eastern Canada. *Bulletin of Canadian Petroleum Geology* **33**: 116-119.
- Pratson, L.F., and Coakley, B.J. 1996. A Model for the Headward Erosion of Submarine Canyons Induced by Downslope-Eroding Sediment Flows. *Geological Society of America Bulletin* **108**: 225-234.
- Pratson, L.F., Ryan, W.B.F., Mountain, G.S., and Twichell, D.C. 1994. Submarine Canyon Initiation by Downslope-Eroding Sediment Flows: Evidence in Late Cenozoic Strata on the New Jersey Continental Slope. *Geological Society of America Bulletin* **106**: 395-412.
- Prothero, D.R., and Schwab, F. 1996. *Sedimentary Geology*. New York, W.H. Freeman and Company. 575 pp.
- Ryan, W.B.F., Cita, M.B., Miller, E.L., Hanselman, D., Nesteroff, W.D., Hecker, B., and Nibbelink, M. 1978. Bedrock Geology in New England Submarine Canyons. *Oceanologica Acta* **1**: 233-254.
- Shepard, F.P. 1981. Submarine Canyons: Multiple Causes and Long-Time Persistence. *The American Association of Petroleum Geologists Bulletin* **65**: 1062-1077.
- Shepard, F.P. and Dill, R.F. 1966. *Submarine Canyons and Other Sea Valleys*. Chicago, Rand McNally and Co. 381 pp.
- Shimeld, J., Williamson, M.A., Cofflin, K.C., and Prior, D.B. in prep. A Buried Paleocene Submarine Canyon System, Offshore Newfoundland. GSC-Atlantic.
- Tankard, A.J. and Welsink, H.J. 1989. Mesozoic Extension and Styles of Basin Formation in Atlantic Canada. *In: Extensional Tectonics and Stratigraphy of the North Atlantic Margins, AAPG Memoir 46. Edited by: Tankard, A.J., and Balkwill, H.R.* Tulsa, Oklahoma, pp. 175-195.

- Twichell, D.C. and Roberts, D.G. 1982. Morphology, Distribution and Development of Submarine Canyons on the United States Atlantic Continental Slope Between Hudson and Baltimore Canyons. *Geology* **10**: 408-412.
- Walker, R.G. 1992. Turbidites and Submarine Fans. *In: Facies Models: Response to Sea Level Change. Edited by: Walker, R.G. and James, N.P.* Geological Association of Canada, St. John's, Newfoundland, pp. 239-264.
- Welsink, H.J., Srivastava, S.P., Tankard, A.J. 1989. Basin Architecture of the Newfoundland Continental Margin and Its Relationship to Ocean Crust Fabric During Extension. *In: Extensional Tectonics and Stratigraphy of the North Atlantic Margins, AAPG Memoir 46. Edited by: Tankard, A.J., and Balkwill, H.R.* Tulsa, Oklahoma, pp. 197-213.
- Williams, H. 1984. Miogeoclines and Suspect Terranes of the Caledonian-Appalachian Orogen: Tectonic Patterns in the North Atlantic Region. *Canadian Journal of Earth Sciences*, **21**: 887-901.
- Williams, H. 1979. Appalachian Orogen in Canada. *Canadian Journal of Earth Sciences*, **16**: 792-807.

## APPENDIX 1: WELLS

AMOCO-Imperial-Skelly Osprey G-84	
<b>Unique Well ID:</b>	300 G84 44500 49150
<b>Location:</b>	44° 43' 28.76" N x 49° 27' 22.99" W
<b>Spud Date:</b>	July 9, 1973
<b>Well Class:</b>	New Field Wildcat
<b>Rotary Table:</b>	85 feet (25.9 m)
<b>Water Depth:</b>	201 feet (61.3 m)
<b>Total Depth:</b>	11, 397 feet (3473.8 m)
<b>Gas/Oil:</b>	None
<b>Status:</b>	Abandoned August 16, 1973

*original units: Imperial*

### WELL HISTORY:

Osprey G-84 is located approximately two hundred and sixteen nautical miles southeast of St. John's Newfoundland, in the Carson Basin. This well was spudded as a new field wildcat on July 9, 1973 in 201 feet of water. The total depth reached was 11,397 feet (3473.8 m). The well was drilled to test a closed anticlinal structure interpreted from seismic data. The structure is present beneath a regional mid-Cretaceous angular unconformity.

The well penetrated 2780 feet of Tertiary age marine sands and shales and 684 feet of Cretaceous marine shales and sands above the angular unconformity. The section below the unconformity included 654 feet of a carbonate-evaporite sequence, 6723 feet of interbedded salt and red shales, and 557 feet of clastic red beds. These last three sections are presumed to be Lower Jurassic or older in age.

No hydrocarbons were encountered during the drilling of the well, and no drill-stem tests were run after completion of well logging. Osprey G-84 was abandoned on August 16, 1973.



## APPENDIX 1: WELLS

<b>Mobil-Gulf Bonniton H-32</b>	
<b>Unique Well ID:</b>	300 H32 46000 48150
<b>Location:</b>	45° 51' 26.79" N x 48° 19' 31.76" W
<b>Spud Date:</b>	December 2, 1973
<b>Well Class:</b>	New Field Wildcat
<b>Rotary Table:</b>	98 feet (29.9 m)
<b>Water Depth:</b>	334 feet (101.8 m)
<b>Total Depth:</b>	10,000 feet (3048.0 m)
<b>Gas/Oil:</b>	Minor gas show
<b>Status:</b>	Abandoned January 2, 1974

*original units: Imperial*

### WELL HISTORY:

Bonniton H-32 is located approximately 244 miles to the southeast of St. John's Newfoundland, in the Carson Basin. This well was spudded as a new field wildcat on December 2, 1973 in 334 feet of water. The total depth reached was 10,000 feet (3048.0 m). The well was drilled over a collapse zone of the Carson Basin interpreted from seismic data.

The well penetrated 4230 feet of Quaternary and Tertiary sediments, 60 feet of Upper Cretaceous, approximately 3300 feet of Lower Cretaceous, and another 2410 feet of Upper Jurassic sediments. No significant hydrocarbon shows were encountered, and consequently the well was plugged and abandoned as of January 2, 1974. No drill-stem tests were run.

## APPENDIX 1: WELLS

<b>AMOCO-Imperial-Skelly Skua E-41</b>	
<b>Unique Well ID:</b>	300 E41 45300 48450
<b>Location:</b>	45° 20' 23.23" N x 48° 52' 26.26" W
<b>Spud Date:</b>	August 31, 1974
<b>Well Class:</b>	New Field Wildcat
<b>Rotary Table:</b>	98 feet (29.9 m)
<b>Water Depth:</b>	272 feet (82.9 m)
<b>Total Depth:</b>	10,626 feet (3238.8 m)
<b>Gas/Oil:</b>	None
<b>Status:</b>	Abandoned October 21, 1974

*original units: Imperial*

### **WELL HISTORY:**

Skua E-41 is located 240 miles southeast of St. John's Newfoundland, in the Carson Basin. The well was drilled as a new field wildcat on August 31, 1974 in 272 feet of water (82.9 m). The total depth reached was 10,626 feet (3238.8 m). The well was drilled near the north edge of the Carson Basin where seismic data showed structural closure within the Jurassic.

The well penetrated 3,294 feet of Quaternary and Tertiary sediments below the sea floor, followed by 931 feet of Cretaceous and 6,031 feet of Jurassic sediments. No significant hydrocarbon shows were encountered. Drill-stem tests were not conducted, and the well was abandoned as of October 21, 1974.

## APPENDIX 1: WELLS

<b>Canterra-PCI St. George J-55</b>	
<b>Unique Well ID:</b>	300 J55 45500 48150
<b>Location:</b>	45° 44' 40" N x 48° 23' 4" W
<b>Spud Date:</b>	April 9, 1986
<b>Well Class:</b>	New Field Wildcat
<b>Rotary Table:</b>	23.5 m
<b>Water Depth:</b>	104.5 m
<b>Total Depth:</b>	4100.2 m
<b>Gas/Oil:</b>	None
<b>Status:</b>	Abandoned

*original units: metric*

### WELL HISTORY:

St. George J-55 was spud April 9, 1986 in 104.5 m of water. The well was drilled to the Upper Jurassic at 4100.5 m of total depth. No prospective hydrocarbons were encountered, and the well was subsequently abandoned.

Amoco-Imperial-Skelly Osprey G-84

<b>FORMATION</b>	<b>Top: CNOPB (1990)</b>	<b>Top: McAlpine (1988)</b>	<b>Tops Used in This Study</b>
Banquereau Formation	0	0	0
Base Tertiary Unconformity	868	867	868 (Early Eocene)
Wyandot Member	868	867	868
Dawson Canyon Formation	868	918 <sup>1</sup>	868
Petrel Member	926	984	-
Eider Unit	1023	-	1023
Cenomanian Unconformity	1023	1056	1023
Iroquois Formation	1056	1056	1056
Argo Formation	1254	1252	1254
Unconformity	-	1692	-
Osprey Formation	-	1692	1692
Eurydice Formation	3304	3306	3304

<sup>1</sup>Wyandot was not recognized as part of the Dawson Canyon Formation until McAlpine (1990).

Amoco-Imperial-Skelly Osprey G-84

<b>Age</b>	<b>Bio-Strat. Tops: Bujak and Williams (1979)</b>
Late Miocene	253.0
Middle Miocene	307.8
Early Miocene	335.3
Middle-Late Oligocene	362.7
Early Oligocene	445.0
Early-Middle Eocene	746.8
Early Eocene	801.6
Late Paleocene?	829.6
Santonian-Campanian	856.5
Turonian-Coniacian	1027.2
Cenomanian	1057.7
Hettangian-Sinemurian	1103.4
Rhaetian	1370.7
(Indeterminate)	1642.9
Carnian-Norian	1917.2

<b>Unconformity</b>	<b>Gap (hiatus or erosion)</b>
Early Eocene	Maastrichtian, Early/Middle Paleocene
Cenomanian	Pleinsbachian, Toarcian, Middle-Late Jurassic, Early Cretaceous



Mobil-Gulf **Bonnition H-32**

<b>FORMATIONS</b>	<b>Tops: CNOPB (1990)</b>	<b>Tops: McAlpine (1988)</b>	<b>Tops Used in This Study</b>
Banquereau Formation	0	0	0
South Mara Member	1268	1268	1268
Unconformity	-	1268	-
Base Tertiary Unconformity	1291	1291	1291 (Early Eocene)
Lower Cretaceous Limestone	1291	-	1291
Dawson Canyon Formation	-	1291	-
Unconformity	-	1301	-
Nautilus Shale	-	1301	-
Unnamed L. Cret. Sandstone	-	1409	-
Whiterose Shale Equivalent	1426	2054	1426
Hibernia Equivalent	1458	-	1458
Unnamed Limestone	-	2407	-
Fortune Bay Shale Equivalent	1640	2491	1640
Jeanne d'Arc Equivalent	1725	2798	1725
Tithonian Unconformity	2054	-	2054
Unconformity	-	2962	-
Rankin Formation	2233	2962	2233

Mobil-Gulf **Bonntonion H-32**

<b>Age</b>	<b>Bio-Strat. Tops: Ascoli (1988)</b>
Early and Middle Miocene	301.8-338.3
Oligocene	548.6
Late Eocene	818.1
Middle Eocene	1020.5
Early Eocene	1296.6
Unconformity	1300.9
Barremian	1307.6
Hauterivian	1874.5
Valanginian	2118.4
Late Berriasian	2209.8
Early Berriasian	2235.1
Late Tithonian	2286
Early Tithonian	2432.9
Late Kimmeridgian	2484.1
Early Kimmeridgian	2590.8

<b>Unconformity</b>	<b>Gaps (hiatus or erosion)</b>
Early Eocene	Aptian, Albian, Late Cretaceous, Paleocene

Amoco-Imperial-Skelly Skua E-41

<b>FORMATION</b>	<b>Tops: CNOBP (1990)</b>	<b>Tops: McAlpine (1988)</b>	<b>Tops Used in This Study</b>
Banquereau Formation	0	0	0
Unconformity	-	1077	1077 (Early Eocene)
South Mara Member	1077	1077	1077
Base Tertiary Unconformity	1117	1117	1117 (Early Paleocene)
Dawson Canyon Formation	1117	1181 <sup>1</sup>	1117
Wyandot Member	1117	1117	1117
Petrel Member	-	1274	-
Cenomanian Unconformity	1319	-	1319
Eider Unit	1319	1319	1319
Aptian Unconformity	1341	1342	1341
Hibernia Equivalent	1341	1342	1341
Fortune Bay Shale Equivalent	1370	1369	1370
Tithonian Unconformity	1571	-	1571
Unconformity	-	1749	-
Rankin Formation	-	1749	1571
Voyager Formation	1571	1994	1590
Downing Formation	2337	2337	2337
Whale Member	-	2814	-

<sup>1</sup>Wyandot was not recognized as part of the Dawson Canyon Formation until McAlpine (1990).

Amoco-Imperial-Skelly Skua E-41

Age	Bio-Strat. Tops: Robertson (1982)	Bio-Strat. Tops: Bujak (1979)
Miocene or younger	-	295.7
Middle Miocene	-	350.5
Early Miocene	-	423.7
Middle-Late Oligocene	-	588.3
Late Eocene/Early Oligocene	-	688.8
Late Eocene	-	824.5
Middle Eocene	-	908.3
Early Eocene	-	990.6
Early Paleocene	-	1072.9
Campanian	-	1158.2
Santonian	-	1292.4
Albian-Santonian	-	1314.3
(Indeterminate)	-	1319.8
Neocomian	1466.1	1357.9
Portlandian (Tithonian)	-	1539.2
Kimmeridgian	1630.7	1585.0
Oxfordian-Early Kimmeridgian	-	1889.0
Oxfordian?	2042.2	-
Late Oxfordian	2179.3	-
Early Oxfordian	2296.7	-
Callovian-Oxfordian	-	2225.0
Late Callovian	2316.8	-
Middle Callovian	2383.5	-
Early Callovian	2423.2	-
Bathonian-Early Callovian	2500.9	-
Middle-Early Bathonian	2598.4	-
Bajocian-Bathonian	2760.0	2347.0
Bajocian	2845.3	-
L.Pliensbachian-Toarcian-Aalenian	-	2856.0
Lower Toarcian-Aalenian	3002.3	-
Lower Pliensbachian-Early Toarcian?	3157.7	-

Unconformity	Gap (hiatus or erosion)
Early Eocene	Middle-Late Paleocene
Early Paleocene	Maastrichtian
Albian-Aptian	Velanginian, Hauterivian, Barremian, Aptian

Canterra-PCI St. George J-55

<b>FORMATIONS</b>	<b>Tops: CNOBP (1990)</b>	<b>Tops: McAlpine (1988)</b>	<b>Tops Used in This Study</b>
Banquereau Formation	0	0	0
Base Tertiary Unconformity	1421	1421	1421 (Early Eocene)
Dawson Canyon Formation	1421	1457 <sup>1</sup>	1421
Wyandot Member	1421	1421	1421
Cenomanian Unconformity	1479	1479	1479
Nautilus Shale Equivalent	1479	1479	1479
Aptian Unconformity	1840	-	1840
Avalon Equivalent	1840	-	1840
“A” Marker Member Equiv.	1840	-	1840
Unnamed L. Cret. Sandstone	-	1857	-
Whiterose Shale Equivalent	2017	3006	2017
Hibernia Equivalent	2385	-	2385
Unnamed Limestone	-	3858	-
Fortune Bay Shale Equivalent	3006	3902	3006
Jeanne d’Arc Equivalent	3287	-	3287
Tithonian Unconformity	3714	-	3714
Rankin Formation	3859	-	3859

<sup>1</sup>Wyandot was not recognized as part of the Dawson Canyon Formation until McAlpine (1990).



Canterra-PCI St. George J-55

<b>Age</b>	<b>Bio-Strat. Tops: (Canterra 1986)</b>
Eocene-Recent	0
Maastrichtian-Paleocene Unconformity	1421
Campanian	1421
Unconformity	1479
Albian	1479
Aptian	1633
Unconformity	1848
Hauterivian-Barremian	1848
Unconformity	3475
Early Kimmeridgian	3475
Late Kimmeridgian	3950

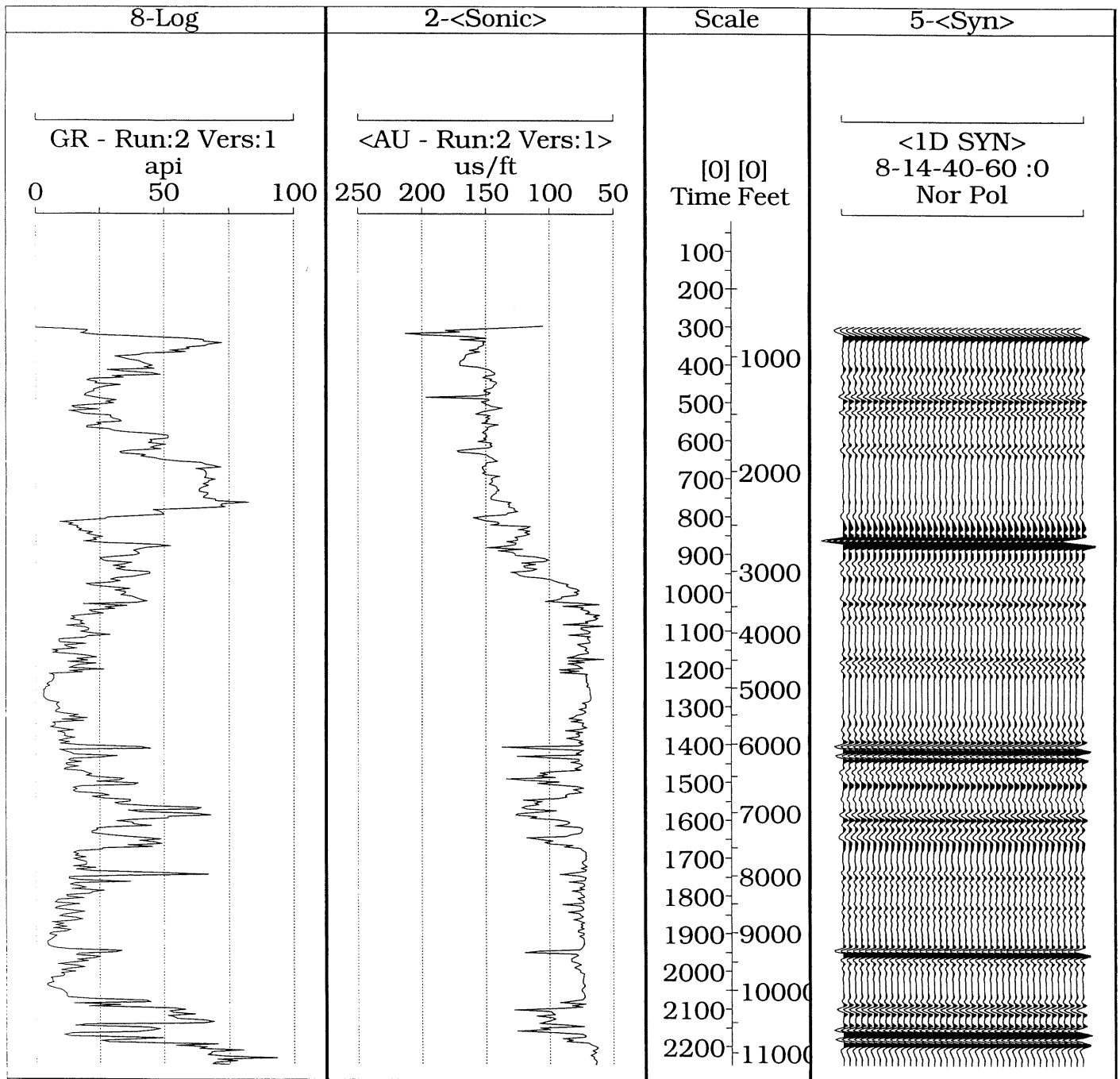
<b>Unconformity</b>	<b>Gaps (hiatus or erosion)</b>
Eocene	Maastrichtian, Paleocene
Campanian?	Cenomanian, Turonian, Coniacian, Santonian
Aptian?	part of Aptian?
Neocomian?	Tithonian, Berriasian, Velanginian

*-resolution of biostratigraphy makes it difficult to pick unconformities*

### APPENDIX 3: SYNTHETIC SEISMOGRAMS

Intersecting lines (within 500 m of each well):

WELL	LINE	SHOTPOINT
<b>Osprey</b>	6307C-85	8100
	6304-85	850
<b>Bonntion</b>	HM81-36	925
	5000-82	100
	PCP81-067C	1738
	PCP81-067D	2500-2520
	6307-85	50
	6165-83	250
	6163-83	250
	CNF82-18	3900
<b>Skua</b>	CGB82-115	550
	HM81-30/3	3300
	6300-85	700
	6307D-85	12400
<b>St. George</b>	6124-83	100
	FC83-49A	4500



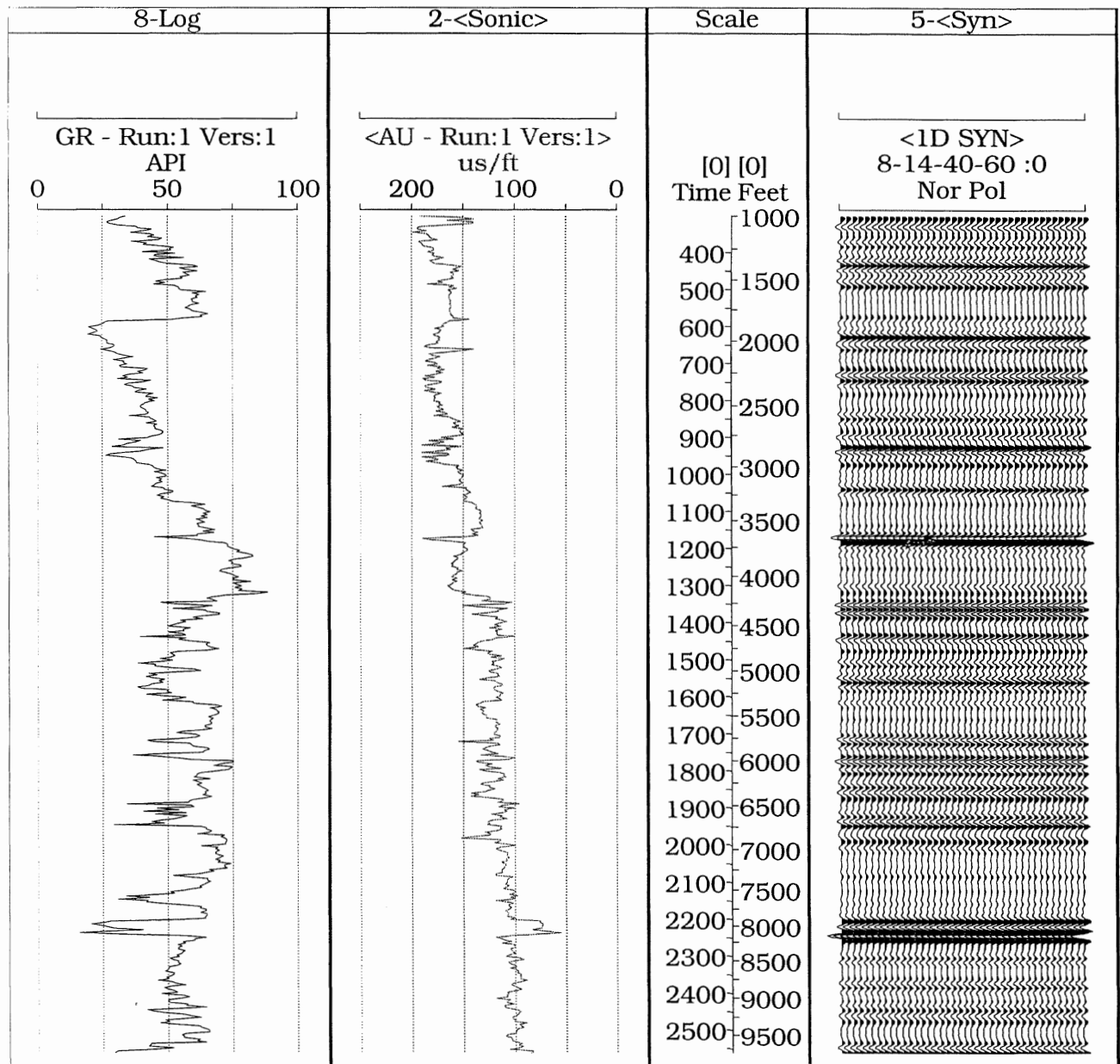
SynTool - Copyright (C) 1991-1996 Landmark Graphics Corp.

Date: Dec 11, 1998 Time: 9:41:26

Osprey G-84  
Scale: 2.5 in/s

Osprey Well for line 6304-85

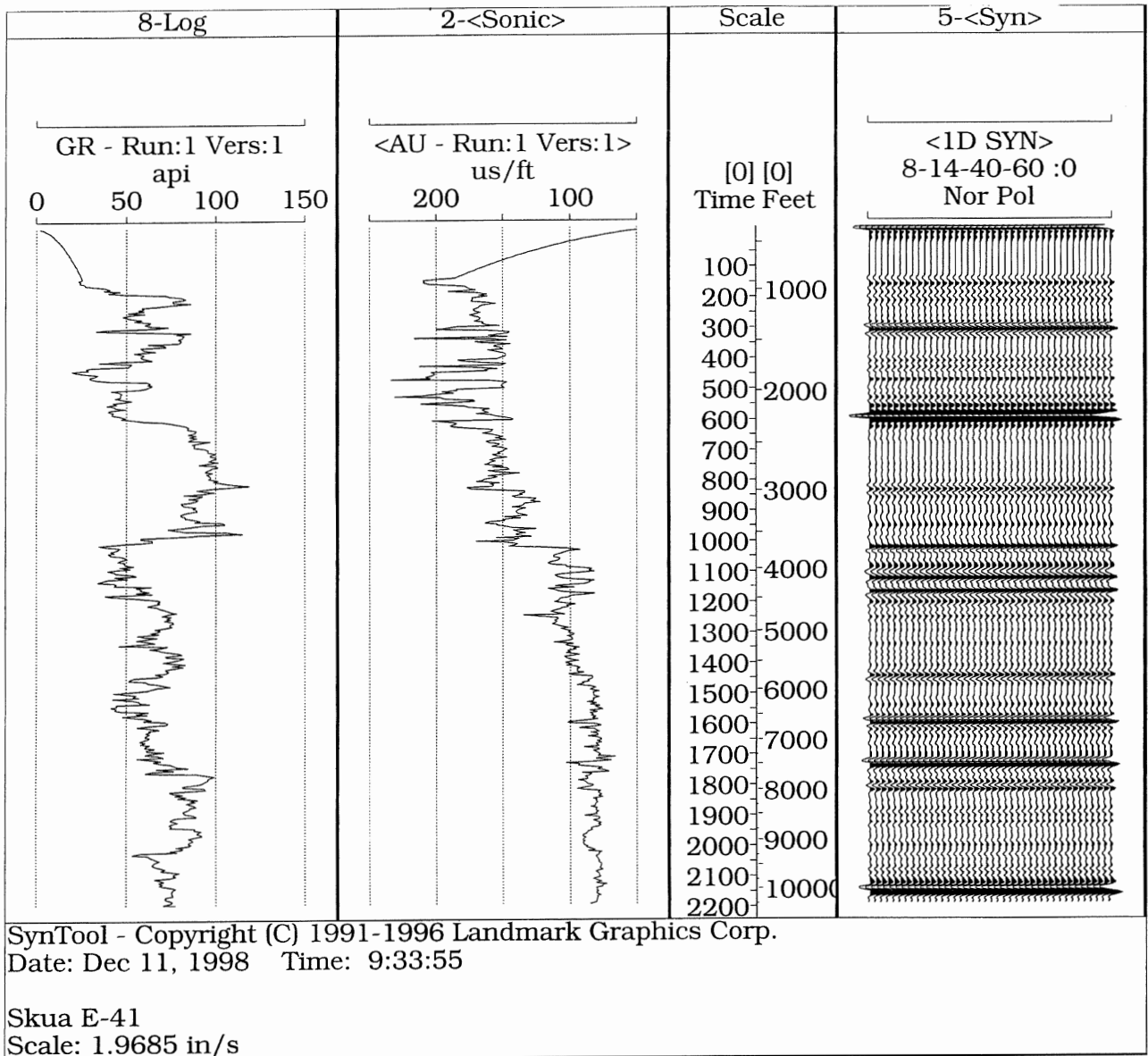
# OSPREY SYNTHETIC SEISMOGRAM



SynTool - Copyright (C) 1991-1996 Landmark  
Date: Jan 7, 1999 Time: 10:10:11

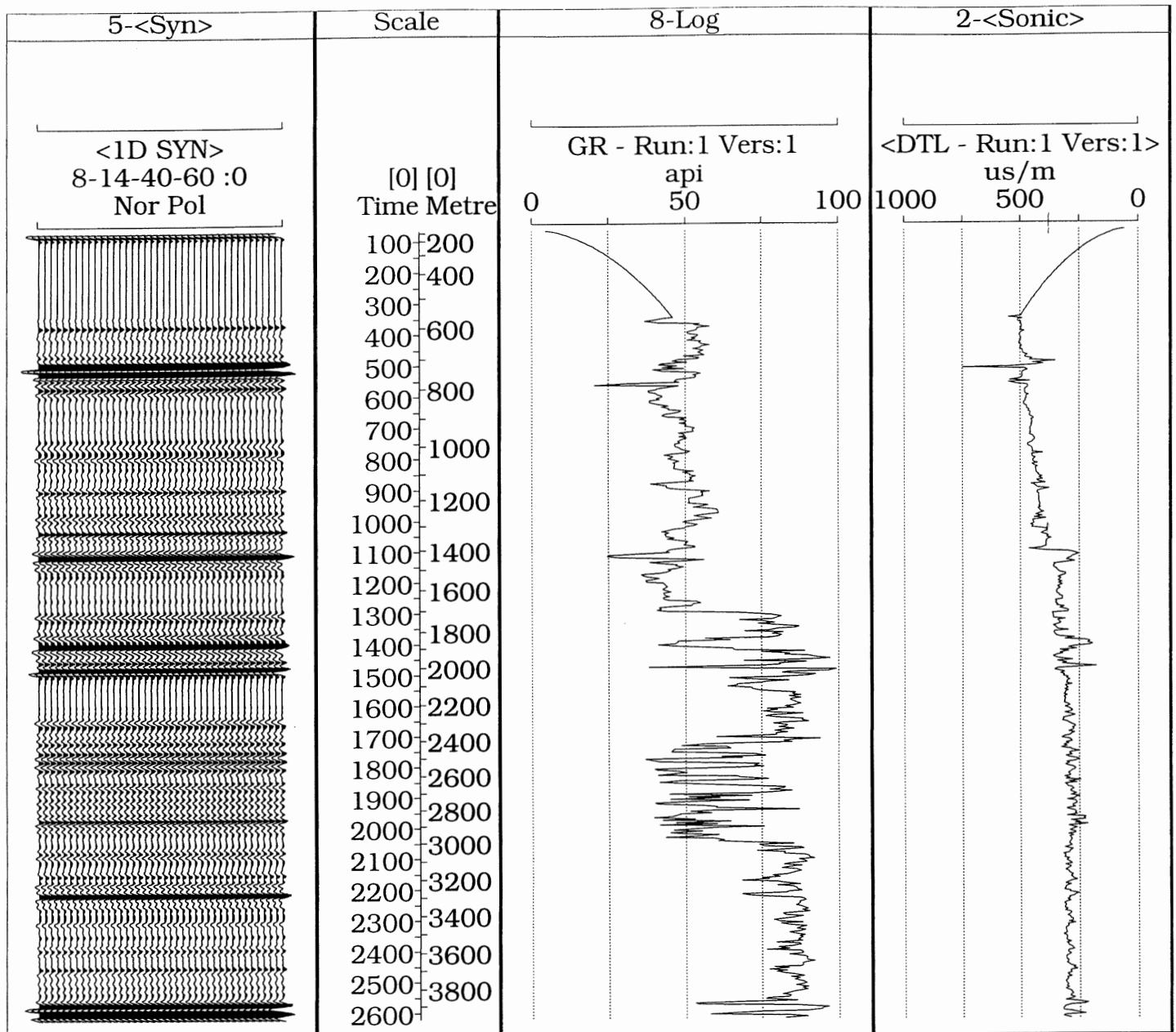
Bonniton H-32  
Scale: 2.5 in/s

## BONNITION SYNTHETIC SEISMOGRAM



Skua Synthetic Seismogram





SynTool - Copyright (C) 1991-1996 Landmark Graphics Corp.  
 Date: Dec 10, 1998 Time: 14:36:24

St. George J-55  
 Scale: 1.9685 in/s

St. George well with 6124-83 line

# ST. GEORGE SYNTHETIC SEISMOGRAM

*Appendix 4: Seismic Sections used in this study of Carson Basin.*

<b>PROJECT</b>	<b>LINES</b>	<b>COMPANY</b>	<b>YEAR</b>
8624-P28-39/40E	5000-82 5002-82 5004-82 5006-82, 5006A 5008-82 5010-82 5012-82 5021-82 5023A-82 5025-82 5027-82 5029-82 5031-82 5033-82	PETROCANADA	1982
8624-P28-61E	6120-83 6122-83 6124-83 6126-83 6128-83 6130-83 6132-83 6134-83 6136-83 6138-83 6139-83 6140-83 6141-83 6142-83 6143-83 6145-83 6147-83 6149-83 6151-83 6153-83 6155-83 6157-83 6159-83 6161-83 6163-83 6165-83 6167-83	PETRO-CANADA	1983
8624-P28-76E	6298-85 6300-85 6302-85 6304-85 6305-85 6306-85 6307-85	PETROCANADA	1985

8624-H6-1E	HM81-17B HM81-30/2 HM81-30/3 HM81-35 HM81-36 HM81-37-3 HM81-38A, 38B HM81-39 HM81-39/2 HM81-40/2 HM81-41 HM81-42	HUSKY OIL	1981
8624-J8-3E	HS-7 HS-8 HS-9 HS-10	IGC RESOURCES	1982
8624-J1-2E	81-73101 81-73102 81-73103 81-73106	ESSO	1982
8624-P3-1E	PCP81-60A, B PCP81-62 PCP81-63 PCP81-65 PCP81-66A,C PCP81-67C, D PCP81-68A PCP81-69,A PCP-81070 PCP81-71A PCP81-72 PCP81-73 PCP81-102	PANCANADIAN	1982
8624-C55-2E	CGB82-25 CGB82-115	CANTERRA	1982
8624-C55-1E	CNF82-104, 104A CNF82-119	CANTERRA	1982
8620-S14-8E	83-2674A 83-4816 83-4832A	SOQUIP	1983
8620-G5-11P	NF79-107	GSI	1980
8624-G5-1P	NF81-109 NF81-116	GSI	1982

8624-G5-2P	NF82-03 NF82-05 NF82-09 NF82-15 NF82-18 NF82-20, 20A NF82-22 NF82-24 NF82-26 NF82-32 NF82-34	GSI	1982
8624-G5-9P	FC83-01B FC83-28, 28A FC83-30, 30A FC83-32, 32A, 32B FC83-34 FC83-39A FC83-41 FC83-43 FC83-47 FC83-49A	GSI	1984
Lithoprobe	85-4, 4A		1985

**Appendix 5: Greyscale Figures and Uninterpreted Seismic Sections**



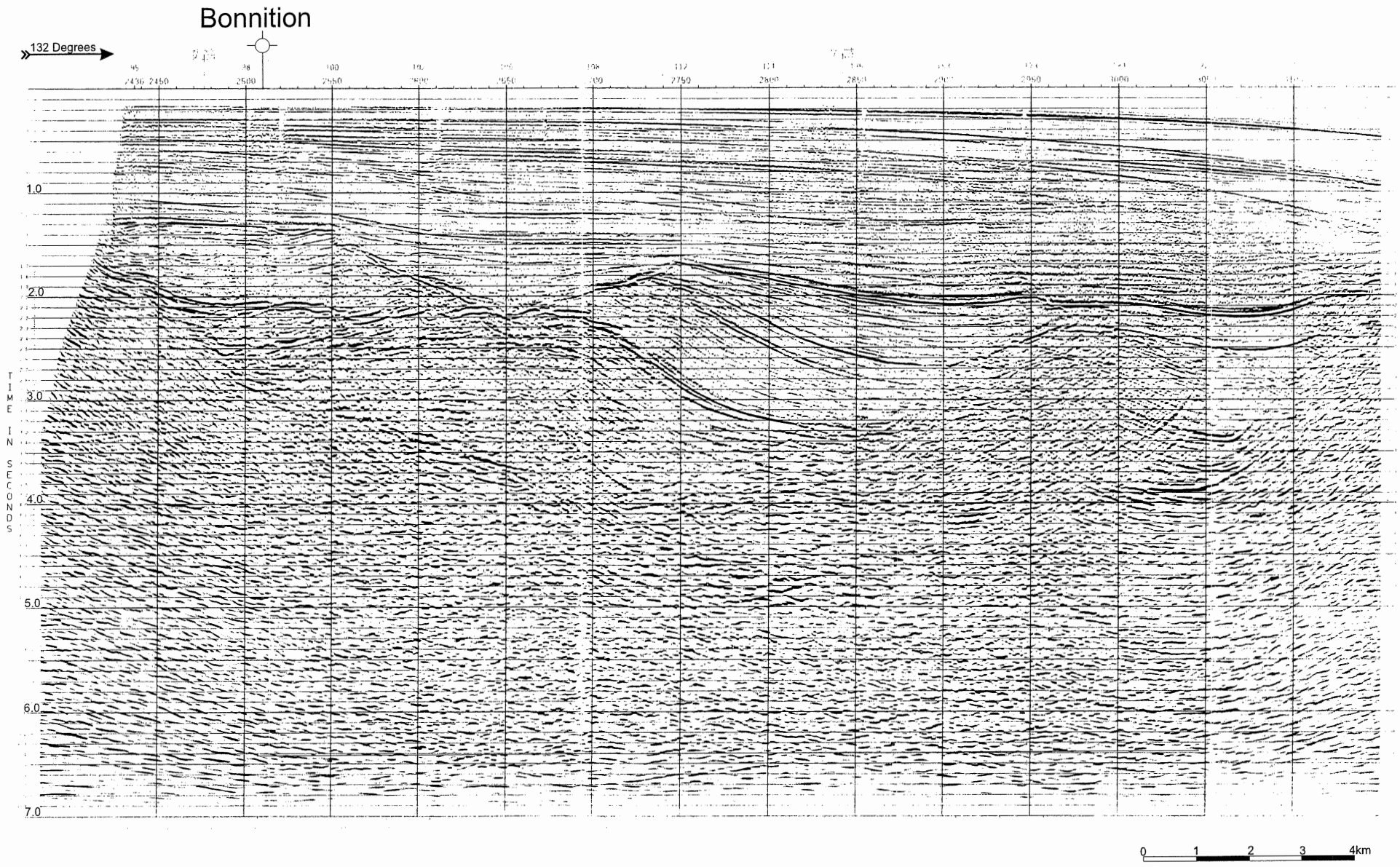


Figure 5.2: PCP81-067D

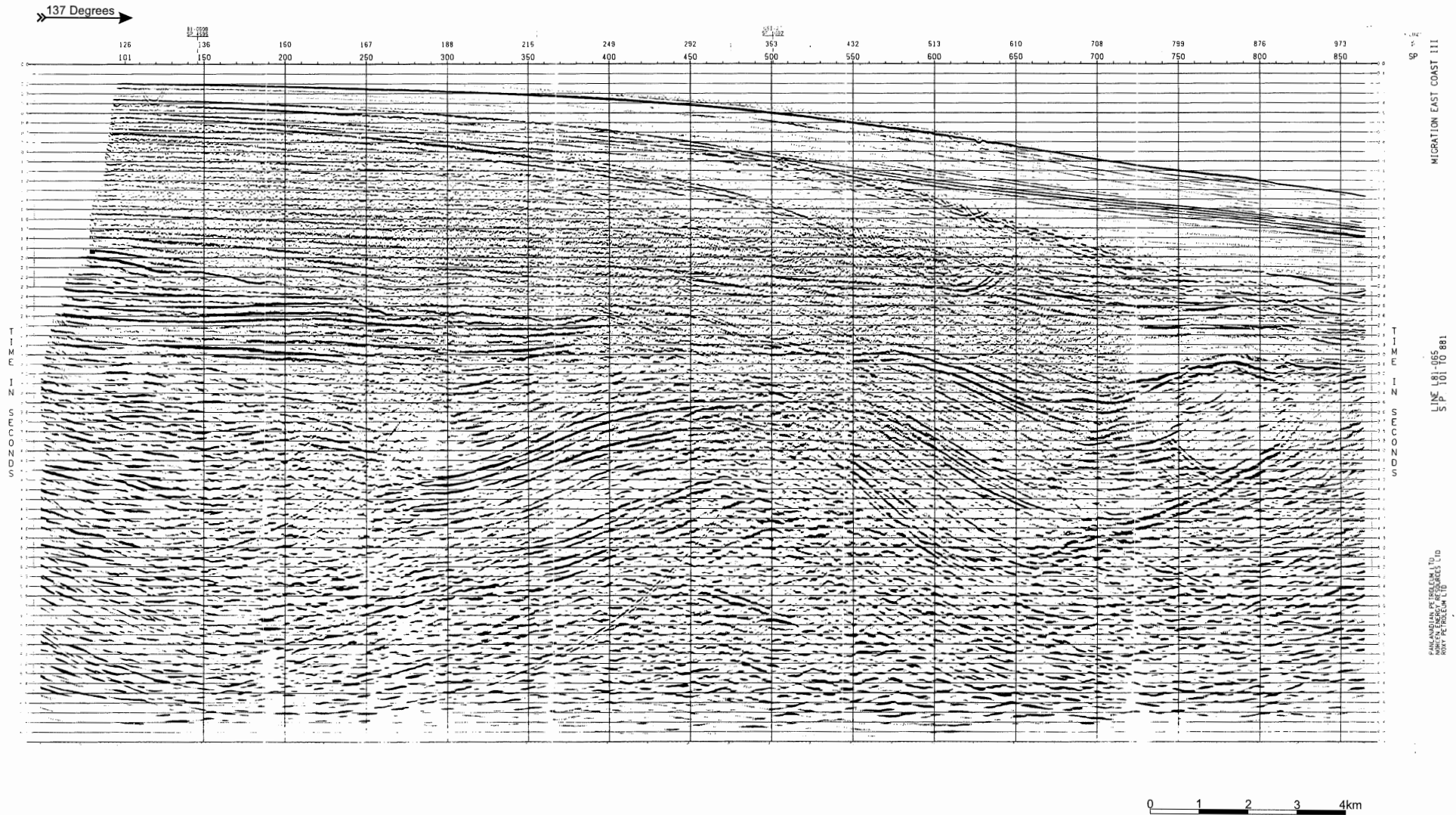


Figure 5.3: PCP81-065

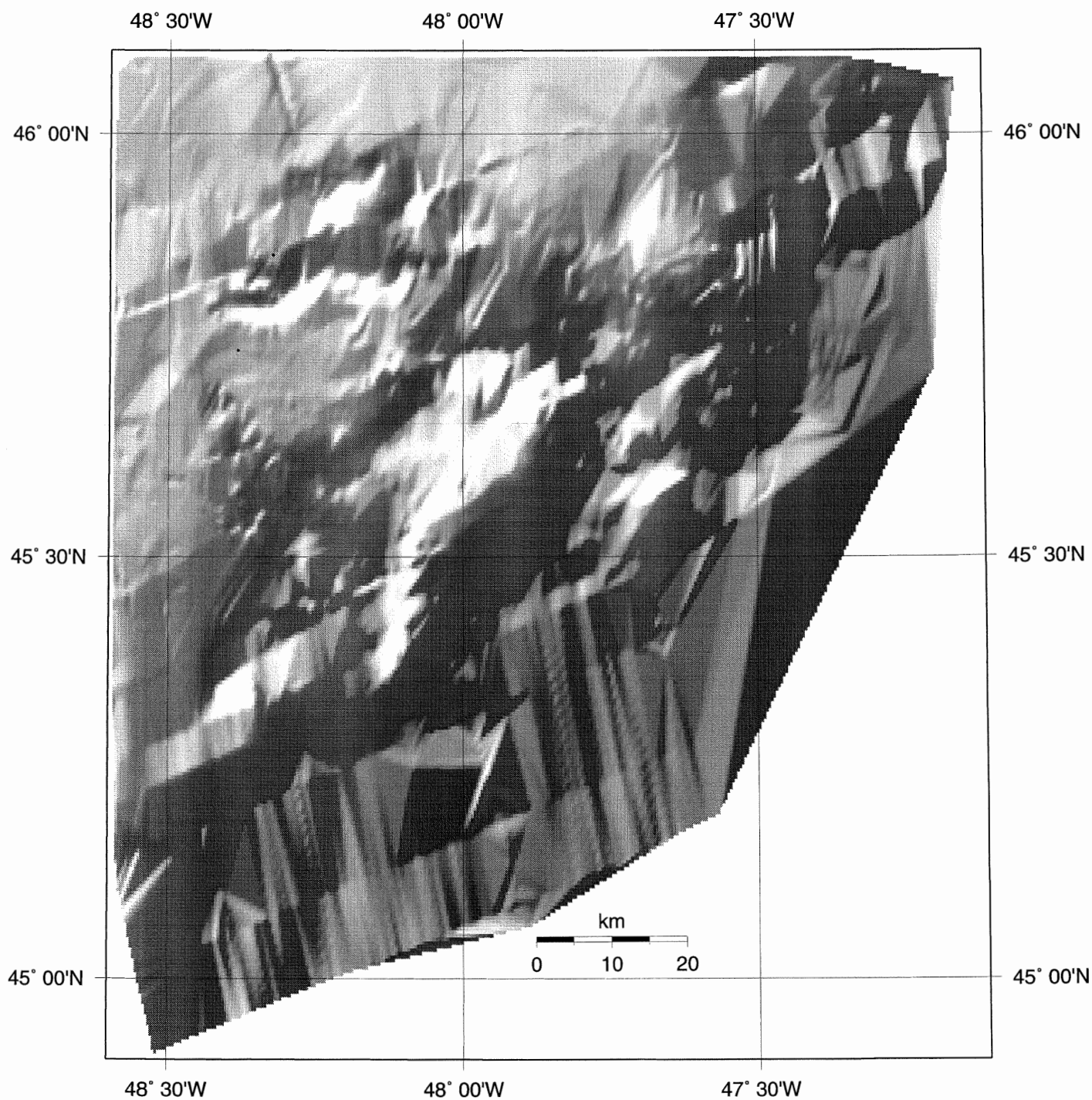


Figure 5.5: Greyscale shaded relief map of Early Eocene Unconformity surface.

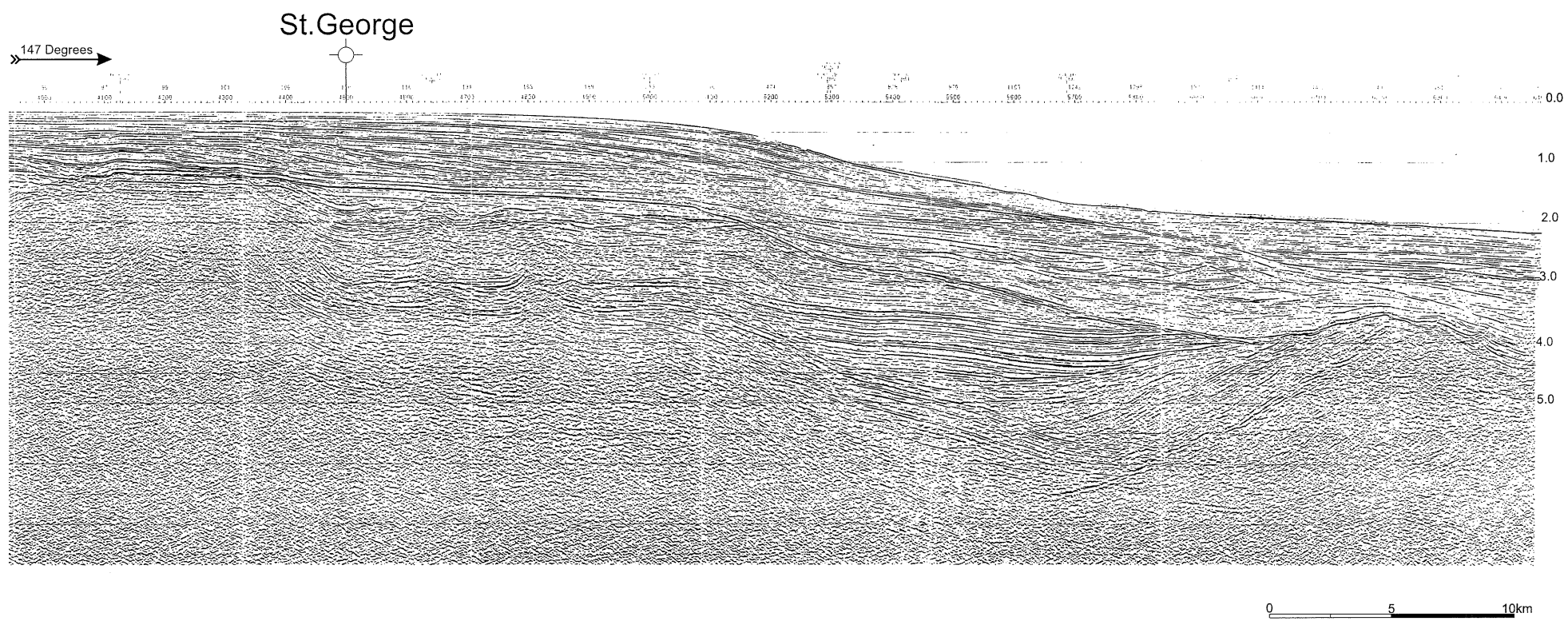


Figure 5.6: FC83-49A



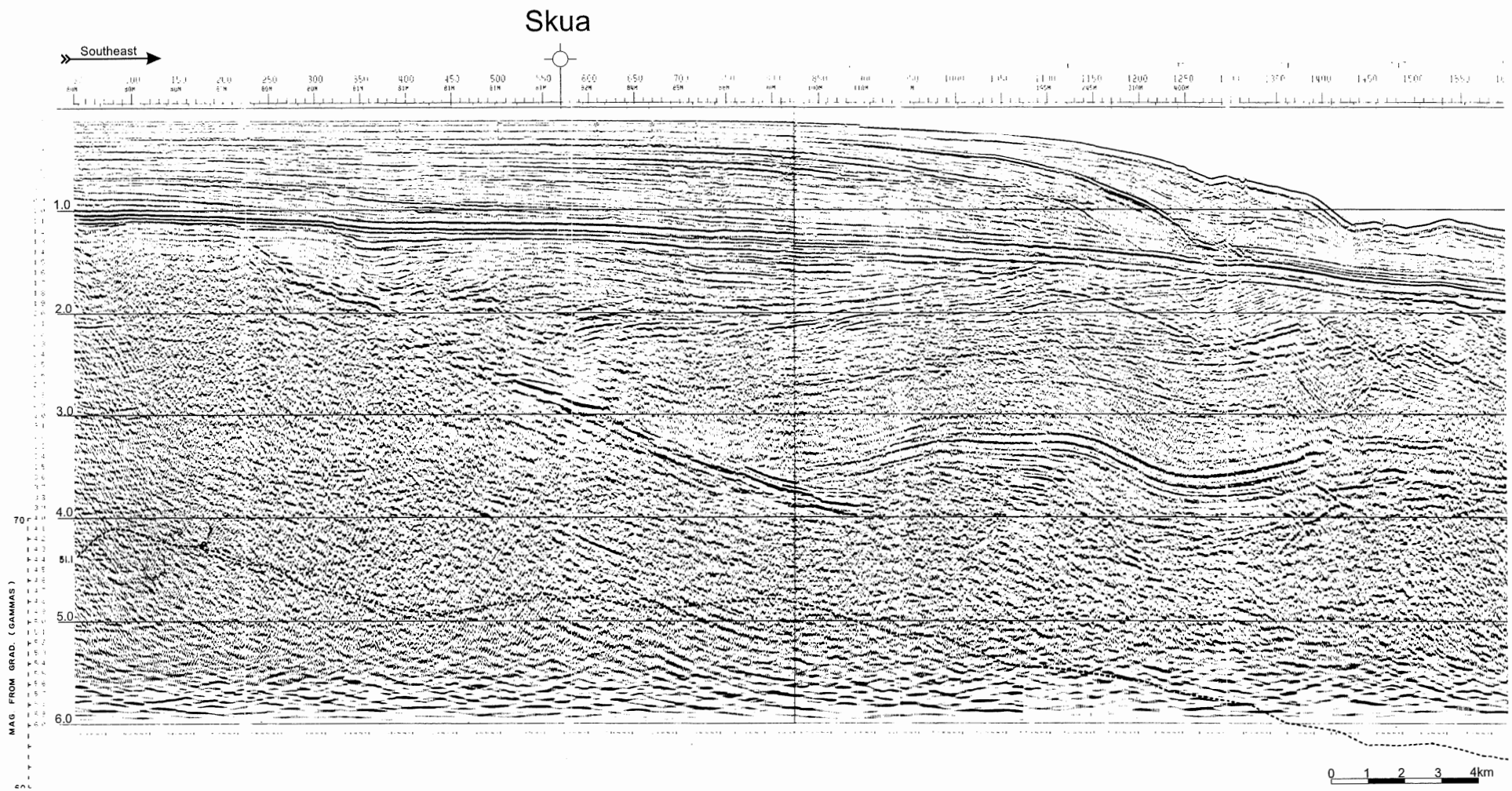


Figure 5.7: CGB82-115

» Southeast

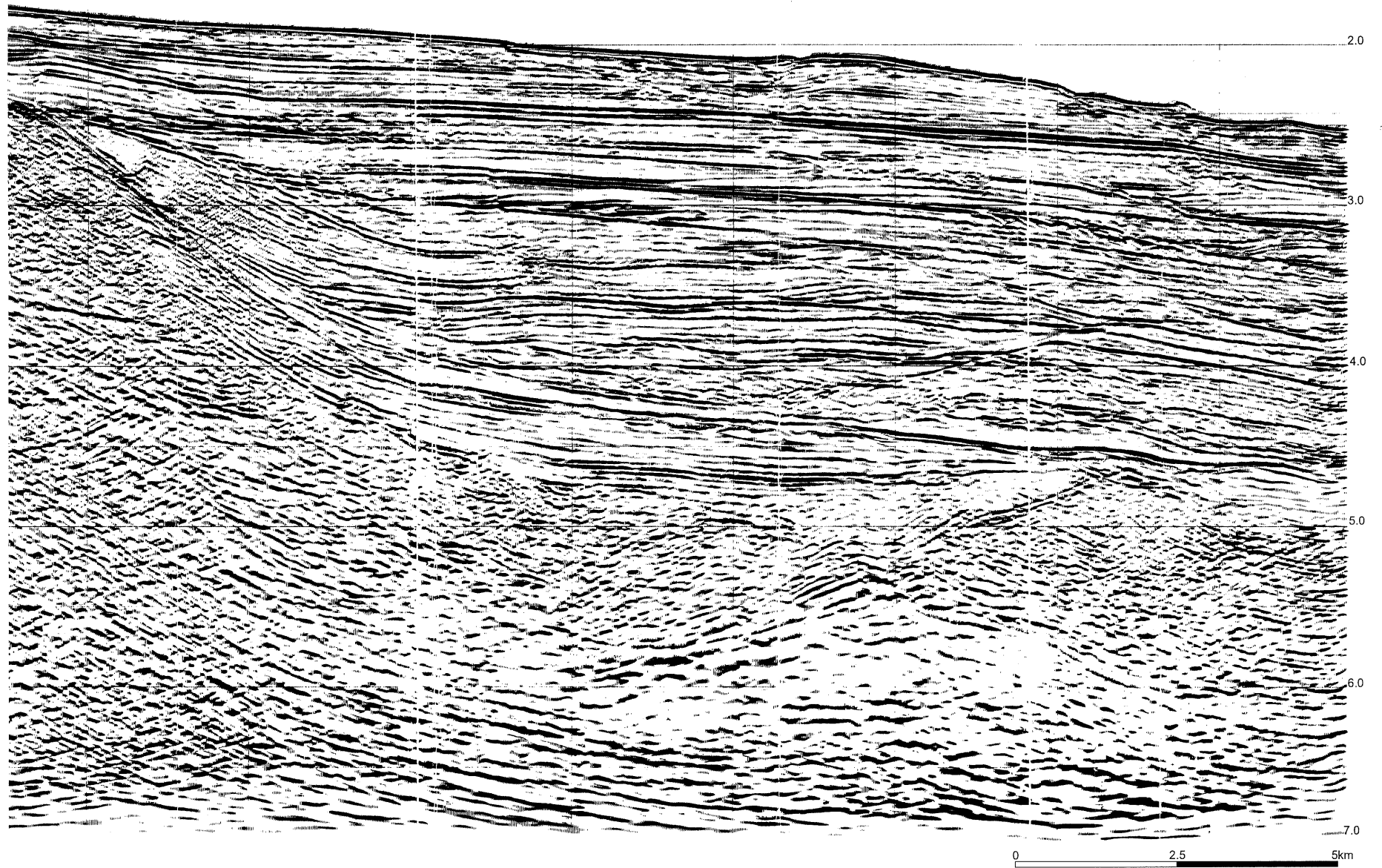


Figure 5.8: 6161-83



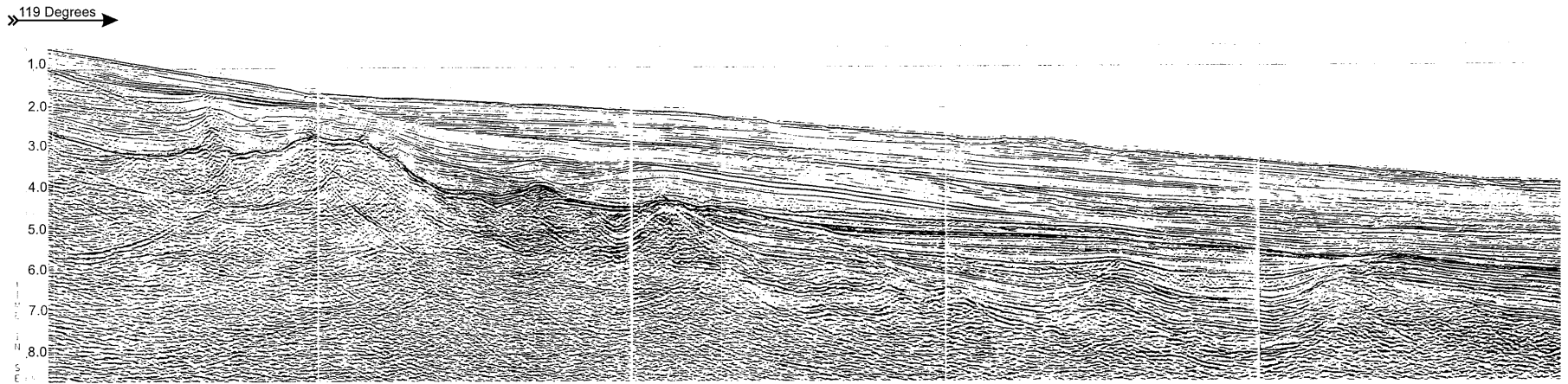
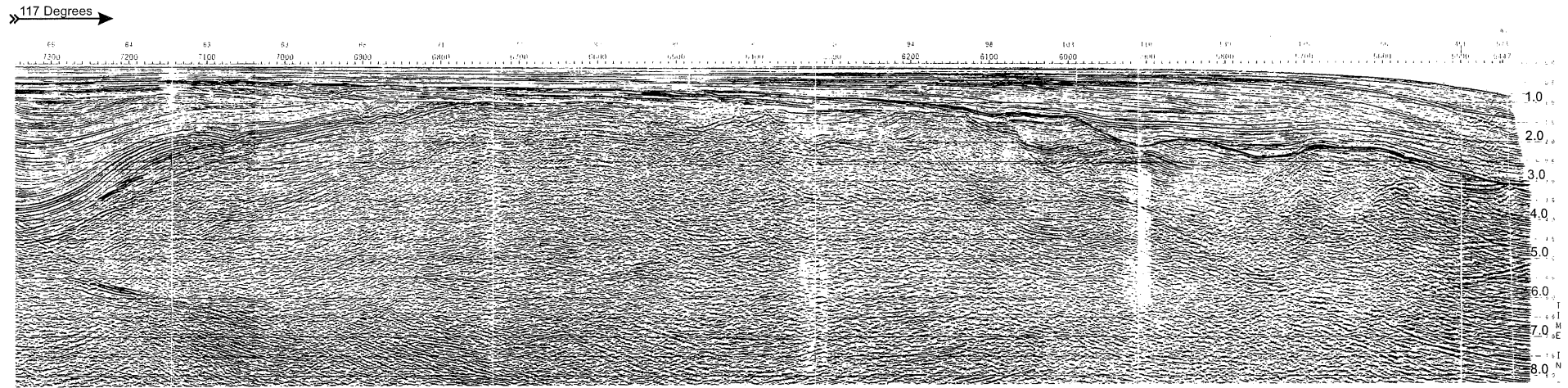


Figure 5.11: Lithoprobe 85-4, 85-4A

0 5 10km

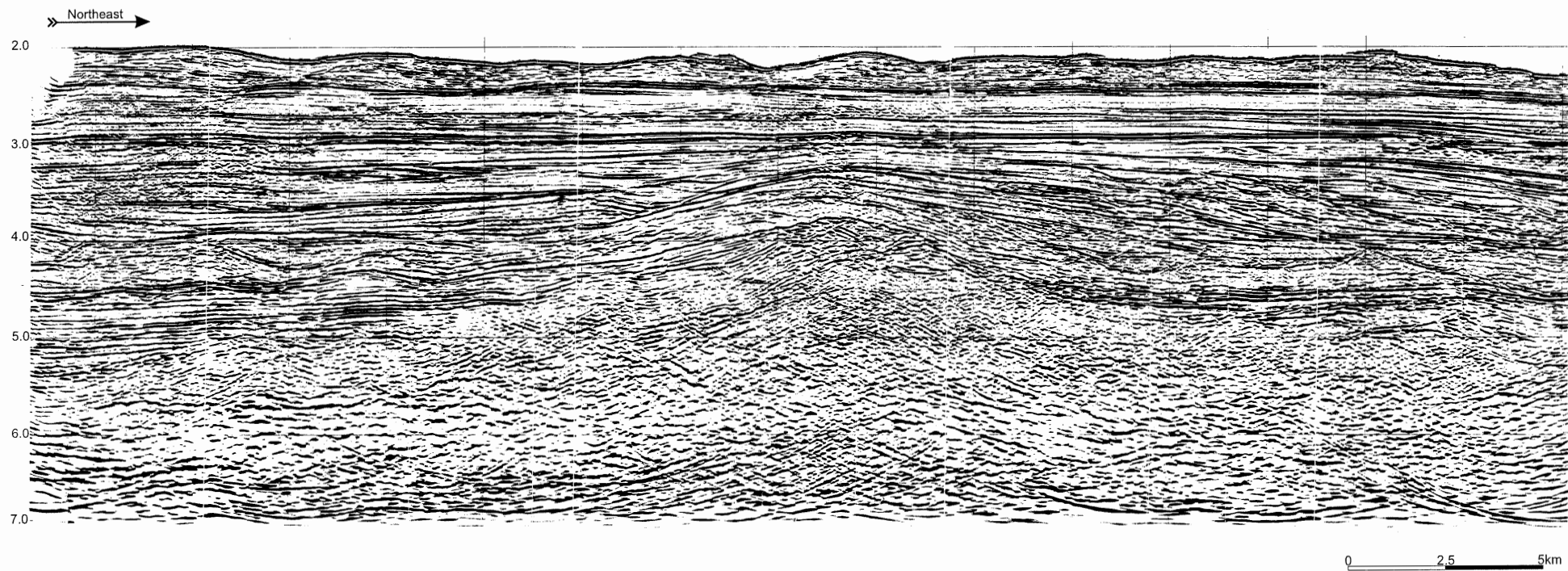


Figure 5.13: 6132-83

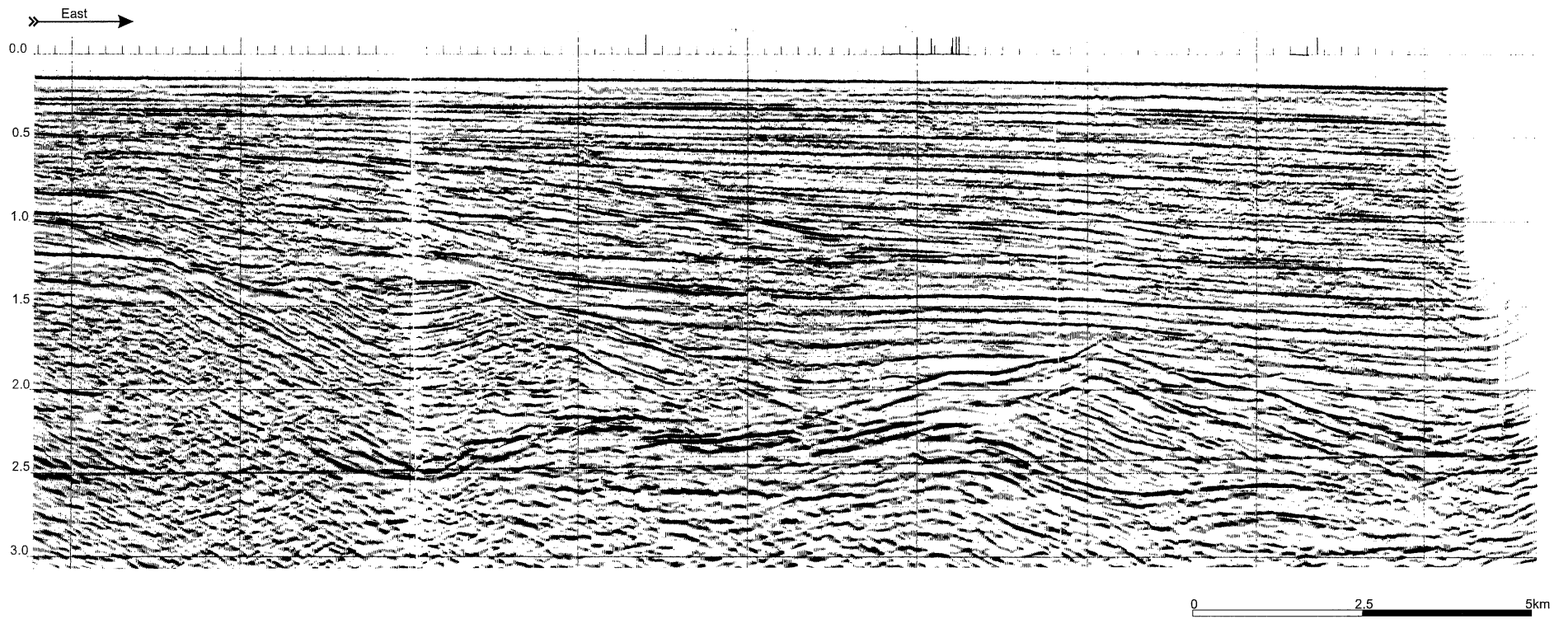


Figure 5.14: 6130-83